

SPECTRAL DECIMATION OF THE MAGNETIC LAPLACIAN ON THE SIERPINSKI GASKET HOFSTADTER'S BUTTERFLY, DETERMINANTS, AND LOOP SOUP ENTROPY

JOE P. CHEN AND RUOYU GUO

ABSTRACT. The magnetic Laplacian (also called the line bundle Laplacian) on a connected weighted graph is a self-adjoint operator wherein the real-valued adjacency weights are replaced by complex-valued weights. When properly interpreted, these complex weights give rise to magnetic fluxes through cycles in the graph.

In this paper we establish the spectrum of the magnetic Laplacian on the Sierpinski gasket graph (SG) where the magnetic fluxes equal α through the smallest upright triangles, and β through the smallest downright triangles. This is achieved upon showing the spectral self-similarity of the magnetic Laplacian via a 3-parameter map involving non-rational functions, which takes into account α , β , and the spectral parameter λ . When $\alpha, \beta \in \{0, \frac{1}{2}\}$, we can list the eigenvalues according to their multiplicities. When not both α and β are in $\{0, \frac{1}{2}\}$, we show that the spectrum is essentially determined by the Julia set of the 3-parameter map.

We provide two applications of our results: 1) demonstrate the true Hofstadter's butterfly appearing in the energy spectrum on SG under uniform magnetic field; and 2) compute the magnetic Laplacian determinant which corresponds to the partition function for random cycle-rooted spanning forests on SG , derive the corresponding asymptotic complexity, and give its probabilistic interpretation in terms of a "loop soup entropy."

CONTENTS

1. Introduction and main results	2
1.1. Magnetic Laplacian	3
1.2. The Sierpinski gasket	4
1.3. Spectrum of the magnetic Laplacian on the Sierpinski gasket	5
1.4. Hofstadter's butterfly meets Sierpinski	9
1.5. Magnetic Laplacian determinants and cycle-rooted spanning forests	10
1.6. Asymptotic complexity and the loop soup entropy	13
1.7. Open questions	15
Organization for the rest of the paper	16
2. Spectral self-similarity of the magnetic Laplacian	16
2.1. Schur complement computation	16
2.2. Diagrammatic analysis	18
2.3. Establishing spectral self-similarity	21
3. Mechanics of spectral decimation	23
3.1. Schur complement & functional identities	23

Date: July 8, 2022.

2010 Mathematics Subject Classification. 05C50; 11C20; 32M25; 37F50; 47A10; 58J50; 82D40;

Key words and phrases. Spectral decimation, Schur complement, magnetic Laplacian, fractals, Hofstadter butterfly, Julia set, Laplacian determinants, matrix-tree theorem, cycle-rooted spanning forests, asymptotic complexity.

This work is an outgrowth of the High Honors Bachelor's thesis by the second-named author at Colgate University, advised by the first-named author. We acknowledge partial financial support from the Research Council of Colgate University, the Simons Foundation (Collaboration Grant for Mathematicians #523544), and the National Science Foundation (DMS-1855604).

3.2. Spectral decimation for the non-exceptional values	24
3.3. Spectral decimation for the exceptional values	25
4. Recursive characterization of the magnetic spectrum	28
4.1. Case-by-case analysis of the exceptional set	29
4.2. Spectrum under (half-)integer fluxes	31
4.3. Spectrum under non-(half-)integer fluxes	36
5. Magnetic Laplacian determinants and CRSF asymptotic complexity	41
Acknowledgements	44
Appendix A. Numerical approximation of the filled Julia set in Figure 3	44
References	45

1. INTRODUCTION AND MAIN RESULTS

Spectral analysis of the magnetic Laplacian on a planar lattice has both theoretical and practical implications. The famous Hofstadter’s butterfly [22] describes the spectrum of a noninteracting electron gas moving on the planar integer lattice under uniform magnetic field, *i.e.*, the magnetic flux through every square cell is constant. Understanding the fractal nature of this spectrum involves the interplay of analysis, geometry, topology, and number theory.

We can also study the magnetic spectrum on other periodic or quasi-periodic planar graph under uniform magnetic field. For instance, we can replace the square lattice by the triangular lattice. From the triangular lattice, we can remove vertices and the attached edges in such a way that the remainder is an infinite blow-up of the Sierpinski gasket graph (SG); see Figure 1. How does the magnetic spectrum vary with the state space? And more importantly, can we find ways to compute the magnetic spectrum as explicitly as possible?

The problem of computing the magnetic spectrum on SG started in the early 1980s [1, 13, 18, 38]. Already then the authors have identified the nesting mechanism for generating the spectrum recursively, and pointed out the existence of localized eigenfunctions associated with certain “exceptional” eigenvalues. Probably the most important claim made was that the magnetic spectrum is given by an analog of Hofstadter’s butterfly shown in [18, Figure 2].¹ We refer the reader to Bellissard’s survey [4] for an overview of spectral problems on quasi-periodic lattices and the renormalization group methods, which includes the magnetic spectral problem on SG .

After [4] there was a lull in activities around the analysis of magnetic Laplacians on fractal spaces. Throughout the 1990s, intense activity surrounded the spectral analysis of the (graph) Laplacian on self-similar sets, starting with Fukushima and Shima [17] and Shima [40]. The first complete characterization of the Laplacian spectrum on the infinite SG lattice was attained by Teplyaev [42], based on an abstract formulation of spectral decimation by him and Malozemov [33]. The said techniques have since been applied to obtaining Laplacian spectra on a variety of self-similar spaces. There are too many subsequent works to list here in this introduction, but we single out the pedagogically influential paper [3].

The 2010s has witnessed a renewal of interest in the study of magnetic Laplacians on fractals. Probably closest to our present work is that of Hyde, Kelleher, Moeller, Rogers, and Seda [23], where they obtained the spectrum on SG in which the magnetic 1-form is locally exact, corresponding to having nonzero flux through a finite number of triangles. Another fractal graph whose magnetic spectrum can be solved exactly is the diamond fractal [5]. On the functional analytic side, we

¹See also [4, Figure 2] for what appears to be a higher-resolution picture of [18, Figure 2], though it is the authors’ opinion that the two pictures have major differences.

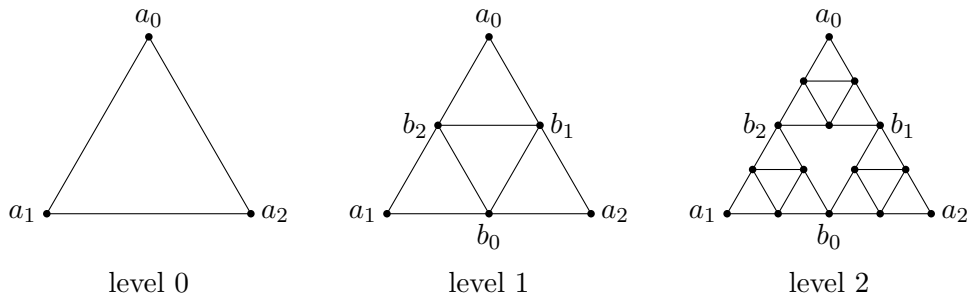


FIGURE 1. The Sierpinski gasket graph of level 0, 1, and 2.

would like to mention recent results on the closability and self-adjointness of, and a Feynman-Kac formula corresponding to, magnetic Laplacians on compact fractal spaces (or more generally, resistance spaces) [19–21].

Despite the aforementioned progress, it may come as a surprise that the original problem of identifying the spectrum of the magnetic Laplacian on SG under uniform magnetic field remains unsolved, more than 30 years since it was first posed [1, 13, 38].

The main purpose of this work is to provide a full solution to this long-standing problem. Via a recursive procedure called **spectral decimation** (see §3 for details, including a few refinements of the arguments in [3] to tailor to the magnetic Laplacian setting), we establish the magnetic spectrum on SG when the flux through each smallest upright triangle (resp. smallest downright triangle) equals α (resp. β), for any $\alpha, \beta \in [0, 1)$.

In the case where $\alpha, \beta \in \{0, \frac{1}{2}\}$, which we refer to as the case of (half-)integer fluxes, we can list the eigenvalues according to their multiplicities (Theorem 1). As a corollary, we compute explicitly the magnetic Laplacian determinants (Theorem 3), which correspond to partition functions for a class of determinantal point processes on SG ; see §1.5 and §1.6 for further details. When $\alpha = \beta = 0$ the magnetic Laplacian degenerates to the usual graph Laplacian, and we recover previously known results [2, 17, 39, 42].

In the other cases where the fluxes are not (half-)integer-valued, the magnetic spectrum is essentially given by the Julia set of a nontrivial 3-parameter map (1.6) (Theorem 2, Corollary 1.4). Historically this 3-parameter map was first obtained by Alexander [1], cf. [4, 13, 18]. For the sake of full transparency, we provide the computations to obtain this map, and explicate the necessity for taking all 3 parameters (α , β , and the spectral parameter λ) into account when generating the Julia set (see §2). Our proofs expand upon the results, and correct an oversight, in the above-mentioned physics literature. To wit, while the authors of [18] rightfully identified a reduction from the 3-parameter map to a 2-parameter one, they neglected the fact that the dynamics of the two maps differ (compare Figures 3 and 5). Our main contribution is to establish the correct analog of “Hofstadter’s butterfly” for a free electron gas moving on SG under uniform magnetic field.

1.1. Magnetic Laplacian. Let $G = (V, E)$ be a locally finite connected graph. The (combinatorial) graph Laplacian on G is $\Delta_G = D_G - A_G$, where D_G and A_G are the degree matrix and the adjacency matrix, respectively. Equivalently,

$$(\Delta_G u)(x) = \sum_{y \sim x} (u(x) - u(y)), \quad u \in \mathbb{R}^V,$$

where the sum is over vertices y connected to x by an edge. Clearly Δ_G is self-adjoint on $\ell^2(V)$. Sometimes it is more convenient to normalize the Laplacian by the degree, i.e., $\mathcal{L}_G = D_G^{-1} \Delta_G$, or

equivalently,

$$(\mathcal{L}_G u)(x) = \frac{1}{\deg_G(x)} \sum_{y \sim x} (u(x) - u(y)), \quad u \in \mathbb{R}^V.$$

This is called the probabilistic graph Laplacian, and it is self-adjoint on $L^2(V, \deg)$. More generally, we introduce a **conductance** function $\mathbf{c} : \{\pm E\} \rightarrow \mathbb{R}_+$ on the set of oriented edges of G , and define the weighted graph Laplacian as

$$(\mathcal{L}_{(G, \mathbf{c})} u)(x) = \sum_{y \sim x} \mathbf{c}_{xy} (u(x) - u(y)), \quad u \in \mathbb{R}^V.$$

We allow $\mathbf{c}_{xy} \neq \mathbf{c}_{yx}$: a natural example is to let \mathbf{c}_{xy} be the transition probability $p(x, y)$ of an irreducible Markov chain on G .

Whereas the adjacency matrix contains entries with values 0 or 1, we now replace the 1's by unit complex numbers to form the magnetic Laplacian. The motivation behind the definition is from differential geometry. Place a copy \mathcal{W}_v of $\mathcal{W} = \mathbb{C}$ at each $v \in V$. We call $\mathcal{W} = \bigoplus_{v \in V} \mathcal{W}_v$ a *complex line bundle* on G . A *unitary connection* Φ on \mathcal{W} satisfies the property that for every oriented edge $e = vv'$, $\phi_{vv'} : \mathcal{W}_v \rightarrow \mathcal{W}_{v'}$ is a unitary complex linear map such that $\phi_{v'v} = \phi_{vv'}^{-1}$. We call $\phi_{vv'}$ the *parallel transport* from v to v' . Two unitary connections Φ and Φ' are *gauge equivalent* if there exists a unitary map $\psi_v : \mathcal{W}_v \rightarrow \mathcal{W}_v$ such that $\psi_{v'} \phi_{vv'} = \phi'_{vv'} \psi_v$, that is, ψ_v gives the change of basis between the two connections.

We may also extend the definition of the line bundle to E . Place a copy \mathcal{W}_e of $\mathcal{W} = \mathbb{C}$ at each $e \in E$. Then define a connection isomorphism $\phi_{ve} = \phi_{ev}^{-1}$ for a vertex $v \in V$ and an edge e containing v , satisfying the condition that if $e = vv'$, then $\phi_{vv'} = \phi_{ev'} \circ \phi_{ve}$, where $\phi_{vv'}$ is the parallel transport from v to v' .

For this paper we choose Φ to be a $U(1)$ connection ω , and the action of $\phi_{vv'}$ is multiplication by a unit complex number $\omega_{vv'}$, satisfying $\omega_{v'v} = \overline{\omega_{vv'}}$.

Now we can define the magnetic Laplacian associated to the connection ω as

$$(1.1) \quad (\mathcal{L}_{(G, \mathbf{c})}^\omega u)(x) = \sum_{y \sim x} \mathbf{c}_{xy} (u(x) - \omega_{xy} u(y)), \quad u \in \mathbb{C}^V.$$

Another way to express (1.1) is $\mathcal{L}_{(G, \mathbf{c})}^\omega = d^* d$, where

$$(1.2) \quad d : \Lambda^0(G, \omega) \rightarrow \Lambda^1(G, \omega), \quad (df)(e) = \phi_{ye} f(y) - \phi_{xe} f(x), \quad e = xy,$$

$$(1.3) \quad d^* : \Lambda^1(G, \omega) \rightarrow \Lambda^0(G, \omega), \quad (d^* \chi)(v) = \sum_{e=v'v} \mathbf{c}_{vv'} \phi_{ev} \chi(e),$$

are, respectively, the gradient and the divergence operators, and $\Lambda^0(G, \omega)$ and $\Lambda^1(G, \omega)$ denote the space of 0-forms and 1-forms on (G, ω) .

We now define the flux through a simple cycle induced by a $U(1)$ connection ω . A sequence P of vertices $\{x_0, x_1, x_2, \dots, x_{m-1}, x_m\}$ is a *path* if $x_i \sim x_{i+1}$ for all $i \in \{0, 1, \dots, m-1\}$, and moreover, a *simple path* if $x_i \neq x_j$ for any pair $i, j \in \{0, 1, \dots, m-1\}$. A path is called a *cycle* (of length m) if $x_m = x_0$. We assign an orientation to each simple cycle γ , and let $\omega(\gamma) = \omega_{x_0 x_1} \omega_{x_1 x_2} \cdots \omega_{x_{m-1} x_0}$ be the product of the parallel transports around γ , also called the *holonomy* of γ .

Definition 1.1. Given (G, ω) , and a simple cycle γ in G with counterclockwise orientation, the **magnetic flux** through γ is defined as the number $\theta \in [0, 1)$ such that the holonomy $\omega(\gamma) = e^{2\pi i \theta}$.

1.2. The Sierpinski gasket. Let $x_0 = (0, 0) := o$, $x_1 = (\frac{1}{2}, \frac{\sqrt{3}}{2})$, and $x_2 = (1, 0)$ be the vertices of a unit equilateral triangle in \mathbb{R}^2 , and \mathfrak{G}_0 be the complete graph on the vertex set $V_0 = \{x_0, x_1, x_2\}$. We introduce three contracting similitudes $\Phi_i : \mathbb{R}^2 \rightarrow \mathbb{R}^2$, $\Phi_i(x) = \frac{1}{2}(x - x_i) + x_i$ for each $i \in \{0, 1, 2\}$. The Sierpinski gasket fractal K is the unique nonempty compact set K such that $K = \bigcup_{i=0}^2 \Phi_i(K)$. To obtain the associated level- N pre-fractal graph \mathfrak{G}_N , $N \geq 1$, we define by induction $\mathfrak{G}_N =$

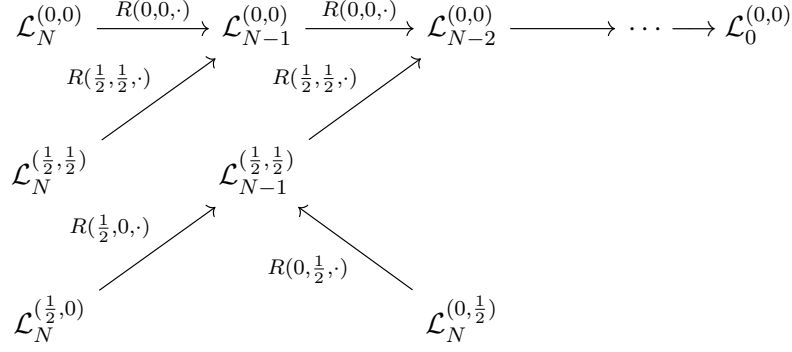


FIGURE 2. Scheme of spectral decimation for the magnetic Laplacians in the case of (half-)integer fluxes.

$\bigcup_{i=0}^2 \Phi_i(\mathfrak{G}_{N-1})$. To make all edges of the graph have unit length, we set $G_N := 2^N \mathfrak{G}_N$, where for $\alpha > 0$ and $\Omega \subset \mathbb{R}^2$ we denote $\alpha\Omega := \{\alpha x : x \in \Omega\}$. The (one-sided) Sierpinski gasket graph SG is then defined to be the infinite graph $\bigcup_{N=0}^{\infty} G_N$. The number of vertices $|V_N|$ in $G_N = (V_N, E_N)$ is easily shown to be $\frac{3^{N+1}+3}{2} =: \dim_N$.

1.3. Spectrum of the magnetic Laplacian on the Sierpinski gasket. Denote by \mathcal{L}_N^ω the magnetic Laplacian on the level- N gasket graph G_N endowed with the $U(1)$ connection ω , that is,

$$(1.4) \quad (\mathcal{L}_N^\omega u)(x) = \sum_{y \sim x} \frac{1}{\deg_{G_N}(x)} (u(x) - \omega_{xy} u(y)), \quad u \in \mathbb{C}^V.$$

It is direct to check that \mathcal{L}_N^ω is self-adjoint on $L^2(V_N, \deg_{G_N})$. Moreover, by embedding SG into the plane, we can unambiguously assign an orientation to each simple cycle, and apply Definition 1.1.

Assumption 1. The magnetic flux through each upright (resp. downright) triangle of side length 1 in the graph distance equals α (resp. β).

It is not difficult to show that for every N , there exists a line bundle connection ω which satisfies Assumption 1. We denote by $\mathcal{L}_N^{(\alpha, \beta)}$ the gauge equivalence class of magnetic Laplacians on G_N which satisfies Assumption 1.

The following notation will be in force throughout the paper. For an operator \mathcal{L} , we denote by $\sigma(\mathcal{L}) := \{z \in \mathbb{C} : \mathcal{L} - zI \text{ is not invertible}\}$ the *spectrum* of \mathcal{L} . The notation $\text{mult}(\mathcal{L}, \lambda)$ (resp. $\text{mult}(P, \lambda)$) represents the *multiplicity* of $\lambda \in \mathbb{C}$ in $\sigma(\mathcal{L})$ (resp. in the zero set of a polynomial function P). In particular, $\text{mult}(\mathcal{L}, \lambda) = 0$ means that $\lambda \notin \sigma(\mathcal{L})$.

Let us introduce the quadratic polynomials

$$\begin{aligned} R(0, 0, \lambda) &= \lambda(5 - 4\lambda), & R\left(\frac{1}{2}, \frac{1}{2}, \lambda\right) &= -(\lambda - 2)(4\lambda - 3), \\ R\left(\frac{1}{2}, 0, \lambda\right) &= -4\lambda^2 + 9\lambda - 3, & R\left(0, \frac{1}{2}, \lambda\right) &= -4\lambda^2 + 7\lambda - 1, \end{aligned}$$

which are special cases of $R(\alpha, \beta, \lambda)$ in (2.24).

It has already been established in [17] that

$$\sigma(\mathcal{L}_N^{(0,0)}) = \left\{0, \frac{3}{2}\right\} \cup \left(\bigcup_{k=0}^{N-1} (R(0, 0, \cdot))^{-k} \left(\frac{3}{4}\right) \right) \cup \left(\bigcup_{k=0}^{N-2} (R(0, 0, \cdot))^{-k} \left(\frac{5}{4}\right) \right),$$

where each (preimage of the) number on the RHS has multiplicity 1, $\frac{3^N+3}{2}$, $\frac{3^{N-k-1}+3}{2}$, and $\frac{3^{N-k-1}-1}{2}$, respectively. Our first theorem provides an explicit description of the magnetic spectra under nonzero (half-)integer fluxes. The relationship between the four magnetic Laplacians is sketched in Figure 2.

Theorem 1 (Magnetic spectra under nonzero (half-)integer fluxes).

$$\sigma(\mathcal{L}_N^{(\frac{1}{2}, \frac{1}{2})}) = \left\{ \frac{1}{2}, \frac{3}{4}, \frac{5}{4}, 2 \right\} \cup \left(R\left(\frac{1}{2}, \frac{1}{2}, \cdot\right) \right)^{-1} \left(\left(\bigcup_{k=0}^{N-2} (R(0, 0, \cdot))^{-k} \left(\frac{3}{4}\right) \right) \cup \left(\bigcup_{k=0}^{N-3} (R(0, 0, \cdot))^{-k} \left(\frac{5}{4}\right) \right) \right),$$

where each (preimage of the) number on the RHS has multiplicity $\frac{3^N+3}{2}$, $\frac{3^{N-1}-1}{2}$, $\frac{3^{N-1}+3}{2}$, 1, $\frac{3^{N-k-2}+3}{2}$, and $\frac{3^{N-k-2}-1}{2}$, respectively.

$$\sigma(\mathcal{L}_N^{(\frac{1}{2}, 0)}) = \left\{ \frac{1}{2}, 1, \frac{5}{4}, \frac{7}{4} \right\} \cup \left(R\left(\frac{1}{2}, 0, \cdot\right) \right)^{-1} \left(\left\{ \frac{3}{4}, \frac{5}{4} \right\} \right) \cup \left(R\left(\frac{1}{2}, 0, \cdot\right) \right)^{-1} \circ \left(R\left(\frac{1}{2}, \frac{1}{2}, \cdot\right) \right)^{-1} \left(\left(\bigcup_{k=0}^{N-3} (R(0, 0, \cdot))^{-k} \left(\frac{3}{4}\right) \right) \cup \left(\bigcup_{k=0}^{N-4} (R(0, 0, \cdot))^{-k} \left(\frac{5}{4}\right) \right) \right),$$

where each (preimage of the) number on the RHS has multiplicity $\frac{3^N+3}{2}$, 1, $\frac{3^{N-1}-1}{2}$, $\frac{3^{N-1}+3}{2}$, $\frac{3^{N-2}-1}{2}$, $\frac{3^{N-2}+3}{2}$, $\frac{3^{N-k-3}+3}{2}$, and $\frac{3^{N-k-3}-1}{2}$, respectively.

$$\sigma(\mathcal{L}_N^{(0, \frac{1}{2})}) = \left\{ \frac{1}{4}, \frac{3}{4}, 1, \frac{3}{2} \right\} \cup \left(R\left(0, \frac{1}{2}, \cdot\right) \right)^{-1} \left(\left\{ \frac{3}{4}, \frac{5}{4} \right\} \right) \cup \left(R\left(0, \frac{1}{2}, \cdot\right) \right)^{-1} \circ \left(R\left(\frac{1}{2}, \frac{1}{2}, \cdot\right) \right)^{-1} \left(\left(\bigcup_{k=0}^{N-3} (R(0, 0, \cdot))^{-k} \left(\frac{3}{4}\right) \right) \cup \left(\bigcup_{k=0}^{N-4} (R(0, 0, \cdot))^{-k} \left(\frac{5}{4}\right) \right) \right),$$

where each (preimage of the) number on the RHS has multiplicity $\frac{3^N+3}{2}$, $\frac{3^{N-1}-1}{2}$, 1, $\frac{3^N+3}{2}$, $\frac{3^{N-2}-1}{2}$, $\frac{3^{N-2}+3}{2}$, $\frac{3^{N-k-3}+3}{2}$, and $\frac{3^{N-k-3}-1}{2}$, respectively.

Observe that each of the 4 spectra above involves the set of backward iterates under $R(0, 0, \cdot)$. Not surprisingly, there is a connection of the (magnetic) spectrum to the Julia set of $R(0, 0, \cdot)$. Recall that the Fatou set $\mathcal{F}(f)$ of a nonconstant holomorphic function f on $\hat{\mathbb{C}} := \mathbb{C} \cup \{\infty\}$ is the domain in which the family of iterates $\{f^n\}_n$ converges uniformly on compacts. The Julia set of f is $\mathcal{J}(f) = \hat{\mathbb{C}} \setminus \mathcal{F}(f)$; by definition it is closed. By [35, Theorem 14.1], the Julia set for any rational map of degree ≥ 2 equals the closure of its set of repelling periodic points. Also, by [35, Corollary 4.13], if z_0 is any point of the Julia set $\mathcal{J}(f)$, then the set of all iterated preimages $\bigcup_{k=0}^{\infty} f^{-k}(z_0)$ is everywhere dense in $\mathcal{J}(f)$.

The polynomial $R(0, 0, \cdot)$ has three fixed points: ∞ (attracting), 0, and 1 (the latter two are repelling). Thus $\{0, 1\} \in \mathcal{J}(R(0, 0, \cdot))$, and $\bigcup_{k=0}^{\infty} (R(0, 0, \cdot))^{-k}(0)$ is everywhere dense in $\mathcal{J}(R(0, 0, \cdot))$. Since $\frac{5}{4} \in R(0, 0, \cdot)^{-1}(0)$, it follows that the closure of $\{0\} \cup \bigcup_{k=0}^{\infty} R(0, 0, \cdot)^{-k}(\frac{5}{4})$ equals $\mathcal{J}(R(0, 0, \cdot))$. Meanwhile, $R(0, 0, \frac{3}{4}) = \frac{3}{2}$ and $(R(0, 0, \cdot))^k(\frac{3}{2}) \rightarrow \infty$ as $k \rightarrow \infty$. So $\frac{3}{2}$ belongs to the Fatou set $(\mathcal{J}(R(0, 0, \cdot)))^c$, and the same goes for the set of all backward iterates $\bigcup_{k=0}^{\infty} (R(0, 0, \cdot))^{-k}(\frac{3}{4})$ by the invariance of the Fatou set under backward/forward iterates. This justifies the decomposition

$$\sigma(\mathcal{L}_{\infty}^{(0, 0)}) = \mathcal{J}(R(0, 0, \cdot)) \cup \left(\bigcup_{k=0}^{\infty} (R(0, 0, \cdot))^{-k} \left(\frac{3}{4}\right) \right) \cup \left\{ \frac{3}{2} \right\}$$

as shown by Teplyaev [42].² In the same paper Teplyaev proved that $\sigma(\mathcal{L}_\infty^{(0,0)})$ is pure point.

Following the above line of reasoning, we express each of the other three magnetic spectra as the union of preimages of the Julia set $\mathcal{J}(R(0,0,\cdot))$ and additional sets.

Corollary 1.2 (Magnetic spectrum on the infinite SG).

$$\begin{aligned}\sigma(\mathcal{L}_\infty^{(\frac{1}{2},\frac{1}{2})}) &= \left(R\left(\frac{1}{2},\frac{1}{2},\cdot\right)\right)^{-1} \left[\mathcal{J}(R(0,0,\cdot)) \cup \left(\bigcup_{k=0}^{\infty} (R(0,0,\cdot))^{-k} \left(\frac{3}{4}\right)\right)\right] \cup \left\{\frac{1}{2}, \frac{5}{4}\right\}, \\ \sigma(\mathcal{L}_\infty^{(\frac{1}{2},0)}) &= \left(R\left(\frac{1}{2},0,\cdot\right)\right)^{-1} \circ \left(R\left(\frac{1}{2},\frac{1}{2},\cdot\right)\right)^{-1} \left[\mathcal{J}(R(0,0,\cdot)) \cup \left(\bigcup_{k=0}^{\infty} (R(0,0,\cdot))^{-k} \left(\frac{3}{4}\right)\right)\right] \\ &\quad \cup \left\{\frac{1}{2}, \frac{7}{4}\right\} \cup \left(R\left(\frac{1}{2},0,\cdot\right)\right)^{-1} \left(\left\{\frac{3}{4}, \frac{5}{4}\right\}\right), \\ \sigma(\mathcal{L}_\infty^{(0,\frac{1}{2})}) &= \left(R\left(0,\frac{1}{2},\cdot\right)\right)^{-1} \circ \left(R\left(\frac{1}{2},\frac{1}{2},\cdot\right)\right)^{-1} \left[\mathcal{J}(R(0,0,\cdot)) \cup \left(\bigcup_{k=0}^{\infty} (R(0,0,\cdot))^{-k} \left(\frac{3}{4}\right)\right)\right] \\ &\quad \cup \left\{\frac{1}{4}, \frac{3}{2}\right\} \cup \left(R\left(0,\frac{1}{2},\cdot\right)\right)^{-1} \left(\left\{\frac{3}{4}, \frac{5}{4}\right\}\right).\end{aligned}$$

In particular, each of the spectra above is pure point.

The situation for non-(half)-integer fluxes is more delicate. At the moment we can hardly say any more than what Theorem 2 below states, but to the best of our knowledge, the result is new.

Theorem 2 (Magnetic spectra under non-(half)-integer fluxes). *Suppose not both of α_N and β_N are in $\{0, \frac{1}{2}\}$. Then*

$$(1.5) \quad \begin{aligned}\sigma\left(\mathcal{L}_N^{(\alpha_N,\beta_N)}\right) &= \left\{\lambda \in \mathbb{R} \setminus \mathcal{E}(\alpha_N,\beta_N) : R(\alpha_N,\beta_N,\lambda) \in \sigma\left(\mathcal{L}_{N-1}^{(\alpha_{N-1},\beta_{N-1})}\right)\right\} \\ &\sqcup \left\{\lambda : \mathcal{D}(\beta_N,\lambda) = 0, \text{mult}\left(\mathcal{L}_N^{(\alpha_N,\beta_N)},\lambda\right) > 0\right\} \sqcup \left\{\begin{array}{ll} \frac{3}{2}, & \text{if } \alpha_N = 0 \\ \frac{1}{2}, & \text{if } \alpha_N = \frac{1}{2} \end{array}\right\},\end{aligned}$$

where

$$\begin{aligned}\mathcal{E}(\alpha,\beta) &= \{\lambda \in \mathbb{R} : \Psi(\alpha,\beta,\lambda) = 0 \text{ or } \mathcal{D}(\beta,\lambda) = 0\}, \\ R(\alpha,\beta,\lambda) &= 1 + \frac{A(\alpha,\beta,\lambda) - 64\mathcal{D}(\beta,\lambda)(1-\lambda)}{16|\Psi(\alpha,\beta,\lambda)|}, \\ A(\alpha,\beta,\lambda) &= 16\lambda^2 - (32 + 4\cos(2\pi\alpha))\lambda + 15 + 4\cos(2\pi\alpha) + \cos(2\pi(\alpha+\beta)), \\ \mathcal{D}(\beta,\lambda) &= -\lambda^3 + 3\lambda^2 - \frac{45}{16}\lambda + \frac{13}{16} - \frac{1}{32}\cos(2\pi\beta), \\ \Psi(\alpha,\beta,\lambda) &= (1-\lambda)^2 - \frac{1}{16} + \frac{1-\lambda}{4}(2e^{-2\pi i\alpha} + e^{-2\pi i(2\alpha+\beta)}) + \frac{1}{16}(e^{-4\pi i\alpha} + 2e^{-2\pi i(\alpha+\beta)}), \\ \theta(\alpha,\beta,\lambda) &= \frac{\arg \Psi(\alpha,\beta,\lambda)}{2\pi} \quad (\arg : \mathbb{C} \rightarrow [0, 2\pi)), \\ \alpha_{N-1} &= \alpha_{\downarrow}(\alpha_N,\beta_N,\lambda) \quad \text{and} \quad \beta_{N-1} = \beta_{\downarrow}(\alpha_N,\beta_N,\lambda), \\ \alpha_{\downarrow}(\alpha,\beta,\lambda) &= 3\alpha + \beta - 3\theta(\alpha,\beta,\lambda) \pmod{1}, \\ \beta_{\downarrow}(\alpha,\beta,\lambda) &= 3\beta + \alpha + 3\theta(\alpha,\beta,\lambda) \pmod{1}.\end{aligned}$$

²For general self-similar Laplacians \mathcal{L}_∞ , we expect that $\sigma(\mathcal{L}_\infty) = \mathcal{J} \cup \mathcal{D}$, where \mathcal{D} is an ‘‘exceptional set’’ which depends sensitively on the graph under study. See [33] for several illustrating examples. An example where $\mathcal{D} = \emptyset$ appears in a one-parameter family of self-similar ‘‘ pq -Laplacians’’ on \mathbb{Z}_+ [9].

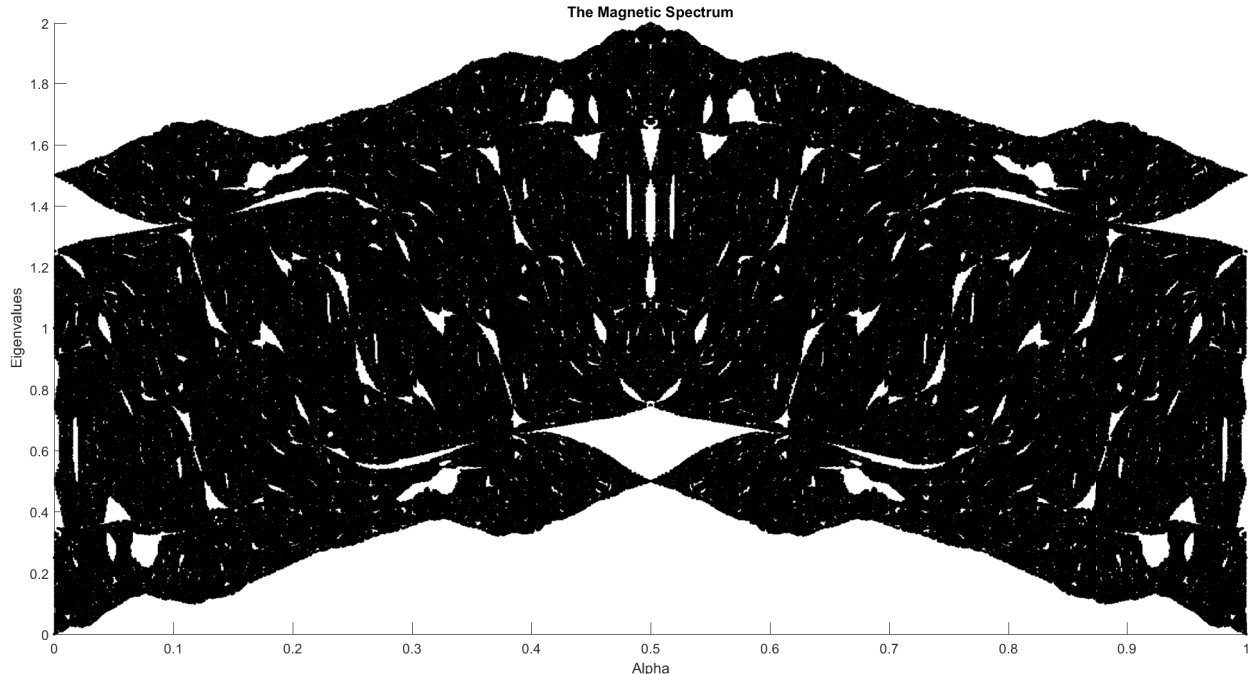


FIGURE 3. The filled Julia set associated with the 3-parameter map $\mathcal{U} : (\alpha, \beta, \lambda) \mapsto (\alpha_{\downarrow}(\alpha, \beta, \lambda), \beta_{\downarrow}(\alpha, \beta, \lambda), R(\alpha, \beta, \lambda))$, with initial condition $(\alpha, \alpha, \lambda)$. We claim that the corresponding Julia set gives the correct approximation of $\sigma(\mathcal{L}_{\infty}^{(\alpha, \alpha)})$. See Appendix A for the MATLAB code used to generate this figure.

On the RHS of (1.5), each element of the first and third set has respective multiplicity

$$\text{mult} \left(\mathcal{L}_{N-1}^{(\alpha_{N-1}, \beta_{N-1})}, R(\alpha_N, \beta_N, \lambda) \right) \quad \text{and} \quad \frac{3^N + 3}{2}.$$

The multiplicity of each element of the second set is given in Proposition 4.5-(G2) and Proposition 4.8-(II.2) below.

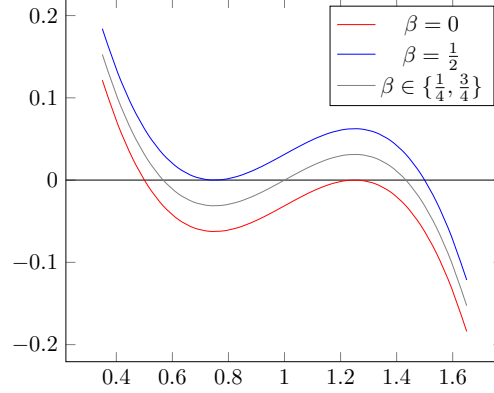
The first set on the RHS of (1.5) is driven by a 3-parameter map

$$(1.6) \quad \mathcal{U} : [0, 1]^2 \times \mathbb{R} \rightarrow [0, 1]^2 \times \mathbb{R}, \quad (\alpha, \beta, \lambda) \mapsto (\alpha_{\downarrow}(\alpha, \beta, \lambda), \beta_{\downarrow}(\alpha, \beta, \lambda), R(\alpha, \beta, \lambda)).$$

Observe the full dependence of the image triple on the domain triple. Unlike Theorem 1, the spectral decimation function $R(\alpha, \beta, \cdot)$ in Theorem 2 is a non-rational function. And given how the flux variables evolve under \mathcal{U} , it is generally not possible to describe the backward iterates of (1.6). The more natural approach is to study forward iterates of (1.6). Figure 3 shows a numerical approximation of the filled Julia set of (1.6) with initial condition $(\alpha, \alpha, \lambda)$. (The Julia set is the boundary of the filled Julia set.)

Observe, however, that in the first set we have excluded points in the **exceptional set for spectral decimation** $\mathcal{E}(\alpha_N, \beta_N)$. Determining which of the exceptional values belong to the spectrum is usually the trickiest part of the spectral decimation program. For this problem we have identified them in the second and third sets on the RHS of (1.5).

The second set includes *at most* the three zeros of the cubic polynomial $\mathcal{D}(\beta, \cdot)$, whose graph is shown in Figure 4. It is easy to verify that $\mathcal{D}(\beta, \cdot)$ does not have a zero of multiplicity 3, and has a double zero only when $\beta \in \{0, \frac{1}{2}\}$ —namely, $\frac{5}{4}$ when $\beta = 0$, and $\frac{3}{4}$ when $\beta = \frac{1}{2}$ —see Lemma 4.2 below. Moreover, since $\mathcal{D}(\beta, \cdot)$ for two different values of β differ by an additive constant, we see that the smallest zero of $\mathcal{D}(\beta, \cdot)$ lies in $[\frac{1}{2}, \frac{3}{4}]$; the middle zero, $[\frac{3}{4}, \frac{5}{4}]$; and the largest zero, $[\frac{5}{4}, \frac{3}{2}]$.

FIGURE 4. The graph of $\mathcal{D}(\beta, \cdot)$.

Identifying which zeros of $\mathcal{D}(\beta_N, \cdot)$ appear in the spectrum is a complicated task, and we defer the case-by-case determination to the latter part of §4.3. That said, we can make the following statements based on the proofs to be presented there.

Proposition 1.3. *Suppose not both of α_N and β_N are in $\{0, \frac{1}{2}\}$.*

(1) *If λ is a simple zero of $\mathcal{D}(\beta_N, \cdot)$ and $\lambda \in \sigma(\mathcal{L}_N^{(\alpha_N, \beta_N)})$, then $R(\alpha_N, \beta_N, \lambda) \in \sigma(\mathcal{L}_{N-1}^{(\alpha_{N-1}, \beta_{N-1})})$.*

(2) *If λ is a double zero of $\mathcal{D}(\beta_N, \cdot)$, then for generic values of α_N , we have that $\lambda \in \sigma(\mathcal{L}_N^{(\alpha_N, \beta_N)})$ whenever $N \geq 3$, with*

$$\text{mult}(\mathcal{L}_N^{(\alpha_N, \beta_N)}, \lambda) = \frac{3^{N-1} - 3}{2} + \text{mult}(\mathcal{L}_{N-1}^{(\alpha_{N-1}, \beta_{N-1})}, R(\alpha_N, \beta_N, \lambda)).$$

The exceptions are when $\alpha_N \in \{\frac{1}{6}, \frac{5}{6}\}$, $\beta_N = 0$ and $\lambda = \frac{5}{4}$, or when $\alpha_N \in \{\frac{1}{3}, \frac{2}{3}\}$, $\beta_N = \frac{1}{2}$ and $\lambda = \frac{3}{4}$, in which case further analysis is required.

Corollary 1.4. *Suppose $\beta_N \notin \{0, \frac{1}{2}\}$. Then*

(1.7)

$$\sigma(\mathcal{L}_N^{(\alpha_N, \beta_N)}) \subseteq \left\{ \lambda \in \mathbb{R} : \Psi(\alpha_N, \beta_N, \lambda) \neq 0, R(\alpha_N, \beta_N, \lambda) \in \sigma(\mathcal{L}_{N-1}^{(\alpha_{N-1}, \beta_{N-1})}) \right\} \sqcup \left\{ \begin{array}{l} \frac{3}{2}, \text{ if } \alpha_N = 0 \\ \frac{1}{2}, \text{ if } \alpha_N = \frac{1}{2} \end{array} \right\}.$$

Moreover, if $\alpha_N, \beta_N \notin \{0, \frac{1}{2}\}$, then

$$(1.8) \quad \left\{ \lambda \in \mathbb{R} : \mathcal{D}(\beta_N, \lambda) \neq 0, R(\alpha_N, \beta_N, \lambda) \in \sigma(\mathcal{L}_{N-1}^{(\alpha_{N-1}, \beta_{N-1})}) \right\} \\ \subseteq \sigma(\mathcal{L}_N^{(\alpha_N, \beta_N)}) \subseteq \left\{ \lambda \in \mathbb{R} : R(\alpha_N, \beta_N, \lambda) \in \sigma(\mathcal{L}_{N-1}^{(\alpha_{N-1}, \beta_{N-1})}) \right\}.$$

1.4. Hofstadter's butterfly meets Sierpinski. Our Theorem 2 and Corollary 1.4 provide the clearest indication that $\sigma(\mathcal{L}_\infty^{(\alpha, \beta)})$ is essentially determined by the Julia set of the 3-parameter map \mathcal{U} (1.6). The second containment in (1.8) states that for *generic* fluxes $\alpha_N, \beta_N \notin \{0, \frac{1}{2}\}$, $\lambda \in \sigma(\mathcal{L}_N^{(\alpha_N, \beta_N)})$ implies $R(\alpha_N, \beta_N, \lambda) \in \sigma(\mathcal{L}_{N-1}^{(\alpha_{N-1}, \beta_{N-1})})$. Iterating this implication inductively on N , using the invariance of the Julia set under forward iterates, and applying the fact that the spectrum is a compact subset of \mathbb{C} , we deduce that

$$\bigcup_{(\alpha, \beta) \notin \{0, \frac{1}{2}\}^2} \sigma(\mathcal{L}_\infty^{(\alpha, \beta)}) \subseteq \mathcal{J}(\mathcal{U}).$$

While we do not resolve the reverse direction in this paper, we expect that for any $(\alpha, \beta) \in [0, 1]^2$, the difference between $\sigma(\mathcal{L}_\infty^{(\alpha, \beta)})$ and the restriction of $\mathcal{J}(\mathcal{U})$ to $\{(\alpha, \beta)\} \times \mathbb{R}$ is a set of small cardinality.

Figure 3 shows the filled Julia set of \mathcal{U} when $\alpha = \beta$. It is our main contention is that this is the correct analog of Hofstadter's butterfly on SG under uniform magnetic field (for the original on \mathbb{Z}^2 see [22]).

At least three versions of the “ SG butterfly” have appeared in the previous literature. We think that [4, Figure 2] and [44], which appears to result from computations on a finite approximating graph G_N , came closest to our Figure 3. Even earlier, the filled Julia set of the 2-parameter map $(\alpha, \lambda) \mapsto (4\alpha, R(\alpha, \alpha, \lambda))$ was presented in [18, Figure 2], which we reproduce from a MATLAB code as Figure 5. The authors of [18] claimed that this 2-parameter map produce a good approximation of $\sigma(\mathcal{L}_\infty^{(\alpha, \alpha)})$. In the same paper they also provided data from superconductivity measurements showing good agreement between theory and experiment.

Upon comparing Figure 3 and Figure 5, especially the bottom of (ground state), and the gaps in, the filled Julia sets, we can safely conclude that this is not the case. In fact, Figure 5 produces the correct approximation of $\sigma(\mathcal{L}_\infty^{(\alpha, \alpha)})$ only when $\alpha \in \{0, \frac{1}{2}\}$, the reason being that $\mathbb{R} \ni \lambda \mapsto \Psi(\alpha, \alpha, \lambda)$ is strictly \mathbb{R} -valued at these flux values. Once $\alpha \notin \{0, \frac{1}{2}\}$, $\mathbb{R} \ni \lambda \mapsto \Psi(\alpha, \alpha, \lambda)$ is in general \mathbb{C} -valued, and its argument $\theta = \arg \Psi$ must be taken into account when deducing the magnetic fluxes.

Here is a take-away message (*cf.* Proposition 2.3 below): If the flux through every smallest upright and downright triangle equals α , then upon decimation, it is *false* that the flux through a next smallest upright (or downright) triangle equal 4α , despite the fact that the flux through a rhombus (formed by adjoining an upright triangle to a downright one) always equals 8α . More importantly, the post-decimation fluxes through each triangle depend on the spectral parameter λ .

Another new aspect of our spectral decimation analysis is that the function $R(\alpha, \beta, \cdot)$ is generally not rational, due to the appearance of $|\Psi(\alpha, \beta, \cdot)|$ in the denominator. All previous mathematical works on spectral decimation [3, 5, 9, 17, 33, 39, 40, 42] involve R rational. While it may seem an unavoidable nuisance to deal with non-rational functions, we nevertheless can carry out spectral decimation after applying some care.

1.5. Magnetic Laplacian determinants and cycle-rooted spanning forests. Using Theorem 1 we can compute the magnetic Laplacian determinant in the case of (half-)integer fluxes. Recall that the determinant \det is the product of all eigenvalues. If 0 is an eigenvalue, then we define \det' to be the product of all nonzero eigenvalues.

The classic Kirchhoff's **matrix-tree theorem** states that on a finite graph G , the number of spanning trees $\tau(G)$ on G equals $\frac{1}{|V(G)|} \det'(\Delta_G)$, or equivalently, the cofactor of Δ_G obtained by removing any one row and any one column. Since we use the probabilistic Laplacian $\mathcal{L}_G = D_G^{-1} \Delta_G$, it is useful to know that

$$(1.9) \quad \tau(G) = \kappa(G) \det'(\mathcal{L}_G), \quad \text{where } \kappa(G) = \frac{\left(\prod_{v \in V(G)} \deg(v) \right)}{\left(\sum_{v \in V(G)} \deg(v) \right)}.$$

This follows from matching the coefficient of t in the identity $\det(\mathcal{L}_G + tI) = (\det D_G)^{-1} \det(\Delta_G + tD_G)$ using the cofactor expansion, and the aforementioned matrix-tree theorem.

Enumeration of spanning trees on SG has already been studied. Set

$$\kappa(G_N) := \frac{\left(\prod_{v \in V_N} \deg(v) \right)}{\left(\sum_{v \in V_N} \deg(v) \right)} = \frac{1}{2} \frac{2^{3^{N+1}}}{3^{N+1}}.$$

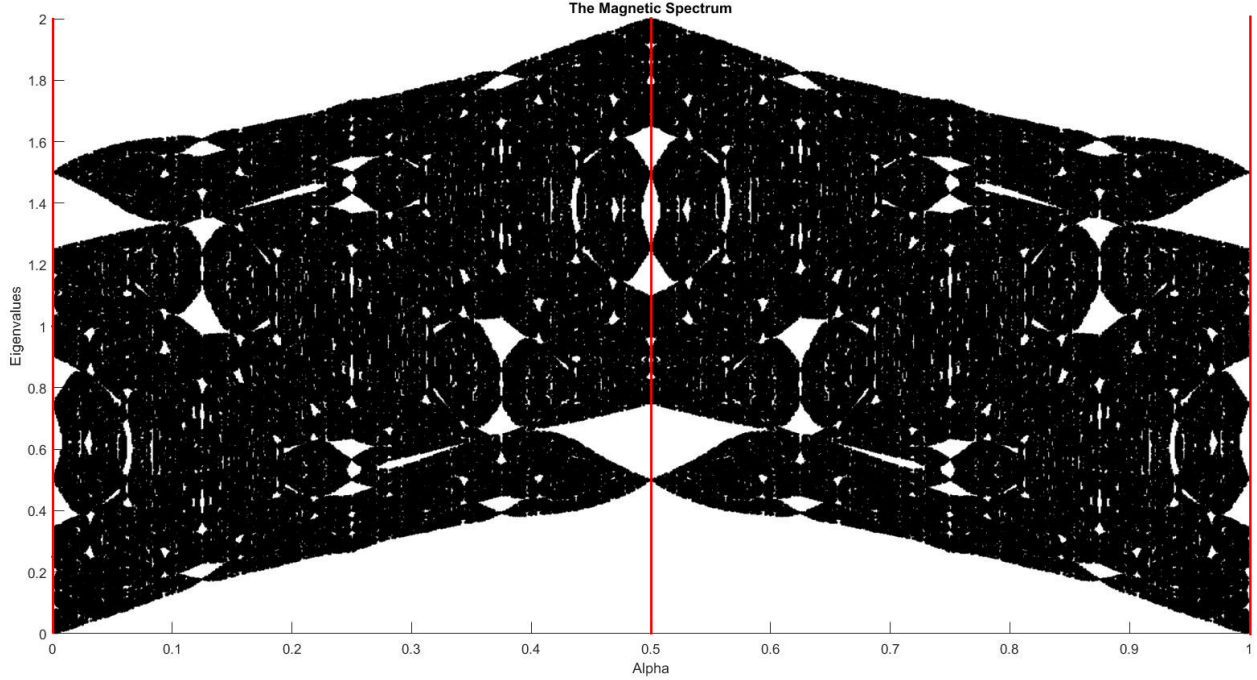


FIGURE 5. The filled Julia set associated with the 2-parameter map $(\alpha, \lambda) \mapsto (4\alpha, R(\alpha, \alpha, \lambda))$, as was used to generate [18, Figure 2]. The corresponding Julia set gives the correct approximation of $\sigma(\mathcal{L}_\infty^{(\alpha, \alpha)})$ only when $\alpha \in \{0, \frac{1}{2}\}$ (red).

It was shown in [7, 43] via a combinatorial approach, and in [2] via spectral decimation and (1.9), that

$$(1.10) \quad \tau(G_N) = \kappa(G_N) \det'(\mathcal{L}_N^{(0,0)}) = 2^{\frac{3^N}{2} - \frac{1}{2}} \cdot 3^{\frac{3^{N+1}}{4} + \frac{N+1}{2} + \frac{1}{4}} \cdot 5^{\frac{3^N}{4} - \frac{N}{2} - \frac{1}{4}}.$$

By placing a uniform probability measure on the set of all spanning trees, *a.k.a.* **uniform spanning trees (USTs)**, we obtain a determinantal point process on the edge set with kernel $K = dGd^*$, where G is the Green's function for random walks. The matrix K is known as the *transfer impedance matrix* [6]. For more properties of USTs on SG and scaling limit questions, see [41].

Our next theorem gives the determinant formulae for the three magnetic Laplacians. The normalization prefactor $\kappa(G_N)$ is used for the same reason as described in (1.9) above.

Theorem 3 (Determinant of the magnetic Laplacian under nonzero (half-)integer fluxes).

$$(1.11) \quad \det(\mathcal{L}_N^{(\frac{1}{2}, \frac{1}{2})}) = \frac{1}{\kappa(G_N)} \cdot 2^{\frac{3^N}{2} + \frac{3}{2}} \cdot 3^{\frac{3^{N-1}}{2} - N - \frac{3}{2}} \cdot 5^{\frac{3^{N-1}}{2} + \frac{3}{2}} \\ \times \left[\prod_{k=0}^{N-2} \left(H(k) + \frac{1}{2} \right)^{\frac{3^{N-k-2} + 3}{2}} \right] \left[\prod_{k=0}^{N-3} \left(H(k) + \frac{5}{2} \right)^{\frac{3^{N-k-2} - 1}{2}} \right],$$

where $H(0) = 26.5$, and for $k \geq 1$, $H(k) = [H(k-1)]^2 - \frac{15}{4}$.

$$(1.12) \quad \det(\mathcal{L}_N^{(\frac{1}{2}, 0)}) = \frac{1}{\kappa(G_N)} \cdot 2^{\frac{13}{6} 3^{N-1} - \frac{5}{2}} \cdot 3^{\frac{3^{N-2}}{2} - N - \frac{3}{2}} \cdot 5^{\frac{5}{2} 3^{N-2} - 1} \cdot 7^{\frac{3^{N-1}}{2} + \frac{3}{2}} \cdot 17^{\frac{3^{N-2}}{2} + \frac{3}{2}} \\ \times \left[\prod_{k=0}^{N-3} \left(\tilde{H}(k) + \frac{1}{2} \right)^{\frac{3^{N-k-3} + 3}{2}} \right] \left[\prod_{k=0}^{N-4} \left(\tilde{H}(k) + \frac{5}{2} \right)^{\frac{3^{N-k-3} - 1}{2}} \right],$$

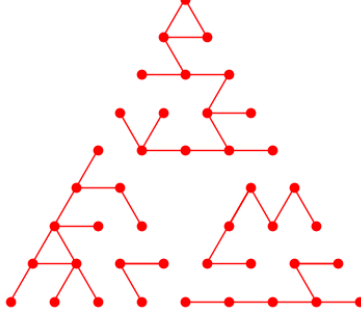


FIGURE 6. An instance of a cycle-rooted spanning forest on the level-3 gasket graph, generated via the sampling algorithm of Kassel and Kenyon [24, p. 938] based on loop-erased random walks. In this case a loop γ is retained with fixed probability $p \in (0, 1)$ for all γ , and a loop of length 2 is allowed, which differs from the setting considered in this paper. Image courtesy of Quan Vu.

where $\tilde{H}(0) = 302.5$, and for $k \geq 1$, $\tilde{H}(k) = [\tilde{H}(k-1)]^2 - \frac{15}{4}$.

$$(1.13) \quad \det(\mathcal{L}_N^{(0, \frac{1}{2})}) = \frac{1}{\kappa(G_N)} \cdot 2^{\frac{13}{6}3^{N-1} - \frac{5}{2}} \cdot 3^{\frac{7}{3}3^{N-1} - N + 3} \cdot 7^{\frac{3^{N-2}}{2} - \frac{1}{2}} \\ \times \left[\prod_{k=0}^{N-3} \left(\hat{H}(k) + \frac{1}{2} \right)^{\frac{3^{N-k-3} + 3}{2}} \right] \left[\prod_{k=0}^{N-4} \left(\hat{H}(k) + \frac{5}{2} \right)^{\frac{3^{N-k-3} - 1}{2}} \right],$$

where $\hat{H}(0) = 86.5$, and for $k \geq 1$, $\hat{H}(k) = [\hat{H}(k-1)]^2 - \frac{15}{4}$.

There is an analog of the matrix-tree theorem for the magnetic Laplacian determinant, established by Forman [14] and Kenyon [27]. To explain this, we recall some definitions from [24, 27], and refer the reader there for more details. A cycle-rooted tree, or *unicycle*, is a tree plus an extra edge to form a single cycle. A **cycle-rooted spanning forest (CRSF)** is a spanning forest whose connected components are unicycles. (See Figure 6 for an illustration.)

Fix a connected graph G , a directed edge conductance function \mathbf{c} on $\{\pm E\}$, and a line bundle connection ω on G . We would like to assign a probability measure on the set of all CRSFs thereon. Declare that each oriented CRSF (OCRSF) occurs with probability proportional to $\prod_{e \in \text{bushes}} \mathbf{c}(e) \prod_{\gamma \in \text{cycles}} \mathbf{C}(\gamma)(1 - \omega(\gamma))$, where the first product runs over all edges in the bushes (that is, not in the cycles), the second product runs over all cycles, $\mathbf{C}(\gamma)$ is the product of the semiconductances along γ , and $\omega(\gamma)$ is the holonomy of γ . The following says that $\det(\mathcal{L}_{(G, \mathbf{c})}^\omega)$ gives the partition function which makes the said CRSF measure a probability measure.

Proposition 1.5 (Matrix-CRSF theorem [27, Theorem 6]). *Let $\mathcal{L}_{(G, \mathbf{c})}^\omega$ be the line bundle Laplacian (1.1). Then*

$$(1.14) \quad \det(\mathcal{L}_{(G, \mathbf{c})}^\omega) = \sum_{\text{OCRSFs}} \prod_{e \in \text{bushes}} \mathbf{c}(e) \prod_{\gamma \in \text{cycles}} \mathbf{C}(\gamma)(1 - \omega(\gamma)).$$

Remark 1.6. Note that if $\mathbf{c}_{xy} = \mathbf{c}_{yx}$ for all $xy \in E$, then (1.14) may be written as a sum over unoriented CRSFs:

$$\det(\mathcal{L}_{(G, \mathbf{c})}^\omega) = \sum_{\text{CRSFs}} \prod_e \mathbf{c}(e) \prod_{\gamma \in \text{cycles}} \left(2 - \omega(\gamma) - \frac{1}{\omega(\gamma)} \right),$$

where the first product is over all edges in the CRSF [27, Theorem 5].

Like the UST process, the CRSF process is also a determinantal point process on the edge set, with kernel $d \left(\mathcal{L}_{(G,c)}^\omega \right)^{-1} d^*$ [27, Theorem 2]. In [24, p. 938] Kassel and Kenyon gave an elementary sampling algorithm for CRSFs based on loop-erased random walks (LERWs) and cycle popping à la Wilson [46], valid for any holonomy $e^{2\pi i \gamma}$ with $\gamma \in [-\frac{1}{4}, \frac{1}{4}]$. Using this algorithm, in combination with facts from LERWs and Brownian loop soups [29], they proved convergence to a loop measure on an oriented Riemannian surface from the CRSF processes on discretizations of the said surface [24, Theorem 20].

1.6. Asymptotic complexity and the loop soup entropy. It is an open problem to study local properties and scaling limits of the CRSF measures on SG . That said, we can use our results on the magnetic Laplacian determinant (Theorem 3) to quantify the **asymptotic complexity** of the CRSF measures.

Let G_∞ be an infinite connected graph which can be exhausted by a sequence of finite connected graphs $\{G_N\}_N$. We define the asymptotic complexity associated with $\mathcal{L}_\infty^\omega$ on G_∞ by

$$(1.15) \quad \mathfrak{h}(G_\infty, \mathcal{L}_\infty^\omega) := \lim_{N \rightarrow \infty} \frac{\log(\kappa(G_N) \det'(\mathcal{L}_N^\omega))}{|V_N|}$$

provided that the RHS limit exists.

The formula (1.15) is classical for the graph Laplacian, *i.e.*, for the enumeration of spanning trees. In [30, 31] R. Lyons introduced the notion of **tree entropy** on G_∞ , gave several equivalent formulations—one of which is the logarithm of a Fuglede-Kadison determinant [16] of the “continuum” Laplacian—and proved that his tree entropy equals (1.15).^{3,4} For old and new results on tree entropy for various graphs, see [2, 10, 30, 31]. As an example, from (1.10) it is direct to show that the tree entropy on SG equals (*cf.* [2, Corollary 5.2])⁵

$$(1.16) \quad \mathfrak{h}(SG, \mathcal{L}_\infty^{(0,0)}) = \frac{\log 2}{3} + \frac{\log 3}{2} + \frac{\log 5}{6}.$$

Our next result gives the asymptotic complexity of each of the three magnetic Laplacians on SG .

³If G_∞ has bounded degree, the proof in [30, Theorem 4.1] suffices. If G_∞ has unbounded degree, then the proof proceeds according to [31, Theorem 3.1], which is based on von Neumann algebras.

⁴The limit of USTs on an infinite connected graph is a spanning forest. On \mathbb{Z}^d the limit is a tree iff $d \leq 4$ [36].

⁵In (1.16) the weights associated to the logarithmic factors are probability weights. This is merely coincidental: for the graphical $(d-1)$ -dimensional Sierpinski simplex, the tree entropy equals $\frac{d-2}{d} \log 2 + \frac{d-2}{d-1} \log d + \frac{d-2}{d(d-1)} \log(d+2)$ [10, Corollary 4.1]. We do not know how to explain this phenomenon in general. Nevertheless, it served as a useful “sanity check” for us when proving Corollary 1.7.

More generally, the tree entropy of a unimodular random infinite connected weighted graph can take values in $[-\infty, \infty)$. For an example of a unimodular random graph with tree entropy equal to $-\infty$, see [31, pp. 308-309].

Corollary 1.7 (Asymptotic complexity of the CRSF measures).

$$\begin{aligned}
\mathfrak{h}(SG, \mathcal{L}_\infty^{(\frac{1}{2}, \frac{1}{2})}) &= \frac{\log 2}{3} + \frac{\log 3}{9} + \frac{\log 5}{9} \\
&+ \frac{2}{9} \cdot \frac{1}{3} \sum_{k=0}^{\infty} \left(\frac{2}{3}\right)^k \frac{\log(H(k) + \frac{1}{2})}{2^{k+1}} + \frac{2}{9} \cdot \frac{1}{3} \sum_{k=0}^{\infty} \left(\frac{2}{3}\right)^k \frac{\log(H(k) + \frac{5}{2})}{2^{k+1}}, \\
\mathfrak{h}(SG, \mathcal{L}_\infty^{(\frac{1}{2}, 0)}) &= \frac{13}{27} \log 2 + \frac{\log 3}{27} + \frac{5}{27} \log 5 + \frac{\log 7}{9} + \frac{\log 17}{27} \\
&+ \frac{2}{27} \cdot \frac{1}{3} \sum_{k=0}^{\infty} \left(\frac{2}{3}\right)^k \frac{\log(\tilde{H}(k) + \frac{1}{2})}{2^{k+1}} + \frac{2}{27} \cdot \frac{1}{3} \sum_{k=0}^{\infty} \left(\frac{2}{3}\right)^k \frac{\log(\tilde{H}(k) + \frac{5}{2})}{2^{k+1}}, \\
\mathfrak{h}(SG, \mathcal{L}_\infty^{(0, \frac{1}{2})}) &= \frac{13}{27} \log 2 + \frac{14}{27} \log 3 + \frac{\log 7}{27} \\
&+ \frac{2}{27} \cdot \frac{1}{3} \sum_{k=0}^{\infty} \left(\frac{2}{3}\right)^k \frac{\log(\hat{H}(k) + \frac{1}{2})}{2^{k+1}} + \frac{2}{27} \cdot \frac{1}{3} \sum_{k=0}^{\infty} \left(\frac{2}{3}\right)^k \frac{\log(\hat{H}(k) + \frac{5}{2})}{2^{k+1}},
\end{aligned}$$

where $H(k)$, $\tilde{H}(k)$, and $\hat{H}(k)$ were defined in Theorem 3.

It can be checked numerically that each of the three asymptotic complexities in Corollary 1.7 is larger than the tree entropy (1.16).

The CRSF asymptotic complexity has a probabilistic interpretation which we explain now. Let G be a finite connected graph, and B be a subset of $V(G)$ which we declare as the boundary set. An **essential CRSF** on (G, B) is a spanning subgraph of G , each of whose connected components is either a unicycle not containing any vertex in B , or a tree containing a unique vertex in B . The corresponding matrix-CRSF theorem is the analog of Proposition 1.5, where on the LHS the Laplacian carries Dirichlet boundary condition on B ,

$$(1.17) \quad (\mathcal{L}_{(G, B, \mathbf{c})}^\omega u)(x) = \sum_{y \sim x} \mathbf{c}_{xy} (u(x) - \omega_{xy} u(y)), \quad u \in \mathbb{C}^{V \setminus B},$$

the sum being over the neighbors y of x (y can be in B); and on the RHS the sum runs over all oriented essential CRSFs. Let us denote the essential CRSF measure on $(G, B, \mathbf{c}, \omega)$ by $\mathbb{P}_{(G, B, \mathbf{c})}^\omega$. Since the conductance will not play a role in the remainder of this discussion, we will suppress the subscript \mathbf{c} in what follows.

Let $\mathcal{L}_{(G, B)}^{\text{Id}}$ be the magnetic Laplacian on (G, B) with the trivial connection. It is easy to see from the definition of the CRSF measure that

$$(1.18) \quad \mathbb{P}_{(G, B)}^\omega[\text{no loops}] = \frac{\det(\mathcal{L}_{(G, B)}^{\text{Id}})}{\det(\mathcal{L}_{(G, B)}^\omega)}.$$

We multiply both sides of the RHS fraction by $\kappa(G)$ (1.9), take the logarithm on the equation, and then divide by $|V(G)|$ to get

$$(1.19) \quad \frac{1}{|V(G)|} \log \mathbb{P}_{(G, B)}^\omega[\text{no loops}] = \frac{\log(\kappa(G) \det(\mathcal{L}_{(G, B)}^{\text{Id}}))}{|V(G)|} - \frac{\log(\kappa(G) \det(\mathcal{L}_{(G, B)}^\omega))}{|V(G)|}.$$

Suppose we have an increasing sequence of graphs with boundary $((G_N, B_N))_N$ tending to G_∞ with $\frac{|B_N|}{|V(G_N)|} \rightarrow 0$. Furthermore, suppose that the essential tree entropy and the essential CRSF asymptotic complexity exist. Then (1.19) says that the difference of the two asymptotic complexities gives the rate of exponential decay in the probability of observing no loops under $\mathbb{P}_{(G_N, B_N)}^\omega$ as

$N \rightarrow \infty$. In light of this identity and the notion of tree entropy, we propose to introduce the **loop soup entropy**⁶ on (G_∞, ω) , a universal object which depends only on the connection ω :

$$(1.20) \quad \mathfrak{h}_{\text{loop}}(G_\infty, \mathcal{L}_\infty^\omega) := \mathfrak{h}(G_\infty, \mathcal{L}_\infty^\omega) - \mathfrak{h}(G_\infty, \mathcal{L}_\infty^{\text{Id}}).$$

Then from (1.19) we obtain

$$(1.21) \quad \lim_{N \rightarrow \infty} \frac{1}{|V(G_N)|} \log \mathbb{P}_{(G_N, B_N)}^\omega [\text{no loops}] = -\mathfrak{h}_{\text{loop}}(G_\infty, \mathcal{L}_\infty^\omega).$$

This can be seen as a quantitative version of [24, Theorem 7], which can then be applied to a wide variety of infinite connected graphs with boundary, including, but not limited to, compact Riemannian surfaces.

Indeed the final result of this paper is to provide meaning to the loop soup entropy on SG . Recall that in defining the magnetic Laplacians on SG , we did not impose any boundary condition. That said, we can add a single point b and connect it to o by an edge of conductance c , and regard $G_N \cup \{b\}$ as the graph with boundary $B = \{b\}$. This one-point modification introduces correction terms on the RHS of (1.21) that vanish as $c \downarrow 0$ for every N . As a result, in the case of nonzero (half-)integer fluxes, we can apply (1.16) and Corollary 1.7 to obtain the loop soup entropy on SG , which carries the probabilistic interpretation (1.21).

Corollary 1.8 (Loop soup entropy on SG). *Let $\mathbb{P}_{N,c}^{(\alpha,\beta)}$ be the essential CRSF measure on $G_N \cup \{b\}$ where an edge of conductance c connects o and b , and with fluxes α and β as before. For $(\alpha, \beta) \in \{(0, \frac{1}{2}), (\frac{1}{2}, 0), (\frac{1}{2}, \frac{1}{2})\}$,*

$$(1.22) \quad \lim_{N \rightarrow \infty} \lim_{c \downarrow 0} \frac{1}{|V_N|} \log \mathbb{P}_{N,c}^{(\alpha,\beta)} [\text{no loops}] = -\mathfrak{h}_{\text{loop}}(SG, \mathcal{L}_\infty^{(\alpha,\beta)}),$$

where $\mathfrak{h}_{\text{loop}}(SG, \mathcal{L}_\infty^{(\alpha,\beta)}) = \mathfrak{h}(SG, \mathcal{L}_\infty^{(\alpha,\beta)}) - \mathfrak{h}(SG, \mathcal{L}_\infty^{(0,0)})$, and each term on the RHS was defined in Corollary 1.7 and (1.16), respectively.

1.7. Open questions. We end this introductory section with several open questions.

1.7.1. Spectral aspects. In the case of (half-)integer fluxes, there are two issues which we have not addressed, but whose answers can be deduced from the methods used in this paper and the references indicated below. One, show that the magnetic Laplacian eigenfunctions with finite support are complete, using the methods of [42]. (See also [37] which considered Dirichlet boundary condition at the origin.) Two, obtain zeta functions associated to \mathcal{L}_N^ω using the methods of [10].⁷ It is, however, unclear if these questions can be addressed in the case of non-(half-)integer fluxes.

1.7.2. Point processes induced by Laplacian determinants. There are many unexplored questions concerning CRSF measures on self-similar graphs or Cayley graphs of self-similar groups, in particular the local statistics of the unicycles. On SG we surmise that the cut point structure of SG will result in the predominance of short unicycles. Numerical simulations suggest a hierarchical structure in the number of connected components, as well as in the distribution of unicycle lengths, in the sampled CRSFs. This reflects the spatial self-similarity of SG .

Open Question 1. Characterize the (unique) limit point(s) of the sequence of CRSF measures on self-similar graphs.

On a broader note, building upon the main result of Lyons [31, Theorem 3.1], we wish to pose the following question.

Open Question 2. Is there a Fuglede-Kadison determinant that corresponds to the CRSF asymptotic complexity (or the loop soup entropy) on a unimodular random graph?

⁶The term ‘‘loop entropy’’ has already been used in the study of polymers such as DNAs and proteins.

⁷See [15] for the derivation of the zeta function associated to the line bundle Laplacian on the discrete tori $(\mathbb{Z}/N\mathbb{Z})^d$.

Finally we believe that studying the magnetic Laplacian and the induced CRSF loop measures may shed light on properties of the abelian sandpile model under stationarity. Recall the well-known bijective correspondence between the sandpile group and spanning trees [32]. Kassel and Kenyon [24, §6, Question 9] have asked if the loop measures may lead to a better understanding of waves of sandpile avalanches. On SG we have two specific questions: to prove that the sandpile avalanches exhibit a power law modulated by log-periodic oscillations, which was numerically observed in [11, 12, 28];⁸ and to find the sandpile height distributions (or their moments, such as the sandpile density).⁹

1.7.3. *Experimental realization of the butterfly.* Last but not least, thanks to advances in scanning electron microscopy and nanoscale engineering over the past 3 decades, there has been impressive progress on measurements of electronic band structures in various (meta)materials, including finite approximations of SG . The most recent work we are aware of is [26]. It would be satisfying to see that our version of the butterfly (Figure 3) “come alive” via a laboratory experiment.

Organization for the rest of the paper. In §2 we demonstrate the spectral self-similarity of the magnetic Laplacian on SG , furnished with all the necessary computations. We then systematically discuss the general mechanics of spectral decimation in §3. This section lays the technical groundwork from which we solve the magnetic spectrum on SG in §4, proving Theorems 1 and 2, Proposition 1.3, and Corollary 1.4. Formulae for the magnetic Laplacian determinants (Theorem 3) and the CRSF asymptotic complexity (Corollary 1.7) are proved in §5.

2. SPECTRAL SELF-SIMILARITY OF THE MAGNETIC LAPLACIAN

2.1. **Schur complement computation.** Let $G_N = (V_N, E_N)$ be the level- N pre-Sierpinski gasket graph. Following (1.4), the magnetic Laplacian \mathcal{L}_N^ω on G_N endowed with $U(1)$ connection ω can be represented in the standard basis by the $|V_N|$ -by- $|V_N|$ matrix

$$(2.1) \quad \mathcal{L}_N^\omega(x, y) = \begin{cases} 1, & \text{if } x = y, \\ -\frac{1}{2}\omega_{xy}, & \text{if } x \in V_0, y \sim x, \\ -\frac{1}{4}\omega_{xy}, & \text{if } x \in V_N \setminus V_0, y \sim x, \\ 0, & \text{else.} \end{cases}$$

Recall that \mathcal{L}_N^ω is self-adjoint on $L^2(V_N, \deg_{G_N})$.

We express the resolvent in block matrix form

$$(2.2) \quad \mathcal{L}_N^\omega - \lambda I = \begin{bmatrix} A - \lambda I & B \\ C & D - \lambda I \end{bmatrix}, \quad \lambda \in \mathbb{C},$$

where the rows and columns are arranged such that

$$\begin{aligned} A &: \ell(V_{N-1}) \rightarrow \ell(V_{N-1}), & B &: \ell(V_N \setminus V_{N-1}) \rightarrow \ell(V_{N-1}), \\ C &: \ell(V_{N-1}) \rightarrow \ell(V_N \setminus V_{N-1}), & D &: \ell(V_N \setminus V_{N-1}) \rightarrow \ell(V_N \setminus V_{N-1}), \end{aligned}$$

where I is the identity matrix of an appropriate size, and $\ell(S) = \mathbb{C}^S$.

Assuming that $D - \lambda I$ is invertible for the moment, we define the **Schur complement** of $\mathcal{L}_N^\omega - \lambda I$ with respect to the minor $D - \lambda I$ as

$$(2.3) \quad S_N^\omega(\lambda) := (A - \lambda I) - B(D - \lambda I)^{-1}C,$$

⁸A power law modulated by log-periodic oscillations was proved for the growth of deterministic single-source abelian sandpile on SG [8].

⁹See [34, Chapter 5] for the proof of sandpile height distributions on the Hanoi tower graphs, a variant of SG . A nice exposition of the connection between sandpile density and the looping rate on periodic planar graphs is [25].

which acts on $\ell(V_{N-1})$. To find the entries of $S_N^\omega(\lambda)$, we label the vertices in V_{N-1} by a_i , and vertices in $V_N \setminus V_{N-1}$ by b_i . Then for $a_i, a_j \in V_{N-1}$ we have

$$(2.4) \quad S_N^\omega(\lambda)(a_i, a_j) = (A - \lambda I)(a_i, a_j) - \sum_{b_k, b_l \in V_N \setminus V_{N-1}} B(a_i, b_k)(D - \lambda I)^{-1}(b_k, b_l)C(b_l, a_j).$$

Recall (2.1). Observe that $(A - \lambda I)(a_i, a_j) = (1 - \lambda)\delta_{a_i a_j}$; $B(a_i, b_k) = -\frac{1}{2}\omega_{a_i b_k}$ if $a_i \in V_0$ and $a_i \sim b_k$, $-\frac{1}{4}\omega_{a_i b_k}$ if $a_i \in V_N \setminus V_0$ and $a_i \sim b_k$, and 0 otherwise; $C(b_l, a_j) = -\frac{1}{4}\omega_{b_l a_j}$ if $b_l \sim a_j$, and 0 otherwise; and $(D - \lambda I)^{-1}$ is zero whenever $b_k \not\sim b_l$. By the nested structure of SG , $(D - \lambda I)^{-1}$ is a block diagonal matrix consisting of 3-by-3 Hermitian matrices, each of which is supported on the inner vertices of a level- $(N - 1)$ cell, and has the same structure. To be concrete, we denote the cell by Λ , and its three inner vertices by b_0, b_1, b_2 . Then

$$(2.5) \quad (D - \lambda I)|_\Lambda(b_i, b_j) = \begin{cases} 1 - \lambda, & \text{if } b_i = b_j, \\ -\frac{1}{4}\omega_{b_i b_j}, & \text{if } b_i \neq b_j. \end{cases}$$

Using Cramer's formula for the matrix inverse, we get

$$(2.6) \quad (D - \lambda I)|_\Lambda^{-1}(b_i, b_j) = \frac{1}{\det((D - \lambda I)|_\Lambda)} \text{adj}((D - \lambda I)|_\Lambda)$$

where

$$(2.7) \quad \det((D - \lambda I)|_\Lambda) = (1 - \lambda)^3 - \frac{3}{16}(1 - \lambda) - \frac{1}{32}\text{Re}(\omega_{b_0 b_1}\omega_{b_1 b_2}\omega_{b_2 b_0}),$$

$$(2.8) \quad \text{adj}((D - \lambda I)|_\Lambda)(b_i, b_i) = (1 - \lambda)^2 - \frac{1}{16}, \quad i \in \{0, 1, 2\},$$

$$(2.9) \quad \text{adj}((D - \lambda I)|_\Lambda)(b_i, b_j) = \frac{1}{4}(1 - \lambda)\omega_{b_i b_j} + \frac{1}{16}\omega_{b_i b_k}\omega_{b_k b_j}, \quad \text{if } i \neq j$$

and $k = k(i, j)$ is the third index in $\{0, 1, 2\} \setminus \{i, j\}$.

In light of the difference between the diagonal and off-diagonal entries of the adjugate matrix, (2.8) and (2.9), we shall rewrite the second term on the RHS of (2.4) by splitting the case $b_l = b_k$ and the case $b_l \neq b_k$; namely, if $a_i \in V_N \setminus V_0$, we have

$$(2.10) \quad \begin{aligned} & \sum_{b_k, b_l} B(a_i, b_k)(D - \lambda I)^{-1}(b_k, b_l)C(b_l, a_j) \\ &= \frac{1}{16} \sum_{b_k \sim \{a_i, a_j\}} \frac{1}{\det((D - \lambda I)|_{\Lambda(b_k)})} \left((1 - \lambda)^2 - \frac{1}{16} \right) \omega_{a_i b_k} \omega_{b_k a_j} \\ & \quad + \frac{1}{16} \sum_{b_k \sim a_i} \sum_{\substack{b_l \sim a_j \\ b_l \neq b_k}} \frac{1}{\det((D - \lambda I)|_{\Lambda(b_k, b_l)})} \omega_{a_i b_k} \left(\frac{1}{4}(1 - \lambda)\omega_{b_k b_l} + \frac{1}{16}\omega_{b_k b_m}\omega_{b_m b_l} \right) \omega_{b_l a_j}, \end{aligned}$$

where $\Lambda(b_1, b_2, \dots)$ denotes the level- $(N - 1)$ cell which contains the vertices b_1, b_2, \dots , and $\{b_k, b_l, b_m\} \subset V_N \setminus V_{N-1}$ form the 3 inner vertices of $\Lambda(b_k, b_l)$. If $a_i \in V_0$, replace the prefactor $\frac{1}{16}$ in the formula (2.10) by $\frac{1}{8}$.

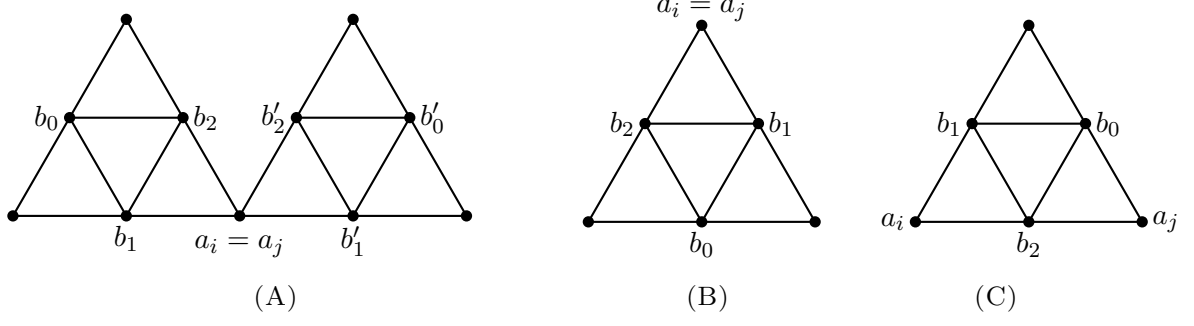


FIGURE 7. The unit cells for diagrammatic analysis used in §2.2.

If $\underline{a_i = a_j} \in V_N \setminus V_0$: We have

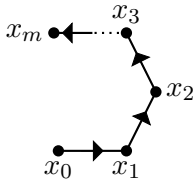
$$\begin{aligned}
 & \sum_{b_k, b_l} B(a_i, b_k) (D - \lambda I)^{-1}(b_k, b_l) C(b_l, a_i) \\
 (2.11) \quad &= \frac{1}{16} \sum_{b_k \sim a_i} \frac{1}{\det((D - \lambda I)|_{\Lambda(b_k)})} \left((1 - \lambda)^2 - \frac{1}{16} \right) \\
 &+ \frac{1}{16} \sum_{b_k \sim a_i} \sum_{\substack{b_l \sim a_i \\ b_l \neq b_k}} \frac{1}{\det((D - \lambda I)|_{\Lambda(b_k, b_l)})} \omega_{a_i b_k} \left(\frac{1}{4} (1 - \lambda) \omega_{b_k b_l} + \frac{1}{16} \omega_{b_k b_m} \omega_{b_m b_l} \right) \omega_{b_l a_i}.
 \end{aligned}$$

Observe that if a_i is contained in two level- $(N - 1)$ cells. We need to pick $\{b_k, b_l\} \sim a_i$ from the same cell to produce a nonzero summand in the second sum.

If $\underline{a_i = a_j} \in V_0$: The formula (2.11) holds with the prefactor $\frac{1}{16}$ replaced by $\frac{1}{8}$. Also, a_i is contained in a unique level- $(N - 1)$ cell.

If $\underline{a_i \neq a_j}$: In (2.10) note that a_i, a_j, b_k, b_l must belong to the same level- $(N - 1)$ cell to produce a nonzero summand. Therefore once we fix a_i and a_j , both sums are localized to the cell $\Lambda(a_i, a_j)$.

2.2. Diagrammatic analysis. To make the results (2.10) and (2.11) more transparent, we introduce a diagrammatic bookkeeping device. Given a path $P = \{x_0, x_1, \dots, x_m\}$, we represent the product of the parallel transports along P , $\omega_{x_0 x_1} \omega_{x_1 x_2} \cdots \omega_{x_{m-1} x_m} =: \omega(P)$, by the diagram



If $\underline{a_i = a_j} \in V_N \setminus V_0$: Consider (2.11) and the diagram in Figure 7(A). We find that there are 4 identical terms in the first summand because $\deg(a_i) = 4$, and there are 8 terms in the second

summand. A diagrammatic representation of (2.11) becomes

$$\begin{aligned}
& \sum_{b_k, b_l} B(a_i, b_k) (D - \lambda I)^{-1} (b_k, b_l) C(b_l, a_i) \\
&= \frac{1}{\mathcal{D}(\beta, \lambda)} \cdot \frac{4}{16} \left((1 - \lambda)^2 - \frac{1}{16} \right) \\
&+ \frac{1}{16} \cdot \frac{1}{\mathcal{D}(\beta, \lambda)} \left(\frac{1}{4} (1 - \lambda) \cdot \begin{array}{c} b_2 \\ \nearrow \quad \searrow \\ b_1 \quad \rightarrow \quad a_i \end{array} + \frac{1}{16} \cdot \begin{array}{c} b_0 \quad \leftarrow \quad b_2 \\ \nearrow \quad \searrow \\ b_1 \quad \rightarrow \quad a_i \end{array} \right) \\
(2.12) \quad &+ \frac{1}{16} \cdot \frac{1}{\mathcal{D}(\beta, \lambda)} \left(\frac{1}{4} (1 - \lambda) \cdot \begin{array}{c} b_2 \\ \nearrow \quad \searrow \\ b_1 \quad \leftarrow \quad a_i \end{array} + \frac{1}{16} \cdot \begin{array}{c} b_0 \quad \rightarrow \quad b_2 \\ \nearrow \quad \searrow \\ b_1 \quad \leftarrow \quad a_i \end{array} \right) \\
&+ \frac{1}{16} \cdot \frac{1}{\mathcal{D}(\beta, \lambda)} \left(\frac{1}{4} (1 - \lambda) \cdot \begin{array}{c} b'_2 \\ \nearrow \quad \searrow \\ a_i \quad \rightarrow \quad b'_1 \end{array} + \frac{1}{16} \cdot \begin{array}{c} b'_2 \quad \leftarrow \quad b'_0 \\ \nearrow \quad \searrow \\ a_i \quad \rightarrow \quad b'_1 \end{array} \right) \\
&+ \frac{1}{16} \cdot \frac{1}{\mathcal{D}(\beta, \lambda)} \left(\frac{1}{4} (1 - \lambda) \cdot \begin{array}{c} b'_2 \\ \nearrow \quad \searrow \\ a_i \quad \leftarrow \quad b'_1 \end{array} + \frac{1}{16} \cdot \begin{array}{c} b'_2 \quad \rightarrow \quad b'_0 \\ \nearrow \quad \searrow \\ a_i \quad \leftarrow \quad b'_1 \end{array} \right)
\end{aligned}$$

where

$$\begin{aligned}
& \mathcal{D}(\beta, \lambda) = \det \left((D - \lambda I)|_{\Lambda(b_0^{(\prime)}, b_1^{(\prime)}, b_2^{(\prime)})} \right) \\
(2.13) \quad &= (1 - \lambda)^3 - \frac{3}{16} (1 - \lambda) - \frac{1}{64} \left(\begin{array}{c} b_2^{(\prime)} \quad \rightarrow \quad b_0^{(\prime)} \\ \nearrow \quad \searrow \\ b_1^{(\prime)} \end{array} + \begin{array}{c} b_2^{(\prime)} \quad \leftarrow \quad b_0^{(\prime)} \\ \nearrow \quad \searrow \\ b_1^{(\prime)} \end{array} \right).
\end{aligned}$$

If $a_i = a_j \in V_0$: $\deg(a_i) = 2$, see Figure 7(B). Formula (2.11) becomes

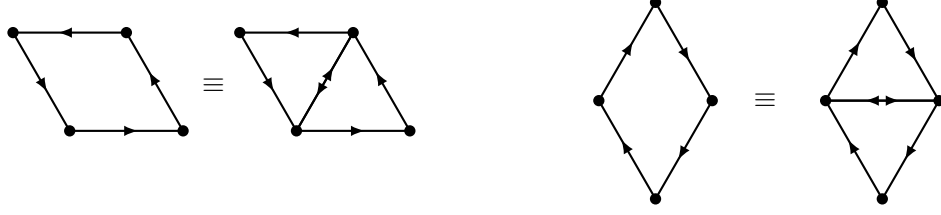
$$\begin{aligned}
& \sum_{b_k, b_l} B(a_i, b_k)(D - \lambda I)^{-1}(b_k, b_l)C(b_l, a_i) \\
&= \frac{2}{8} \cdot \frac{1}{\mathcal{D}(\beta, \lambda)} \left((1 - \lambda)^2 - \frac{1}{16} \right) \\
(2.14) \quad &+ \frac{1}{8} \cdot \frac{1}{\mathcal{D}(\beta, \lambda)} \cdot \left(\frac{1}{4} \cdot (1 - \lambda) \cdot \begin{array}{c} a_i \\ \nearrow \quad \searrow \\ b_2 \quad b_1 \end{array} + \frac{1}{16} \cdot \begin{array}{c} a_i \\ \nearrow \quad \searrow \\ b_2 \quad b_1 \\ \downarrow \\ b_0 \end{array} \right) \\
&+ \frac{1}{8} \cdot \frac{1}{\mathcal{D}(\beta, \lambda)} \cdot \left(\frac{1}{4} \cdot (1 - \lambda) \cdot \begin{array}{c} a_i \\ \searrow \quad \nearrow \\ b_2 \quad b_1 \end{array} + \frac{1}{16} \cdot \begin{array}{c} a_i \\ \searrow \quad \nearrow \\ b_2 \quad b_1 \\ \downarrow \\ b_0 \end{array} \right).
\end{aligned}$$

If $a_i \neq a_j$ and $a_i \in V_N \setminus V_0$: see Figure 7(C). Formula (2.10) writes

$$\begin{aligned}
& \sum_{b_k, b_l} B(a_i, b_k)(D - \lambda I)^{-1}(b_k, b_l)C(b_l, a_j) \\
&= \frac{1}{16} \cdot \frac{1}{\mathcal{D}(\beta, \lambda)} \left((1 - \lambda)^2 - \frac{1}{16} \right) \cdot \left(\begin{array}{c} a_i \quad b_2 \quad a_j \\ \longrightarrow \quad \longrightarrow \end{array} \right) \\
&+ \frac{1}{16} \cdot \frac{1}{\mathcal{D}(\beta, \lambda)} \cdot \frac{1}{4} (1 - \lambda) \cdot \left(\begin{array}{c} b_1 \\ \nearrow \quad \searrow \\ a_i \quad b_2 \quad a_j \\ \downarrow \end{array} + \begin{array}{c} b_1 \quad b_0 \\ \nearrow \quad \longrightarrow \quad \searrow \\ a_i \quad b_2 \quad a_j \end{array} + \begin{array}{c} b_0 \\ \nearrow \quad \searrow \\ a_i \quad b_2 \quad a_j \\ \downarrow \end{array} \right) \\
(2.15) \quad &+ \frac{1}{16} \cdot \frac{1}{\mathcal{D}(\beta, \lambda)} \cdot \frac{1}{16} \cdot \left(\begin{array}{c} b_1 \quad b_0 \\ \nearrow \quad \searrow \quad \nearrow \quad \searrow \\ a_i \quad b_2 \quad a_j \end{array} + \begin{array}{c} b_1 \quad b_0 \\ \nearrow \quad \longrightarrow \quad \searrow \\ a_i \quad b_2 \quad a_j \end{array} + \begin{array}{c} b_1 \quad b_0 \\ \nearrow \quad \searrow \\ a_i \quad b_2 \quad a_j \end{array} \right) \\
&= \frac{1}{16} \cdot \frac{1}{\mathcal{D}(\beta, \lambda)} \cdot \left(\begin{array}{c} a_i \quad b_2 \quad a_j \\ \longrightarrow \quad \longrightarrow \end{array} \right) \cdot \left((1 - \lambda)^2 - \frac{1}{16} \right) \\
&+ \frac{1 - \lambda}{64\mathcal{D}(\beta, \lambda)} \cdot \left(\begin{array}{c} a_i \quad b_2 \quad a_j \\ \longrightarrow \quad \longrightarrow \end{array} \right) \cdot \left(\begin{array}{c} b_1 \\ \nearrow \quad \searrow \\ a_i \quad b_2 \end{array} + \begin{array}{c} b_1 \quad b_0 \\ \nearrow \quad \longrightarrow \quad \searrow \\ a_i \quad b_2 \quad a_j \end{array} + \begin{array}{c} b_0 \\ \nearrow \quad \searrow \\ b_2 \quad a_j \end{array} \right) \\
&+ \frac{1}{256\mathcal{D}(\beta, \lambda)} \cdot \left(\begin{array}{c} a_i \quad b_2 \quad a_j \\ \longrightarrow \quad \longrightarrow \end{array} \right) \cdot \left(\begin{array}{c} b_1 \quad b_0 \\ \nearrow \quad \searrow \quad \nearrow \quad \searrow \\ a_i \quad b_2 \quad a_j \end{array} + \begin{array}{c} b_1 \quad b_0 \\ \nearrow \quad \longrightarrow \quad \searrow \\ a_i \quad b_2 \quad a_j \end{array} + \begin{array}{c} b_1 \quad b_0 \\ \nearrow \quad \searrow \\ b_2 \quad a_j \end{array} \right).
\end{aligned}$$

If $a_i \neq a_j$ and $a_i \in V_0$, $\sum_{b_k, b_l} B(a_i, b_k)(D - \lambda I)^{-1}(b_k, b_l)C(b_l, a_i)$ is half of equation (2.15).

2.3. Establishing spectral self-similarity. Using Assumption 1 we can simplify the expressions for the Schur complement. Note the following equivalent holonomy diagrams.



Therefore we can reexpress (2.12), (2.13), and (2.14) to get

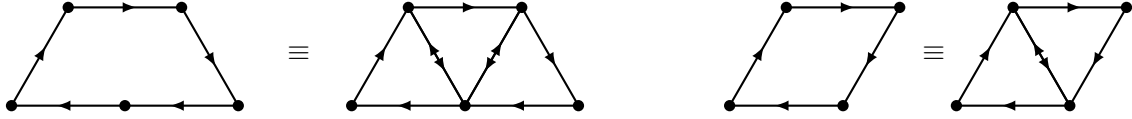
$$(2.16) \quad S_N^\omega(\alpha, \beta, \lambda)(a_i, a_i) = 1 - \lambda - \frac{A(\alpha, \beta, \lambda)}{64\mathcal{D}(\beta, \lambda)}$$

where

$$(2.17) \quad A(\alpha, \beta, \lambda) = 16\lambda^2 - (32 + 4\cos(2\pi\alpha))\lambda + 15 + 4\cos(2\pi\alpha) + \cos(2\pi(\alpha + \beta)),$$

$$(2.18) \quad \mathcal{D}(\beta, \lambda) = -\lambda^3 + 3\lambda^2 - \frac{45}{16}\lambda + \frac{13}{16} - \frac{1}{32}\cos(2\pi\beta).$$

Similarly, due to the equivalent holonomy diagrams



we can rewrite (2.15) to get

$$(2.19) \quad S_N^\omega(\alpha, \beta, \lambda)(a_i, a_j) = -\frac{\Psi(\alpha, \beta, \lambda)\omega_{a_i a_j}}{16\mathcal{D}(\beta, \lambda)},$$

where

$$(2.20) \quad \Psi(\alpha, \beta, \lambda) = (1 - \lambda)^2 - \frac{1}{16} + \frac{1 - \lambda}{4}(2e^{-2\pi i\alpha} + e^{-2\pi i(2\alpha + \beta)}) + \frac{1}{16}(e^{-4\pi i\alpha} + 2e^{-2\pi i(\alpha + \beta)}).$$

Note that the exponents of (2.20) all carry a negative sign since the orientation of the edge $a_i a_j$ is counterclockwise, while the diagrams in (2.15) have clockwise orientation. If the orientation of $a_i a_j$ is clockwise, replace all the exponents in $S_N^\omega(a_i, a_j)$ with a positive sign.

We summarize the preceding arguments as follows.

Proposition 2.1. *Let $\Delta_{a_i a_j}$ be the upright triangle that the edge $a_i a_j$ belongs to, and b_2 be the midpoint of a_i and a_j . We have*

$$(2.21) \quad S_N^\omega(\alpha, \beta, \lambda)(a_i, a_j) = \begin{cases} 1 - \lambda - \frac{A(\alpha, \beta, \lambda)}{64\mathcal{D}(\beta, \lambda)} & \text{if } a_i = a_j, \\ -\frac{\Psi(\alpha, \beta, \lambda)\omega_{a_i b_2}\omega_{b_2 a_j}}{16\mathcal{D}(\beta, \lambda)} & \text{if } a_i \neq a_j, a_i \in V_N \setminus V_0 \text{ and } \Delta_{a_i a_j} \text{ is traversed CCW,} \\ -\frac{\Psi(\alpha, \beta, \lambda)\omega_{a_i b_2}\omega_{b_2 a_j}}{8\mathcal{D}(\beta, \lambda)} & \text{if } a_i \neq a_j, a_i \in V_0 \text{ and } \Delta_{a_i a_j} \text{ is traversed CCW,} \\ -\frac{\overline{\Psi(\alpha, \beta, \lambda)\omega_{a_i b_2}\omega_{b_2 a_j}}}{16\mathcal{D}(\beta, \lambda)} & \text{if } a_i \neq a_j, a_i \in V_N \setminus V_0 \text{ and } \Delta_{a_i a_j} \text{ is traversed CW,} \\ -\frac{\overline{\Psi(\alpha, \beta, \lambda)\omega_{a_i b_2}\omega_{b_2 a_j}}}{8\mathcal{D}(\beta, \lambda)} & \text{if } a_i \neq a_j, a_i \in V_0 \text{ and } \Delta_{a_i a_j} \text{ is traversed CW,} \end{cases}$$

where $A(\alpha, \beta, \lambda)$, $\mathcal{D}(\beta, \lambda)$, and $\Psi(\alpha, \beta, \lambda)$ were defined respectively in (2.17), (2.18), and (2.20).

Corollary 2.2 (Spectral decimation identity). *The Schur complement in Proposition 2.1 can be reexpressed as*

$$(2.22) \quad S_N^\omega(\alpha, \beta, \lambda) = \phi(\alpha, \beta, \lambda)(\mathcal{L}_{N-1}^\Omega - R(\alpha, \beta, \lambda)), \quad \lambda \in \mathbb{C},$$

where \mathcal{L}_{N-1}^Ω is the magnetic Laplacian on V_{N-1} with $U(1)$ connection Ω , a self-adjoint operator on $L^2(V_{N-1}, \text{deg})$, and $R(\alpha, \beta, \lambda)$ is the spectral decimation function. Specifically:

(1) If $\mathbb{R} \ni \lambda \mapsto \Psi(\alpha, \beta, \lambda)$ is \mathbb{R} -valued, then

$$(2.23) \quad \phi(\alpha, \beta, \lambda) = \frac{\Psi(\alpha, \beta, \lambda)}{4\mathcal{D}(\beta, \lambda)},$$

$$(2.24) \quad R(\alpha, \beta, \lambda) = 1 + \frac{A(\alpha, \beta, \lambda) - 64\mathcal{D}(\beta, \lambda)(1 - \lambda)}{16\Psi(\alpha, \beta, \lambda)},$$

$$(2.25) \quad \Omega_{ab}(\alpha, \beta) = \omega_{ac}\omega_{cb}.$$

(2) If $\mathbb{R} \ni \lambda \mapsto \Psi(\alpha, \beta, \lambda)$ is \mathbb{C} -valued, then

$$(2.26) \quad \phi(\alpha, \beta, \lambda) = \frac{|\Psi(\alpha, \beta, \lambda)|}{4\mathcal{D}(\beta, \lambda)},$$

$$(2.27) \quad R(\alpha, \beta, \lambda) = 1 + \frac{A(\alpha, \beta, \lambda) - 64\mathcal{D}(\beta, \lambda)(1 - \lambda)}{16|\Psi(\alpha, \beta, \lambda)|},$$

$$(2.28) \quad \theta(\alpha, \beta, \lambda) = \frac{\arg \Psi(\alpha, \beta, \lambda)}{2\pi} \quad (\arg : \mathbb{C} \rightarrow [0, 2\pi)),$$

$$(2.29) \quad \Omega_{ab}(\alpha, \beta, \lambda) = \omega_{ac}\omega_{cb}e^{2\pi i\theta(\alpha, \beta, \lambda)}.$$

In both cases, $a \sim c \sim b$, and the upright triangle to which the edge ab belongs is traversed counter-clockwise.

Two important remarks are in order. First, $A(\alpha, \beta, \lambda)$, $\mathcal{D}(\beta, \lambda)$, and $\Psi(\alpha, \beta, \lambda)$ are all independent of the level N , and therefore so is $R(\alpha, \beta, \lambda)$. This is the essence of spectral self-similarity and what allows us to characterize the spectrum recursively. Second, in Corollary 2.2-(1), the connection Ω is manifestly independent of λ , whereas in Corollary 2.2-(2) Ω receives an extra ‘‘twist’’ by a unit complex number $e^{2\pi i\theta}$, which depends on λ in general. *There is no easy way to eliminate this twist via conjugation, gauge transformation, or else.*

The following was first noted by [1] and invoked later in [4, 18].

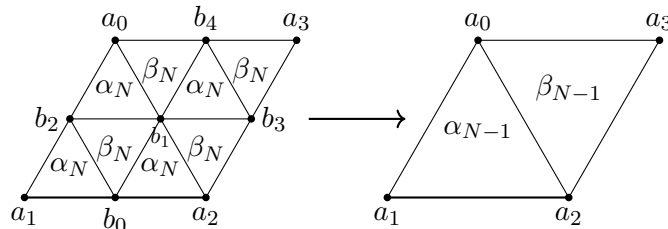
Proposition 2.3 (Evolution of the magnetic flux under spectral decimation). *Let the magnetic flux going through every upright triangle on level N be α_N , and downright triangle, β_N . Then*

$$(2.30) \quad \alpha_{N-1} = \alpha_\downarrow(\alpha_N, \beta_N, \lambda) = 3\alpha_N + \beta_N - 3\theta(\alpha_N, \beta_N, \lambda),$$

$$(2.31) \quad \beta_{N-1} = \beta_\downarrow(\alpha_N, \beta_N, \lambda) = 3\beta_N + \alpha_N + 3\theta(\alpha_N, \beta_N, \lambda),$$

so $\alpha_{N-1} + \beta_{N-1} = 4(\alpha_N + \beta_N)$. Specifically, in the setting of Corollary 2.2-(1), $\theta \equiv 0$.

Proof. By (2.25) or (2.29), $\Omega_{a_1 a_2}(\alpha, \beta, \lambda) = \omega_{a_1 b_0}\omega_{b_0 a_2}e^{2\pi i\theta(\alpha, \beta, \lambda)}$; see the diagram below.



By Definition 1.1,

$$\begin{aligned} e^{2\pi i \alpha_{N-1}} &= \Omega_{a_1 a_2} \Omega_{a_2 a_0} \Omega_{a_0 a_1} = \omega_{a_1 b_0} \omega_{b_0 a_2} \omega_{a_2 b_1} \omega_{b_1 a_0} \omega_{a_0 b_2} \omega_{b_2 a_1} e^{2\pi i (3\theta(\alpha, \beta, \lambda))} \\ &= e^{2\pi i (3\alpha_N + \beta_N)} e^{2\pi i (3\theta(\alpha_N, \beta_N, \lambda))} = e^{2\pi i (3\alpha_N + \beta_N + 3\theta(\alpha_N, \beta_N, \lambda))}, \end{aligned}$$

and similarly for $e^{2\pi i \beta_{N-1}}$. This implies (2.30) and (2.31). \square

3. MECHANICS OF SPECTRAL DECIMATION

In this section we give a general account of Schur complementation and the spectral decimation procedure. The results of this section are essentially given in [3]. However, in order to make this account self-contained, and to explain the subtleties involved in the procedure, we provide—and sometimes repeat—the proofs which already appeared in [3].

3.1. Schur complement & functional identities. We start with an elementary matrix identity. Observe that $A - BD^{-1}C$ is the Schur complement of the block matrix with respect to the D block.

Proposition 3.1. *Suppose $\begin{bmatrix} A & B \\ C & D \end{bmatrix}$ is a square block matrix with the square block D invertible.*

Then

$$\begin{bmatrix} A & B \\ C & D \end{bmatrix} = \begin{bmatrix} A - BD^{-1}C & BD^{-1} \\ 0 & I \end{bmatrix} \begin{bmatrix} I & 0 \\ C & D \end{bmatrix}.$$

Furthermore, the block matrix is invertible with inverse

$$\begin{aligned} (3.1) \quad \begin{bmatrix} A & B \\ C & D \end{bmatrix}^{-1} &= \begin{bmatrix} I & 0 \\ -D^{-1}C & D^{-1} \end{bmatrix} \begin{bmatrix} (A - BD^{-1}C)^{-1} & -(A - BD^{-1}C)^{-1}BD^{-1} \\ 0 & I \end{bmatrix} \\ &= \begin{bmatrix} 0 & 0 \\ 0 & D^{-1} \end{bmatrix} + \begin{bmatrix} I \\ -D^{-1}C \end{bmatrix} (A - BD^{-1}C)^{-1} \begin{bmatrix} I & -BD^{-1} \end{bmatrix}. \end{aligned}$$

Let V be a countable set, μ be a nonnegative measure on V , and $L^2(V, \mu)$ be the Hilbert space of \mathbb{C} -valued functions on V with inner product $\langle f, g \rangle = \sum_{x \in V} \bar{f}(x)g(x)\mu(x)$. Let $M : L^2(V, \mu) \rightarrow L^2(V, \mu)$; equivalently, we may regard M as a square matrix of size $|V|$ with entries $M_{ij} = \langle \delta_i, M\delta_j \rangle$.

Suppose $V = V_{\parallel} \sqcup V_{\perp}$. Naturally, we can project functions in $L^2(V, \mu)$ to $L^2(V_{\parallel}, \mu)$ and $L^2(V_{\perp}, \mu)$, respectively, and denote the corresponding projection operators by P_{\parallel} and P_{\perp} . Their conjugates are

$$P_b^* : L^2(V_b, \mu) \rightarrow L^2(V, \mu), \quad (P_b^* f)(x) = f(x)\mathbf{1}_{\{x \in V_b\}}, \quad b \in \{\parallel, \perp\}$$

Note that $P_b P_b^* = I_b$, the identity on $L^2(V_b, \mu)$.

Combining the preceding facts, we see that Proposition 3.1 implies the following. Suppose M can be expressed in the “block form”

$$A = P_{\parallel} M P_{\parallel}^*, \quad B = P_{\parallel} M P_{\perp}^*, \quad C = P_{\perp} M P_{\parallel}^*, \quad D = P_{\perp} M P_{\perp}^*,$$

with D invertible. Then (3.1) says that

$$M^{-1} = P_{\perp}^* D^{-1} P_{\perp} + \left(P_{\parallel}^* - P_{\perp}^* D^{-1} C \right) (A - BD^{-1}C)^{-1} (P_{\parallel} - BD^{-1} P_{\perp}).$$

For spectral analysis it is more pertinent to consider the resolvent $(M - xI)^{-1}$, $x \in \mathbb{C}$. In this case, assuming that $D - xI_{\perp}$ is invertible, we have

$$\begin{aligned} (3.2) \quad (M - xI)^{-1} &= P_{\perp}^* (D - xI_{\perp})^{-1} P_{\perp} \\ &+ \left(P_{\parallel}^* - P_{\perp}^* (D - xI_{\perp})^{-1} C \right) \left((A - xI_{\parallel}) - B(D - xI_{\perp})^{-1} C \right)^{-1} (P_{\parallel} - B(D - xI_{\perp})^{-1} P_{\perp}). \end{aligned}$$

(From this point on we often drop the notation I_{\parallel} or I_{\perp} , unless the context demands its presence.)

Finally, recall the functional calculus $f(M) = \sum_{\lambda \in \sigma(M)} f(\lambda)E_\lambda(M)$, where $E_\lambda(M) : L^2(V, \mu) \rightarrow L^2(V, \mu)$ is the eigenprojector of M associated with eigenvalue λ . It is then direct to verify that

$$(3.3) \quad E_\lambda(M) = \lim_{x \rightarrow \lambda} (\lambda - x)(M - x)^{-1}.$$

We will be especially interested in expressing the eigenprojector in terms of A, B, C , and D , using the RHS of (3.3) in conjunction with the formula (3.2). Of course we will need to justify the limit as $x \rightarrow \lambda \in \sigma(M)$, which will be done on a case-by-case basis.

3.2. Spectral decimation for the non-exceptional values. Let us introduce the following condition which will be in force for the rest of the section.

Definition 3.2 (Spectral similarity). Let $V_\parallel \subset V$. We say that two self-adjoint operators $M : L^2(V, \mu) \rightarrow L^2(V, \mu)$ and $L : L^2(V_\parallel, \mu) \rightarrow L^2(V_\parallel, \mu)$ are **spectrally similar** if there exist scalar-valued functions ϕ and R which map \mathbb{R} to \mathbb{R} such that

$$(3.4) \quad (A - x) - B(D - x)^{-1}C = \phi(x)(L - R(x))$$

for all $x \in \mathbb{C}$. It follows that

$$(3.5) \quad P_\parallel(M - x)^{-1}P_\parallel^* \left(\stackrel{(3.2)}{=} ((A - x) - B(D - x)^{-1}C)^{-1} \right) = [\phi(x)]^{-1}(L - R(x))^{-1}$$

for all $x \in \mathbb{C}$ whenever the RHS is defined.

Remark 3.3. In Definition 3.2, no assumption is made on the dependence of M or L on the spectral parameter x . (In the example of Corollary 2.2-(2), $L = \mathcal{L}_{N-1}^\Omega$ depends on x .) Also we do not specify extra conditions (such as continuity or differentiability) on ϕ and R at the moment.

In order for (3.4) and (3.5) to make sense as they are, $D - x$ should be invertible, and $\phi(x) \neq 0$. Any x that fails either condition is said to be **exceptional**, and we refer to the set of all such x as the **exceptional set (for spectral decimation)**, denoted

$$(3.6) \quad \mathcal{E} = \{x \in \mathbb{C} : x \in \sigma(D) \text{ or } \phi(x) = 0\}.$$

Since M is self-adjoint on $L^2(V, \mu)$, our goal is to determine which $\lambda \in \mathbb{R}$ belongs to the spectrum $\sigma(M)$. The following result is the spectral decimation identity when $\lambda \in \mathbb{R}$ is not exceptional, which mirrors [3, Proposition 4.1].

Lemma 3.4. *Suppose $\lambda \in \mathbb{R}$ is such that $\lambda \notin \mathcal{E}$, and moreover $\lim_{\mathbb{R} \ni x \rightarrow \lambda} \phi(x) \frac{R(\lambda) - R(x)}{\lambda - x}$ exists and does not equal 0. Then*

$$(3.7) \quad E_\lambda(M) = \left(\lim_{\mathbb{R} \ni x \rightarrow \lambda} \frac{1}{\phi(x)} \frac{\lambda - x}{R(\lambda) - R(x)} \right) \left(P_\parallel^* - P_\perp^*(D - \lambda)^{-1}C \right) E_{R(\lambda)}(L) \left(P_\parallel - B(D - \lambda)^{-1}P_\perp \right).$$

Consequently, $\lambda \in \sigma(M)$ if and only if $R(\lambda) \in \sigma(L)$, and there is a one-to-one correspondence between eigenfunctions of L with eigenvalue $R(\lambda)$ and eigenfunctions of M with eigenvalue λ , given by

$$\text{Image}(E_{R(\lambda)}(L)) \ni f \mapsto \left(P_\parallel^* - P_\perp^*(D - \lambda)^{-1}C \right) f \in \text{Image}(E_\lambda(M)).$$

In particular, $\text{mult}(M, \lambda) = \text{mult}(L, R(\lambda))$.

Proof. Combining (3.2) and (3.5) we find

$$(3.8) \quad (\lambda - x)(M - x)^{-1} = P_\perp^*(\lambda - x)(D - x)^{-1}P_\perp + \left(P_\parallel^* - P_\perp^*(D - x)^{-1}C \right) (\lambda - x)[\phi(x)]^{-1}(L - R(x))^{-1} \left(P_\parallel - B(D - x)^{-1}P_\perp \right).$$

According to (3.3) it suffices to take the limit of (3.8) as $\mathbb{R} \ni x \rightarrow \lambda$. Based on the assumptions, the quantities in blue (resp. purple) remain bounded (resp. vanish) in the limit, and in particular the first term on the RHS tends to 0. To unravel the second term on the RHS, we insert the identity $I_{\parallel} = E_{R(\lambda)}(L) + (I_{\parallel} - E_{R(\lambda)}(L))$ between $(L - R(x))^{-1}$ and $P_{\parallel} - B(D - x)^{-1}P_{\perp}$, resulting in the following expression:

(3.9)

$$\left(P_{\parallel}^* - P_{\perp}^*(D - x)^{-1}C \right) (\lambda - x) [\phi(x)]^{-1} (L - R(x))^{-1} E_{R(\lambda)}(L) (P_{\parallel} - B(D - x)^{-1}P_{\perp})$$

(3.10)

$$+ \left(P_{\parallel}^* - P_{\perp}^*(D - x)^{-1}C \right) (\lambda - x) [\phi(x)]^{-1} (L - R(x))^{-1} (I_{\parallel} - E_{R(\lambda)}(L)) (P_{\parallel} - B(D - x)^{-1}P_{\perp}).$$

Observer that in (3.10), the image of $I_{\parallel} - E_{R(\lambda)}(L)$ is the orthogonal complement of the eigenspace of L with eigenvalue $R(\lambda)$, and $L - R(\lambda)$ is invertible on this space. Therefore (3.10) vanishes in the limit $x \rightarrow \lambda$. As for (3.9), we are in the eigenspace of L with eigenvalues $R(\lambda)$, and $L - R(\lambda)$ is not invertible. That said, we can multiply and divide (3.9) by $R(\lambda) - R(x)$,

(3.11)

$$\left(P_{\parallel}^* - P_{\perp}^*(D - x)^{-1}C \right) \frac{\lambda - x}{R(\lambda) - R(x)} [\phi(x)]^{-1} (R(\lambda) - R(x)) (L - R(x))^{-1} E_{R(\lambda)}(L) (P_{\parallel} - B(D - x)^{-1}P_{\perp}).$$

By functional calculus again, $\lim_{x \rightarrow \lambda} (R(\lambda) - R(x)) (L - R(x))^{-1} = E_{R(\lambda)}(L)$. So the proof is complete provided that $\frac{1}{\phi(x)} \frac{\lambda - x}{R(\lambda) - R(x)}$ has a nonsingular limit as $x \rightarrow \lambda$. \square

Actually (3.7) says more. Since the LHS of (3.7) is a bounded operator, if $\lim_{R \ni x \rightarrow \lambda} \left| \frac{1}{\phi(x)} \frac{\lambda - x}{R(\lambda) - R(x)} \right| = \infty$, then (3.7) holds only if $E_{R(\lambda)}(L) = 0$. In turn $E_{\lambda}(M) = 0$. In what follows, we will encounter similar situations where the scalar prefactor diverges, and we may argue that this divergence should not exist by the aforementioned rationale.

3.3. Spectral decimation for the exceptional values. If λ is exceptional the spectral decimation argument is suitably modified. Here are two items of note.

Lemma 3.5. *Under Definition 3.2:*

- (1) If $\phi(\lambda) \neq 0$, then $(D - \lambda)^{-1}$ is bounded on the image of $E_{R(\lambda)}(L)$.
- (2) If both ϕ and ϕR are bounded in a neighborhood of λ , then $BE_{\lambda}(D)C = 0$.

Proof. (1): If $\phi(\lambda) \neq 0$, we use (3.4) to find that whenever f is an eigenfunction of L with eigenvalue $R(\lambda)$, then

$$(3.12) \quad ((A - \lambda) - B(D - \lambda)^{-1}C) f = \phi(\lambda)(L - R(\lambda))f = 0.$$

Given that $A - \lambda$, B , and C are all bounded, it follows that $(D - \lambda)^{-1}$ must be bounded on the image of $E_{R(\lambda)}(L)$.

(2): Multiply (3.4) on both sides by $(\lambda - x)$ to get

$$(\lambda - x)(A - x) - B(\lambda - x)(D - x)^{-1}C = (\lambda - x)\phi(x)(L - R(x)).$$

Noting that both $A - x$ and $\phi(x)(L - R(x))$ remain bounded as $x \rightarrow \lambda$, we take the limit on the above equation to find $-BE_{\lambda}(D)C = 0$. \square

With the above in mind, we continue to use (3.2), (3.3), and (3.5) altogether to derive an expression for the eigenprojector $E_{\lambda}(M)$. The general strategy proceeds as follows: first decide whether $\lambda \in \sigma(D)$ (which determines the invertibility of $D - \lambda$), then insert the identity $I_{\parallel} =$

$E_{R(\lambda)}(L) + (I_{\parallel} - E_{R(\lambda)}(L))$ in the expression for $(\lambda - x)(M - x)^{-1}$ à la (3.9) and (3.10), and finally identify conditions which ensure the existence of the limits as $\mathbb{R} \ni x \rightarrow \lambda$.

The next result generalizes [3, Proposition 4.1], in the sense that we only require the existence of \mathbb{R} -limits (as opposed to \mathbb{C} -limits) of the various functions that arise naturally in the eigenprojector expression. For the sake of easy reference, we keep the same numbering of the cases as in [3, Proposition 4.1].

Lemma 3.6. *Suppose $\lambda \in \mathbb{R}$.*

(ii) *If $\lambda \notin \sigma(D)$, $\phi(\lambda) = 0$, and moreover $\lim_{\mathbb{R} \ni x \rightarrow \lambda} \frac{\phi(x)}{\lambda - x} \neq 0$ and $\lim_{\mathbb{R} \ni x \rightarrow \lambda} \phi(x) \frac{R(\lambda) - R(x)}{\lambda - x} \neq 0$, then*

$$(3.13) \quad \begin{aligned} E_{\lambda}(M) &= \left(P_{\parallel}^* - P_{\perp}^*(D - \lambda)^{-1}C \right) \left(\lim_{\mathbb{R} \ni x \rightarrow \lambda} \frac{(\lambda - x)[\phi(x)]^{-1}}{R(\lambda) - R(x)} \right) E_{R(\lambda)}(L) (P_{\parallel} - B(D - \lambda)^{-1}P_{\perp}) \\ &+ \left(P_{\parallel}^* - P_{\perp}^*(D - \lambda)^{-1}C \right) \left(\lim_{\mathbb{R} \ni x \rightarrow \lambda} \frac{\lambda - x}{\phi(x)} \right) (L - R(\lambda))^{-1} (I_{\parallel} - E_{R(\lambda)}(L)) (P_{\parallel} - B(D - \lambda)^{-1}P_{\perp}). \end{aligned}$$

In particular, $\text{mult}(M, \lambda) = |V_{\parallel}|$.

(iii) *If $\lambda \in \sigma(D)$, $\lim_{\mathbb{R} \ni x \rightarrow \lambda} [\phi(x)]^{-1} = 0$, and moreover $\lim_{\mathbb{R} \ni x \rightarrow \lambda} \phi(x)(\lambda - x) \neq 0$ and $\left| \frac{\lambda - x}{R(\lambda) - R(x)} \right|$ is bounded in a neighborhood of λ , then*

$$(3.14) \quad E_{\lambda}(M) = P_{\perp}^* E_{\lambda}(D) P_{\perp} + P_{\perp}^* E_{\lambda}(D) C \left(\lim_{\mathbb{R} \ni x \rightarrow \lambda} \frac{1}{\phi(x)(\lambda - x)} \right) (L - R(\lambda))^{-1} (I_{\parallel} - E_{R(\lambda)}(L)) B E_{\lambda}(D) P_{\perp}.$$

In particular, $E_{\lambda}(M)(P_{\perp}^ E_{\lambda}(D) P_{\perp}) = E_{\lambda}(M)$, so any eigenfunction of M with eigenvalue λ vanishes on V_{\parallel} , and $\text{mult}(M, \lambda) = \text{mult}(D, \lambda) - (|V_{\parallel}| - \text{mult}(L, R(\lambda)))$.*

(iv) *If $\lambda \in \sigma(D)$, both ϕ and ϕR are bounded in a neighborhood of λ , $\phi(\lambda) \neq 0$, and moreover $\lim_{\mathbb{R} \ni x \rightarrow \lambda} \phi(x) \frac{R(\lambda) - R(x)}{\lambda - x} \neq 0$, then*

$$(3.15) \quad \begin{aligned} E_{\lambda}(M) &= P_{\perp}^* E_{\lambda}(D) P_{\perp} \\ &+ \left(P_{\parallel}^* - P_{\perp}^*(D - \lambda)^{-1}C \right) \left(\lim_{\mathbb{R} \ni x \rightarrow \lambda} \frac{1}{\phi(x)} \frac{\lambda - x}{R(\lambda) - R(x)} \right) E_{R(\lambda)}(L) (P_{\parallel} - B(D - \lambda)^{-1}P_{\perp}). \end{aligned}$$

In particular, $E_{\lambda}(M)(P_{\perp}^ E_{\lambda}(D) P_{\perp}) = P_{\perp}^* E_{\lambda}(D) P_{\perp}$, the two components on the RHS of (3.15) are mutually orthogonal in $L^2(V, \mu)$, and $\text{mult}(M, \lambda) = \text{mult}(D, \lambda) + \text{mult}(L, R(\lambda))$.*

(v) *If $\lambda \in \sigma(D)$, $\lim_{\mathbb{R} \ni x \rightarrow \lambda} [\phi(x)]^{-1} = 0$, and moreover $\lim_{\mathbb{R} \ni x \rightarrow \lambda} \phi(x)(\lambda - x) \neq 0$ and $\lim_{\mathbb{R} \ni x \rightarrow \lambda} \frac{1}{\phi(x)} \frac{\lambda - x}{R(\lambda) - R(x)} \neq 0$, then*

$$(3.16) \quad \begin{aligned} E_{\lambda}(M) &= P_{\perp}^* E_{\lambda}(D) P_{\perp} + P_{\perp}^* E_{\lambda}(D) C \left(\lim_{\mathbb{R} \ni x \rightarrow \lambda} \frac{1}{\phi(x)(\lambda - x)} \right) (L - R(\lambda))^{-1} (I_{\parallel} - E_{R(\lambda)}(L)) B E_{\lambda}(D) P_{\perp} \\ &+ \left(P_{\parallel}^* - P_{\perp}^*(D - \lambda)^{-1}C \right) \left(\lim_{\mathbb{R} \ni x \rightarrow \lambda} \frac{1}{\phi(x)} \frac{\lambda - x}{R(\lambda) - R(x)} \right) E_{R(\lambda)}(L) (P_{\parallel} - B(D - \lambda)^{-1}P_{\perp}). \end{aligned}$$

which implies generally that $\text{mult}(M, \lambda) = \text{mult}(D, \lambda) - |V_{\parallel}| + 2\text{mult}(L, R(\lambda))$. If none of the corresponding eigenfunctions vanishes on V_{\parallel} , then the first two terms on the RHS of (3.16) vanish, and $\text{mult}(M, \lambda) = \text{mult}(L, R(\lambda))$.

(vi) *If $\lambda \notin \sigma(D)$, $\phi(\lambda) = 0$, $\lim_{\mathbb{R} \ni x \rightarrow \lambda} [R(x)]^{-1} = 0$, and moreover $x \mapsto (\lambda - x)[\phi(x)]^{-1}$ is bounded in a neighborhood of λ , then $E_{\lambda}(M) = 0$, i.e., $\text{mult}(M, \lambda) = 0$.*

Proof. Our starting point is the combination of (3.2) and (3.5). Let us note right away that

$$\begin{aligned} \lambda \notin \sigma(D) & \text{ implies } \lim_{x \rightarrow \lambda} P_{\perp}^*(\lambda - x)(D - x)^{-1}P_{\perp} = 0, \\ \lambda \in \sigma(D) & \text{ implies } \lim_{x \rightarrow \lambda} P_{\perp}^*(\lambda - x)(D - x)^{-1}P_{\perp} = P_{\perp}^*E_{\lambda}(D)P_{\perp}. \end{aligned}$$

So this reduces our analysis to the second term on the RHS of (3.8), namely:

$$(3.17) \quad \left(P_{\parallel}^* - P_{\perp}^*(D - x)^{-1}C \right) (\lambda - x)[\phi(x)]^{-1}(L - R(x))^{-1}(I_{\parallel} - E_{R(\lambda)}(L)) (P_{\parallel} - B(D - x)^{-1}P_{\perp}).$$

As in the proof of Lemma 3.4, terms which stay bounded (resp. vanish) as $\mathbb{R} \ni x \rightarrow \lambda$ are highlighted in blue (resp. purple).

(ii): By the assumptions, (3.17) reads

$$\begin{aligned} & \left(P_{\parallel}^* - P_{\perp}^*(D - x)^{-1}C \right) (\lambda - x)[\phi(x)]^{-1}(L - R(x))^{-1}(P_{\parallel} - B(D - x)^{-1}P_{\perp}) \\ &= \left(P_{\parallel}^* - P_{\perp}^*(D - x)^{-1}C \right) \frac{(\lambda - x)[\phi(x)]^{-1}}{R(\lambda) - R(x)} (R(\lambda) - R(x))(L - R(x))^{-1}E_{R(\lambda)}(L)(P_{\parallel} - B(D - x)^{-1}P_{\perp}) \\ &+ \left(P_{\parallel}^* - P_{\perp}^*(D - x)^{-1}C \right) (\lambda - x)[\phi(x)]^{-1}(L - R(x))^{-1}(I_{\parallel} - E_{R(\lambda)}(L)) (P_{\parallel} - B(D - x)^{-1}P_{\perp}). \end{aligned}$$

(iii): By the assumptions, (3.17) reads

$$\begin{aligned} & \left(P_{\parallel}^* - P_{\perp}^*(D - x)^{-1}C \right) \frac{(\lambda - x)[\phi(x)]^{-1}}{R(\lambda) - R(x)} (R(\lambda) - R(x))(L - R(x))^{-1}E_{R(\lambda)}(L)(P_{\parallel} - B(D - x)^{-1}P_{\perp}) \\ &+ \left(P_{\parallel}^* - P_{\perp}^*(D - x)^{-1}C \right) (\lambda - x)[\phi(x)]^{-1}(L - R(x))^{-1}(I_{\parallel} - E_{R(\lambda)}(L)) (P_{\parallel} - B(D - x)^{-1}P_{\perp}). \end{aligned}$$

For the first term, the boundedness of $(D - \lambda)^{-1}$ follows from Lemma 3.5-(1). We further note that $\lim_{x \rightarrow \lambda} (R(\lambda) - R(x))(L - R(x))^{-1} = E_{R(\lambda)}(L)$ by the functional calculus, and $[\phi(\lambda)]^{-1} = 0$ by assumption. In fact, we would like to show that $\lim_{x \rightarrow \lambda} \frac{\lambda - x}{R(\lambda) - R(x)} [\phi(x)]^{-1} = 0$, and it suffices to have $\left| \frac{\lambda - x}{R(\lambda) - R(x)} \right|$ to be bounded in a neighborhood of λ . Consequently the first term vanishes in the limit.

The second term requires more care, as we do not know *a priori* that $D - \lambda$ is invertible. So we expand it as the sum of four terms

$$\begin{aligned} & P_{\parallel}^*(\lambda - x)[\phi(x)]^{-1}(L - R(x))^{-1}(I_{\parallel} - E_{R(\lambda)}(L))P_{\parallel} \\ & - P_{\perp}^*(\lambda - x)(D - x)^{-1}C[\phi(x)]^{-1}(L - R(x))^{-1}(I_{\parallel} - E_{R(\lambda)}(L))P_{\parallel} \\ & - P_{\parallel}^*[\phi(x)]^{-1}(L - R(x))^{-1}(I_{\parallel} - E_{R(\lambda)}(L))B(\lambda - x)(D - x)^{-1}P_{\perp} \\ & + P_{\perp}^*(\lambda - x)(D - x)^{-1}C[\phi(x)(\lambda - x)]^{-1}(L - R(x))^{-1}(I_{\parallel} - E_{R(\lambda)}(L))B(\lambda - x)(D - x)^{-1}P_{\perp}. \end{aligned}$$

It can be seen readily that the first three lines vanish in the limit, whereas the fourth line converges to

$$P_{\perp}^*E_{\lambda}(D)C \left(\lim_{\mathbb{R} \ni x \rightarrow \lambda} \frac{1}{\phi(x)(\lambda - x)} \right) (L - R(\lambda))^{-1}(I_{\parallel} - E_{R(\lambda)}(L))BE_{\lambda}(D)P_{\perp}$$

given the assumptions. The eigenprojector formula (3.14) follows.

Observe that the image of $E_{\lambda}(M)$ is contained in the image of $P_{\perp}^*E_{\lambda}(D)P_{\perp}$. More specifically,

$$\text{rank}(P_{\perp}^*E_{\lambda}(D)P_{\perp}) - \text{rank}(E_{\lambda}(M)) = \text{rank}(I_{\parallel} - E_{R(\lambda)}(L)),$$

from which the multiplicity formula follows.

(iv): By the assumptions and Lemma 3.5-(1), (3.17) reads

$$\begin{aligned} & \left(P_{\parallel}^* - P_{\perp}^*(D-x)^{-1}C \right) \frac{(\lambda-x)[\phi(x)]^{-1}}{R(\lambda)-R(x)} (R(\lambda)-R(x))(L-R(x))^{-1} E_{R(\lambda)}(L) (P_{\parallel} - B(D-x)^{-1}P_{\perp}) \\ & + \left(P_{\parallel}^* - P_{\perp}^*(D-x)^{-1}C \right) (\lambda-x)[\phi(x)]^{-1} (L-R(x))^{-1} (I_{\parallel} - E_{R(\lambda)}(L)) (P_{\parallel} - B(D-x)^{-1}P_{\perp}). \end{aligned}$$

The first term tends to

$$\left(P_{\parallel}^* - P_{\perp}^*(D-\lambda)^{-1}C \right) \left(\lim_{\mathbb{R} \ni x \rightarrow \lambda} \frac{1}{\phi(x)} \frac{\lambda-x}{R(\lambda)-R(x)} \right) E_{R(\lambda)}(L) (P_{\parallel} - B(D-\lambda)^{-1}P_{\perp}).$$

The second term is again trickier, being the sum of

$$\begin{aligned} & P_{\parallel}^*(\lambda-x)[\phi(x)]^{-1} (L-R(x))^{-1} (I_{\parallel} - E_{R(\lambda)}(L)) P_{\parallel} \\ & - P_{\perp}^*(\lambda-x)(D-x)^{-1}C[\phi(x)]^{-1} (L-R(x))^{-1} (I_{\parallel} - E_{R(\lambda)}(L)) P_{\parallel} \\ & - P_{\parallel}^*[\phi(x)]^{-1} (L-R(x))^{-1} (I_{\parallel} - E_{R(\lambda)}(L)) B(\lambda-x)(D-x)^{-1}P_{\perp} \\ & + P_{\perp}^*(D-x)^{-1}C[\phi(x)]^{-1} (L-R(x))^{-1} (I_{\parallel} - E_{R(\lambda)}(L)) B(\lambda-x)(D-x)^{-1}P_{\perp}, \end{aligned}$$

where the vanishing purple terms in the last 3 lines are due to Lemma 3.5-(2). Altogether the entire sum vanishes in the limit. This proves (3.15). Observe that the two terms on the RHS of (3.15) are mutually orthogonal, from which the remaining claims follow.

(vi): This is a straightforward extension of (iii). In particular, if none of the corresponding eigenfunctions vanishes on V_{\parallel} , then by (iii) the first two terms on the RHS of (3.16) vanishes.

(vii): Since the spectrum of an operator is compact, $(L-R(x))^{-1}$ remains bounded—in fact tends to 0—as $R(x) \rightarrow R(\lambda) = \infty$. Thus (3.17) reads

$$\left(P_{\parallel}^* - P_{\perp}^*(D-x)^{-1}C \right) (\lambda-x)[\phi(x)]^{-1} (L-R(x))^{-1} (P_{\parallel} - B(D-x)^{-1}P_{\perp})$$

which vanishes in the limit. \square

4. RECURSIVE CHARACTERIZATION OF THE MAGNETIC SPECTRUM

In this section we explicitly characterize the spectrum $\sigma(\mathcal{L}_N^{\omega})$ under Assumption 1, thereby proving Theorems 1 and 2. Our approach is to specialize the results from §3 to

$$V = V_N, \quad V_{\parallel} = V_{N-1}, \quad V_{\perp} = V \setminus V_{\parallel}, \quad M = \mathcal{L}_N^{\omega}, \quad L = \mathcal{L}_{N-1}^{\Omega},$$

and involve all the functions referenced in Corollary 2.2.

As a first step, we make a distinction between the case of (half)-integer fluxes $\alpha, \beta \in \{0, \frac{1}{2}\}$ and the remaining cases. This is made not just for convenience, but actually reflects the dichotomy between cases (1) and (2) in Corollary 2.2.

Proposition 4.1. *The function $\mathbb{R} \ni \lambda \mapsto \Psi(\alpha, \beta, \lambda)$ is \mathbb{R} -valued if and only if $\alpha, \beta \in \{0, \frac{1}{2}\}$.*

Proof. From (2.20) we have

$$\operatorname{Im}(\Psi(\alpha, \beta, \lambda)) = (2 \sin(2\pi\alpha) + \sin(2\pi(2\alpha + \beta))) \frac{1-\lambda}{4} + \frac{1}{16} (\sin(4\pi\alpha) + 2 \sin(2\pi(\alpha + \beta))),$$

which is identically zero for all $\lambda \in \mathbb{R}$ if and only if

$$2 \sin(2\pi\alpha) + \sin(2\pi(2\alpha + \beta)) = 0 \quad \text{and} \quad \sin(4\pi\alpha) + 2 \sin(2\pi(\alpha + \beta)) = 0.$$

Using the shorthands $X = \cos(2\pi\alpha)$ and $Y = \cos(2\pi\beta)$, and applying several trig identities (double-angle formula, sum-to-product formula), we rewrite the last condition as

$$(4.1) \quad (2 + 2XY)\sqrt{1-X^2} = (1-2X^2)\sqrt{1-Y^2},$$

$$(4.2) \quad \text{and} \quad (X+Y)\sqrt{1-X^2} = -X\sqrt{1-Y^2}.$$

TABLE 1. Case I. The **bold-faced** number is a double zero of $\mathcal{D}(\beta, \cdot)$.

α	β	$\Psi(\alpha, \beta, x)$	\mathbb{R} -valued zeros of $\Psi(\alpha, \beta, \cdot)$
0	0	$(1-x)^2 + \frac{3}{4}(1-x) + \frac{1}{8}$	$\frac{\mathbf{5}}{\mathbf{4}}, \frac{3}{2}$
0	$\frac{1}{2}$	$(1-x)^2 + \frac{1}{4}(1-x) - \frac{1}{8}$	$\frac{\mathbf{3}}{\mathbf{4}}, \frac{3}{2}$
$\frac{1}{2}$	0	$(1-x)^2 - \frac{1}{4}(1-x) - \frac{1}{8}$	$\frac{1}{2}, \frac{\mathbf{5}}{\mathbf{4}}$
$\frac{1}{2}$	$\frac{1}{2}$	$(1-x)^2 - \frac{3}{4}(1-x) + \frac{1}{8}$	$\frac{1}{2}, \frac{\mathbf{3}}{\mathbf{4}}$

Now square both sides of (4.1) and (4.2) and simplify to get

$$(4.3) \quad (4X^4 + 8X^3Y - 8XY) - Y^2 - 4X^2(Y^2 - 1) + 4X(Y^2 - 1) - 3 = 0,$$

$$(4.4) \quad X^4 + 2X^3Y - 2XY = Y^2.$$

Using (4.4) we replace $4X^4 + 8X^3Y - 8XY$ by $4Y^2$ in (4.3), which can then be simplified to yield $(4X^2 - 4X + 3)(Y^2 - 1) = 0$. So $X = \cos(2\pi\alpha) = -\frac{1}{2}$ or $\frac{3}{2}$ (the latter is impossible), or $Y = \cos(2\pi\beta) = \pm 1$. In addition, by substituting $-\frac{1}{2}$ for X in (4.1), we see that $Y = \frac{3 \pm i\sqrt{2}}{2}$ is \mathbb{C} -valued, so X cannot be $-\frac{1}{2}$. Thus it must be that $\cos(2\pi\beta) = \pm 1$, so $\beta = 0$ or $\frac{1}{2}$. In turn $\cos(2\pi\alpha)$ has to be ± 1 , *i.e.*, $\alpha = 0$ or $\frac{1}{2}$. \square

We shall refer to the case $\alpha, \beta \in \{0, \frac{1}{2}\}$ as Case I.

4.1. Case-by-case analysis of the exceptional set. In this subsection we systematically identify the exceptional set for spectral decimation of \mathcal{L}_N^ω , *cf.* (3.6). In fact, since $\sigma(\mathcal{L}_N^\omega) \subset \mathbb{R}$, it suffices to consider only consider real numbers in this set, namely:

$$(4.5) \quad \mathcal{E}(\alpha, \beta) = \{x \in \mathbb{R} : \mathcal{D}(\beta, x) = 0 \text{ or } \phi(\alpha, \beta, x) = 0\}.$$

Recalling the cubic polynomial (2.18), which is the characteristic polynomial of a Hermitian 3×3 matrix, we see that the three zeros of $\mathcal{D}(\beta, \cdot)$ (which does not depend on α) belong to $\mathcal{E}(\alpha, \beta)$. For reasons to be made clear later, we shall determine if any of the zeros have multiplicity.

Lemma 4.2. *The cubic polynomial $\mathcal{D}(\beta, \cdot)$, (2.18), has a multiple zero only if:*

- $\beta = 0$, in which case the zeros are $\frac{5}{4}$ (double) and $\frac{1}{2}$;
- $\beta = \frac{1}{2}$, in which case the zeros are $\frac{3}{4}$ (double) and $\frac{3}{2}$.

Proof. It is easy to see that for any β , $\mathcal{D}(\beta, \cdot)$ cannot have a triple zero, since there is no $c \in \mathbb{R}$ such that $\mathcal{D}(\beta, x) = -(x-c)^3$. To exhibit the double zeros, we find $c, c' \in \mathbb{R}$ such that $\mathcal{D}(\beta, x) = -(x-c)^2(x-c')$. The RHS can be expanded to give $-x^3 + (c' + 2c)x^2 - c(2c' + c)x + c'c^2$. Equating the coefficients on both sides leads to the system of equations $c' + 2c = 3$, $c(2c' + c) = \frac{45}{16}$, and $c'c^2 = \frac{13}{16} - \frac{1}{32} \cos(2\pi\beta)$. The claim follows. \square

So it remains to identify the \mathbb{R} -valued zeros of $\phi(\alpha, \beta, \cdot)$, *cf.* (2.23) or (2.26). Actually we shall identify the \mathbb{R} -valued zeros of $\Psi(\alpha, \beta, \cdot)$, and check if any of them happens also to be a zero of $\mathcal{D}(\beta, \cdot)$.

In Case I, we indicate in Table 1 the quadratic polynomial Ψ and its \mathbb{R} -valued zeros.

Beyond Case I we must apply Corollary 2.2-(2). The next natural scenario is when exactly one of α and β belongs to $\{0, \frac{1}{2}\}$. We call this Case II. In this case there is only one \mathbb{R} -valued zero of $\Psi(\alpha, \beta, \cdot)$, see Table 2.

TABLE 2. Case II. The **bold-faced** number is a double zero of $\mathcal{D}(\beta, \cdot)$.

α	β	$\Psi(\alpha, \beta, x)$	\mathbb{R} -valued zero of $\Psi(\alpha, \beta, \cdot)$
0	$\notin \{0, \frac{1}{2}\}$	$((1-x) + \frac{1}{2}) ((1-x) + \frac{1}{4}e^{-2\pi i\beta})$	$\frac{3}{2}$
$\notin \{0, \frac{1}{2}\}$	$\frac{1}{2}$	$((1-x) - \frac{1}{4}) ((1-x) - \frac{1}{4}e^{-4\pi i\alpha} + \frac{1}{2}e^{-2\pi i\alpha} + \frac{1}{4})$	$\frac{3}{4}$
$\frac{1}{2}$	$\notin \{0, \frac{1}{2}\}$	$((1-x) - \frac{1}{2}) ((1-x) + \frac{1}{4}e^{-2\pi i\beta})$	$\frac{1}{2}$
$\notin \{0, \frac{1}{2}\}$	0	$((1-x) + \frac{1}{4}) ((1-x) + \frac{1}{4}e^{-4\pi i\alpha} + \frac{1}{2}e^{-2\pi i\alpha} - \frac{1}{4})$	$\frac{5}{4}$

Now we consider $\alpha, \beta \notin \{0, \frac{1}{2}\}$. It turns out that there is a line in the (α, β) -parameter space on which $\Psi(\alpha, \beta, \cdot)$ has an \mathbb{R} -valued zero. This line corresponds to having half-integer fluxes through all the upright triangles of side length 2 in the graph distance.

Proposition 4.3. *Suppose $\alpha, \beta \notin \{0, \frac{1}{2}\}$. Then $\Psi(\alpha, \beta, \cdot)$ has an \mathbb{R} -valued zero if and only if $3\alpha + \beta = \frac{1}{2} \pmod{1}$. If so, this zero is unique, equals $1 + \frac{1}{2} \cos(2\pi\alpha)$, and is not a zero of $\mathcal{D}(\beta, \cdot)$.*

Proof. We solve $\operatorname{Re}(\Psi(\alpha, \beta, x)) = 0$ and $\operatorname{Im}(\Psi(\alpha, \beta, x)) = 0$ simultaneously. Let us mention that the assumption $\alpha, \beta \notin \{0, \frac{1}{2}\}$ implies that $\sin(2\pi\alpha) \neq 0$ and $\sin(2\pi\beta) \neq 0$. Denoting $\eta = 1 - x$, we have

$$\operatorname{Re}(\Psi(\alpha, \beta, \lambda)) = \eta^2 + \frac{\eta}{4} (2 \cos(2\pi\alpha) + \cos(2\pi(2\alpha + \beta))) + \frac{1}{16} (\cos(4\pi\alpha) + 2 \cos(2\pi(\alpha + \beta)) - 1),$$

$$\operatorname{Im}(\Psi(\alpha, \beta, \lambda)) = \frac{\eta}{4} (2 \sin(2\pi\alpha) + \sin(2\pi(2\alpha + \beta))) + \frac{1}{16} (\sin(4\pi\alpha) + 2 \sin(2\pi(\alpha + \beta))).$$

Then $\operatorname{Im}(\Psi) = 0$ is equivalent to

$$(4.6) \quad \eta = -\frac{1}{4} \cdot \frac{\sin(4\pi\alpha) + 2 \sin(2\pi(\alpha + \beta))}{2 \sin(2\pi\alpha) + \sin(2\pi(2\alpha + \beta))}.$$

Substitute this into $\operatorname{Re}(\Psi) = 0$ to get

$$\frac{(\sin(4\pi\alpha) + 2 \sin(2\pi(\alpha + \beta)))^2}{(2 \sin(2\pi\alpha) + \sin(2\pi(2\alpha + \beta)))^2} - \frac{(2 \cos(2\pi\alpha) + \cos(2\pi(2\alpha + \beta)))(\sin(4\pi\alpha) + 2 \sin(2\pi(\alpha + \beta)))}{2 \sin(2\pi\alpha) + \sin(2\pi(2\alpha + \beta))} + (\cos(4\pi\alpha) + 2 \cos(2\pi(\alpha + \beta)) - 1) = 0.$$

Now multiply both sides by $[2 \sin(2\pi\alpha) + \sin(2\pi(2\alpha + \beta))]^2$, a nonzero quantity, to get

$$\begin{aligned} & [\sin(4\pi\alpha) + 2 \sin(2\pi(\alpha + \beta))]^2 - [2 \sin(2\pi\alpha) + \sin(2\pi(2\alpha + \beta))]^2 \\ & - (2 \sin(2\pi\alpha) + \sin(2\pi(2\alpha + \beta))) \times [(2 \cos(2\pi\alpha) + \cos(2\pi(2\alpha + \beta)))(\sin(4\pi\alpha) + 2 \sin(2\pi(\alpha + \beta))) \\ & - (\cos(4\pi\alpha) + 2 \cos(2\pi(\alpha + \beta)))(2 \sin(2\pi\alpha) + \sin(2\pi(2\alpha + \beta)))] = 0. \end{aligned}$$

Combining the appropriate terms in the last square bracket and using the sum-to-difference formulas for sine, we can simplify the last equation to

$$(4.7) \quad \begin{aligned} & [\sin(4\pi\alpha) + \sin(2\pi(2\alpha + \beta)) + 2 \sin(2\pi(\alpha + \beta)) + 2 \sin(2\pi\alpha)] \\ & \times [\sin(4\pi\alpha) - \sin(2\pi(2\alpha + \beta)) + 2 \sin(2\pi(\alpha + \beta)) - 2 \sin(2\pi\alpha)] \\ & - 3 \sin(2\pi\beta)(2 \sin(2\pi\alpha) + \sin(2\pi(2\alpha + \beta))) = 0. \end{aligned}$$

Another application of the sum-to-product formulas on the sine functions reduces the expressions in the square brackets of (4.7), giving rise to

$$\begin{aligned} & 2 \cos(\pi\beta) \cdot [2 \sin(\pi(2\alpha + \beta)) + \sin(\pi(4\alpha + \beta))] \times 2 \sin(\pi\beta) \cdot [2 \cos(\pi(2\alpha + \beta)) - \cos(\pi(4\alpha + \beta))] \\ & - 3 \sin(2\pi\beta)(2 \sin(2\pi\alpha) + \sin(2\pi(2\alpha + \beta))) = 0. \end{aligned}$$

We then divide both sides by $2 \sin(2\pi\beta) = 2 \cos(\pi\beta) \sin(\pi\beta)$ to get

$$(4.8) \quad [2 \sin(\pi(2\alpha + \beta)) + \sin(\pi(4\alpha + \beta))][2 \cos(\pi(2\alpha + \beta)) - \cos(\pi(4\alpha + \beta))] - \frac{3}{2}(2 \sin(2\pi\alpha) + \sin(2\pi(2\alpha + \beta))) = 0.$$

Now we expand the first term on the LHS of (4.8), and use the double-angle formula and the sum-to-difference formulas for sine to simplify (4.8) to

$$(4.9) \quad \frac{1}{2}(\sin(2\pi(2\alpha + \beta)) - \sin(2\pi(4\alpha + \beta))) - \sin(2\pi\alpha) = 0.$$

Applying again the sum-to-product formula to the first term on the LHS of (4.9), we get

$$\sin(2\pi\alpha)(\cos(2\pi(3\alpha + \beta)) + 1) = 0.$$

Since $\sin(2\pi\alpha) \neq 0$, it must be that $\cos(2\pi(3\alpha + \beta)) + 1 = 0$, *i.e.*, $3\alpha + \beta = \frac{1}{2} \pmod{1}$. Finally, substitute this back into (4.6) leads to the conclusion that $1 + \frac{1}{2} \cos(2\pi\alpha)$ is the only zero of $\Psi(\alpha, \beta, \cdot)$. \square

In a nutshell, we have established four cases from which the exceptional set for spectral decimation is analyzed. They are:

Case I: $\alpha, \beta \in \{0, \frac{1}{2}\}$. Spectral decimation can be carried out explicitly (§4.2).

Case II: Only one of α and β is in $\{0, \frac{1}{2}\}$. There is only one \mathbb{R} -valued zero of $\Psi(\alpha, \beta, \cdot)$, which may or may not be a (double) zero of $\mathcal{D}(\beta, \cdot)$.

Case III: $3\alpha + \beta = \frac{1}{2} \pmod{1}$, excluding flux values already discussed in Cases A & B. There is only one \mathbb{R} -valued zero of $\Psi(\alpha, \beta, \cdot)$, and it is not a zero of $\mathcal{D}(\beta, \cdot)$.

Case IV: The remaining case. There are no \mathbb{R} -valued zeros of $\Psi(\alpha, \beta, \cdot)$.

These are indicated in the flux parameter space in Figure 8, and we summarize our main findings as follows.

Proposition 4.4 (Exceptional set for spectral decimation of \mathcal{L}_N^ω). *The exceptional set $\mathcal{E}(\alpha, \beta)$ consists of:*

- The three zeros of $\mathcal{D}(\beta, \cdot)$; and
- The corresponding values x in Table 3 if any of the conditions in the first column is met.

TABLE 3

Condition	Value x to be added to $\mathcal{E}(\alpha, \beta)$
$\alpha = 0$	$\frac{3}{2}$
$\alpha = \frac{1}{2}$	$\frac{1}{2}$
$3\alpha + \beta = \frac{1}{2} \pmod{1}$	$1 + \frac{1}{2} \cos(2\pi\alpha)$

4.2. Spectrum under (half-)integer fluxes. In this subsection we solve $\sigma(\mathcal{L}_N^\omega)$ in Case I, and thereby proving Theorem 1. Here we use Corollary 2.2-(1), where all the functions are explicit polynomial or rational functions. This allows us to spectrally decimate \mathcal{L}_N^ω all the way to $\mathcal{L}_0^{(0,0)}$, as Figure 2 indicates.

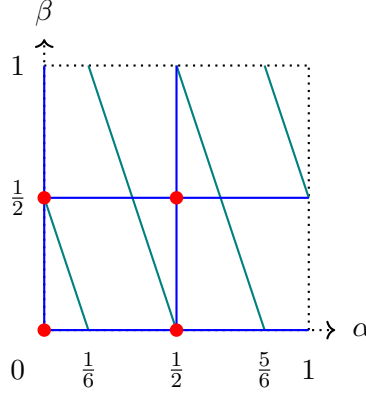


FIGURE 8. The four cases in the analysis of the exceptional set for spectral decimation of \mathcal{L}_N^ω , indicated in the flux parameter space $(\alpha, \beta) \in [0, 1) \times [0, 1)$: **Case I**, **Case II**, **Case III**, and **Case IV** (white space).

4.2.1. $\alpha_N = \beta_N = 0$. We have $\alpha_{N-1} = 3\alpha_N + \beta_N = 0$ and $\beta_{N-1} = 3\beta_N + \alpha_N = 0$. This case corresponds to spectral decimation of the usual graph Laplacian, which has been solved in [42, Section 3] (see also [3, Section 5]). In the literature mentioned, the first three steps below are obtained by first observing that 1 is an eigenvalue on level 0, and then using Lemma 3.4 and the appropriate cases in Lemma 3.6. For the last two steps, we observe that the eigenvalues $\frac{3}{4}$ and $\frac{5}{4}$ first appear on level 1 and level 2, respectively, and that they lead to their corresponding series by spectral decimation.

$$\Psi(0, 0, \lambda) = \left(\lambda - \frac{3}{2}\right) \left(\lambda - \frac{5}{4}\right), \quad \mathcal{D}(0, \lambda) = -\frac{1}{32}(2\lambda - 1)(4\lambda - 5)^2,$$

$$\phi(0, 0, \lambda) = -\frac{\lambda - \frac{3}{2}}{(\lambda - \frac{1}{2})(4\lambda - 5)}, \quad R(0, 0, \lambda) = \lambda(5 - 4\lambda), \quad \mathcal{E}(0, 0) = \left\{\frac{1}{2}, \frac{5}{4}, \frac{3}{2}\right\}.$$

The enumeration of the spectrum proceeds in 5 steps.

(1) $\text{mult}(\mathcal{L}_N^{(0,0)}, 0) = 1$ by induction on N and Lemma 3.4. This result is consistent with the Perron-Frobenius theorem.

(2) $\frac{3}{2} \in \mathcal{E}(0, 0)$, and $\text{mult}(\mathcal{L}_N^{(0,0)}, \frac{3}{2}) = \frac{3^N + 3}{2}$ by Lemma 3.6-(ii).

(3) $\frac{1}{2} \in \mathcal{E}(0, 0)$, and $\text{mult}(\mathcal{L}_N^{(0,0)}, \frac{1}{2}) = 0$ by Lemma 3.6-(iii).

(4) $\frac{3}{4}$ -series: For $k \in \{0, 1, \dots, N-1\}$, $\text{mult}(\mathcal{L}_N^{(0,0)}, (R(0, 0, \cdot))^{-k}(\frac{3}{4})) = \frac{3^{N-k-1} + 3}{2}$ by Lemma 3.4 and Lemma 3.6-(iii).

(5) $\frac{5}{4}$ -series: For $k \in \{0, 1, \dots, N-1\}$, $\text{mult}(\mathcal{L}_N^{(0,0)}, (R(0, 0, \cdot))^{-k}(\frac{5}{4})) = \frac{3^{N-k-1} - 1}{2}$ by Lemma 3.4 and Lemma 3.6-(iii). Note that $\text{mult}(\mathcal{L}_N^{(0,0)}, (R(0, 0, \cdot))^{-(N-1)}(\frac{5}{4})) = 0$.

Adding the multiplicities from these 5 items, we have

$$1 + \frac{3^N + 3}{2} + \sum_{k=0}^{N-1} \frac{3^{N-k-1} + 3}{2} \cdot 2^k + \sum_{k=0}^{N-2} \frac{3^{N-k-1} - 1}{2} \cdot 2^k = \frac{3^{N+1} + 3}{2} = \dim_N,$$

which gives the correct dimension count.

As an aside, note that the preimage of \mathbb{R}_+ under $R(0, 0, \cdot)$ is $[0, \frac{5}{4}]$. It is then direct to see that $\sigma(\mathcal{L}_N^{(0,0)})$ is contained in $[0, \frac{5}{4}] \cup \{\frac{3}{2}\}$.

4.2.2. $\alpha_N = \beta_N = \frac{1}{2}$. We have $\alpha_{N-1} = 3\alpha_N + \beta_N = 0$ and $\beta_{N-1} = 3\beta_N + \alpha_N = 0$,

$$\begin{aligned} \Psi\left(\frac{1}{2}, \frac{1}{2}, \lambda\right) &= \left(\lambda - \frac{1}{2}\right)\left(\lambda - \frac{3}{4}\right), \quad \mathcal{D}\left(\frac{1}{2}, \lambda\right) = -\frac{1}{32}(2\lambda - 3)(4\lambda - 3)^2, \\ \phi\left(\frac{1}{2}, \frac{1}{2}, \lambda\right) &= -\frac{\lambda - \frac{1}{2}}{(\lambda - \frac{3}{2})(4\lambda - 3)}, \quad R\left(\frac{1}{2}, \frac{1}{2}, \lambda\right) = -(\lambda - 2)(4\lambda - 3), \quad \mathcal{E}\left(\frac{1}{2}, \frac{1}{2}\right) = \left\{\frac{1}{2}, \frac{3}{4}, \frac{3}{2}\right\}. \end{aligned}$$

(1) Since $0 \in \sigma(\mathcal{L}_{N-1}^{(0,0)})$, we consider its preimages under $R(\frac{1}{2}, \frac{1}{2}, \cdot)$, which are 2 and $\frac{3}{4}$ (exceptional). Since $\phi(\frac{1}{2}, \frac{1}{2}, 2) \neq 0$ and $\mathcal{D}(\frac{1}{2}, 2) \neq 0$, we can apply Lemma 3.4 to get

$$\text{mult}\left(\mathcal{L}_N^{(\frac{1}{2}, \frac{1}{2})}, 2\right) = \text{mult}\left(\mathcal{L}_{N-1}^{(0,0)}, 0\right) = 1.$$

Next we treat each of the three exceptional values.

(2) We see that $\mathcal{D}(\frac{1}{2}, \frac{1}{2}) \neq 0$ and $\phi(\frac{1}{2}, \frac{1}{2}, \frac{1}{2}) = 0$. So Lemma 3.6-(ii) applies and

$$\text{mult}\left(\mathcal{L}_N^{(\frac{1}{2}, \frac{1}{2})}, \frac{1}{2}\right) = \frac{3^N + 3}{2}.$$

(3) Since $\mathcal{D}(\frac{1}{2}, \frac{3}{4}) = 0$, $\phi(\frac{1}{2}, \frac{1}{2}, \cdot)$ has a pole at $\frac{3}{4}$, and $R(\frac{1}{2}, \frac{1}{2}, \frac{3}{4}) = 0$, Lemma 3.6-(iii) applies and

$$\text{mult}\left(\mathcal{L}_N^{(\frac{1}{2}, \frac{1}{2})}, \frac{3}{4}\right) = 3^{N-1} \cdot 2 - \frac{3^N + 3}{2} + \text{mult}\left(\mathcal{L}_{N-1}^{(0,0)}, 0\right) = \frac{3^{N-1} - 1}{2}.$$

(4) The last exceptional value $\frac{3}{2}$ satisfies the same conditions as $\frac{3}{4}$, and $R(\frac{1}{2}, \frac{1}{2}, \frac{3}{2}) = \frac{3}{2}$, so Lemma 3.6-(iii) applies.

$$\text{mult}\left(\mathcal{L}_N^{(\frac{1}{2}, \frac{1}{2})}, \frac{3}{2}\right) = 3^{N-1} - \frac{3^N + 3}{2} + \text{mult}\left(\mathcal{L}_{N-1}^{(0,0)}, \frac{3}{2}\right) = 0.$$

(5) We need to consider the other preimage of $\frac{3}{2}$ under $R(\frac{1}{2}, \frac{1}{2}, \cdot)$, which is $\frac{5}{4}$. Given that $\mathcal{D}(\frac{1}{2}, \frac{5}{4}) \neq 0$ and $\phi(\frac{1}{2}, \frac{1}{2}, \frac{5}{4}) \neq 0$, Lemma 3.4 applies.

$$\text{mult}\left(\mathcal{L}_N^{(\frac{1}{2}, \frac{1}{2})}, \frac{5}{4}\right) = \text{mult}\left(\mathcal{L}_{N-1}^{(0,0)}, \frac{3}{2}\right) = \frac{3^{N-1} + 3}{2}.$$

(6) We learned that all the eigenvalues in $\sigma(\mathcal{L}_{N-1}^{(0,0)})$, except 0 and $\frac{3}{2}$ whose preimages we have considered, belong to the $\frac{3}{4}$ -series or $\frac{5}{4}$ -series, and lie in $[0, \frac{3}{2}]$. Since $R(\frac{1}{2}, \frac{1}{2}, \lambda) = -4(\lambda - \frac{11}{8})^2 + \frac{25}{16}$, then each eigenvalue of the $\frac{3}{4}$ -series and $\frac{5}{4}$ -series has two positive real preimages under $R(\frac{1}{2}, \frac{1}{2}, \cdot)$. We have

$$\begin{aligned} \text{mult}\left(\mathcal{L}_N^{(\frac{1}{2}, \frac{1}{2})}, \left(R\left(\frac{1}{2}, \frac{1}{2}, \cdot\right)\right)^{-1} \circ (R(0, 0, \cdot))^{-k}\left(\frac{3}{4}\right)\right) &= \frac{3^{N-k-2} + 3}{2}, \quad k \in \{0, 1, \dots, N-2\}, \\ \text{mult}\left(\mathcal{L}_N^{(\frac{1}{2}, \frac{1}{2})}, \left(R\left(\frac{1}{2}, \frac{1}{2}, \cdot\right)\right)^{-1} \circ (R(0, 0, \cdot))^{-k}\left(\frac{5}{4}\right)\right) &= \frac{3^{N-k-2} - 1}{2}, \quad k \in \{0, 1, \dots, N-3\}. \end{aligned}$$

These give rise to

$$2\left(\dim_{N-1} - \text{mult}\left(\mathcal{L}_{N-1}^{(0,0)}, \frac{3}{2}\right) - \text{mult}\left(\mathcal{L}_{N-1}^{(0,0)}, 0\right)\right) = 2\left(\dim_{N-1} - \frac{3^{N-1} + 3}{2} - 1\right) = 2(3^{N-1} - 1)$$

many eigenvalues.

The total count of eigenvalues from the foregoing 6 items is

$$1 + \frac{3^N + 3}{2} + \frac{3^{N-1} - 1}{2} + 0 + \frac{3^{N-1} + 3}{2} + 2(3^{N-1} - 1) = \frac{3^{N+1} + 3}{2} = \dim_N,$$

as desired.

As an aside, note that the eigenvalues in the first 5 items do not fall into the interval $(\frac{1}{2}, \frac{3}{4})$. Also, the eigenvalues in item 6, which are preimages of $R(\frac{1}{2}, \frac{1}{2}, \cdot)$, are in $[\frac{3}{4}, 2]$, also outside of $(\frac{1}{2}, \frac{3}{4})$. This is consistent with the gap $(\frac{1}{2}, \frac{3}{4})$ observed in the numerically generated spectrum shown in Figure 3.

4.2.3. $\alpha_N = \frac{1}{2}, \beta_N = 0$. In this case $\alpha_{N-1} = 3\alpha_N + \beta_N = \frac{1}{2}$ and $\beta_{N-1} = 3\beta_N + \alpha_N = \frac{1}{2}$,

$$\begin{aligned} \Psi\left(\frac{1}{2}, 0, \lambda\right) &= \left(\lambda - \frac{1}{2}\right) \left(\lambda - \frac{5}{4}\right), \quad \mathcal{D}(0, \lambda) = -\frac{1}{32}(2\lambda - 1)(4\lambda - 5)^2, \\ \phi\left(\frac{1}{2}, 0, \lambda\right) &= -\frac{1}{4\lambda - 5}, \quad R\left(\frac{1}{2}, 0, \lambda\right) = -4\lambda^2 + 9\lambda - 3, \quad \mathcal{E}\left(\frac{1}{2}, 0\right) = \left\{\frac{1}{2}, \frac{5}{4}\right\}. \end{aligned}$$

We consider the two values in the exceptional set first.

(1) The first exceptional value $\frac{1}{2}$ satisfies $\mathcal{D}(0, \frac{1}{2}) = 0$ and $\phi(\frac{1}{2}, 0, \frac{1}{2}) \neq 0$. Moreover, both ϕ and ϕR are bounded in a neighborhood of $\frac{1}{2}$, and $\partial_\lambda R(\frac{1}{2}, 0, \frac{1}{2}) \neq 0$. Also $R(\frac{1}{2}, 0, \frac{1}{2}) = \frac{1}{2}$. Therefore Lemma 3.6-(iv) applies and

$$\text{mult}\left(\mathcal{L}_N^{(\frac{1}{2}, 0)}, \frac{1}{2}\right) = 3^{N-1} + \text{mult}\left(\mathcal{L}_{N-1}^{(\frac{1}{2}, \frac{1}{2})}, \frac{1}{2}\right) = 3^{N-1} + \frac{3^{N-1} + 3}{2} = \frac{3^N + 3}{2}.$$

(2) The second exceptional value $\frac{5}{4}$ satisfies all the conditions in Lemma 3.6-(iii). We also know that $R(\frac{1}{2}, 0, \frac{5}{4}) = 2$. So we get

$$\text{mult}\left(\mathcal{L}_N^{(\frac{1}{2}, 0)}, \frac{5}{4}\right) = 3^{N-1} \cdot 2 - \frac{3^N + 3}{2} + \text{mult}\left(\mathcal{L}_{N-1}^{(\frac{1}{2}, \frac{1}{2})}, 2\right) = \frac{3^{N-1} - 1}{2}.$$

The next two items deal with the other preimages of $\frac{1}{2}$ and 2, which appeared in the first two steps and belong to $\sigma(\mathcal{L}_{N-1}^{(\frac{1}{2}, \frac{1}{2})})$.

(3) $\frac{7}{4}$ is the other preimage of $\frac{1}{2}$ under $R(\frac{1}{2}, 0, \cdot)$. Lemma 3.4 applies and

$$\text{mult}\left(\mathcal{L}_N^{(\frac{1}{2}, 0)}, \frac{7}{4}\right) = \text{mult}\left(\mathcal{L}_{N-1}^{(\frac{1}{2}, \frac{1}{2})}, \frac{1}{2}\right) = \frac{3^{N-1} + 3}{2}.$$

(4) 1 is the other preimage of 2 under $R(\frac{1}{2}, 0, \cdot)$. Lemma 3.4 applies and

$$\text{mult}\left(\mathcal{L}_N^{(\frac{1}{2}, 0)}, 1\right) = \text{mult}\left(\mathcal{L}_{N-1}^{(\frac{1}{2}, \frac{1}{2})}, 2\right) = 1.$$

(5) We apply Lemma 3.4 to all eigenvalues of $\sigma(\mathcal{L}_{N-1}^{(\frac{1}{2}, \frac{1}{2})}) \setminus \{\frac{1}{2}, 2\}$. First, we would like to investigate $\frac{3}{4}$ and $\frac{3}{2}$, which are the remaining two values in $\mathcal{E}(\frac{1}{2}, \frac{1}{2})$. Since $\frac{3}{2} \notin \sigma(\mathcal{L}_{N-1}^{(\frac{1}{2}, \frac{1}{2})})$, we can ignore it. As for $\frac{3}{4}$, its preimages do not lie in $\mathcal{E}(\frac{1}{2}, 0)$, so Lemma 3.4 applies. Moreover, all eigenvalues in $\sigma(\mathcal{L}_{N-1}^{(\frac{1}{2}, \frac{1}{2})}) \setminus \{\frac{1}{2}, 2\}$ are in $[\frac{3}{4}, 2]$ and $R(\frac{1}{2}, 0, \lambda) = -4(\lambda - \frac{9}{8})^2 + \frac{33}{16}$, so Lemma 3.4 applies and they all have two positive real preimages under $R(\frac{1}{2}, 0, \cdot)$. So in total they contribute to $\sigma(\mathcal{L}_N^{(\frac{1}{2}, 0)})$

$$2 \left(\dim_{N-1} - \text{mult}\left(\mathcal{L}_{N-1}^{(\frac{1}{2}, \frac{1}{2})}, 2\right) - \text{mult}\left(\mathcal{L}_{N-1}^{(\frac{1}{2}, \frac{1}{2})}, \frac{1}{2}\right) \right) = \frac{2 \cdot 3^N - 2 \cdot 3^{N-1} - 4}{2}$$

eigenvalues.

The total count of eigenvalues is

$$\frac{3^N + 3}{2} + \frac{3^{N-1} - 1}{2} + \frac{3^{N-1} + 3}{2} + 1 + \frac{2 \cdot 3^N - 2 \cdot 3^{N-1} - 4}{2} = \frac{3^{N+1} + 3}{2} = \dim_N.$$

4.2.4. $\alpha_N = 0, \beta_N = \frac{1}{2}$. In this case $\alpha_{N-1} = 3\alpha_N + \beta_N = \frac{1}{2}$ and $\beta_{N-1} = 3\beta_N + \alpha_N = \frac{1}{2}$,

$$\begin{aligned} \Psi\left(0, \frac{1}{2}, \lambda\right) &= \left(\lambda - \frac{3}{4}\right) \left(\lambda - \frac{3}{2}\right), \quad \mathcal{D}\left(\frac{1}{2}, \lambda\right) = -\frac{1}{32}(2\lambda - 3)(4\lambda - 3)^2, \\ \phi\left(0, \frac{1}{2}, \lambda\right) &= -\frac{1}{4\lambda - 3}, \quad R\left(0, \frac{1}{2}, \lambda\right) = -4\lambda^2 + 7\lambda - 1, \quad \mathcal{E}\left(0, \frac{1}{2}\right) = \left\{\frac{3}{4}, \frac{3}{2}\right\}. \end{aligned}$$

The analysis is very similar to that of the previous case $\alpha_N = \frac{1}{2}, \beta_N = 0$.

We consider the two values in the exceptional set first.

(1) The first value $\frac{3}{2}$ is in $\sigma(D)$, and $\phi\left(0, \frac{1}{2}, \lambda\right)$ is neither 0 at $\frac{3}{2}$ nor has a pole at $\frac{3}{2}$. We also know that $R\left(0, \frac{1}{2}, \frac{3}{2}\right) = \frac{1}{2}$. Therefore, we shall apply Lemma 3.6-(iv) to get

$$\text{mult}\left(\mathcal{L}_N^{(0, \frac{1}{2})}, \frac{3}{2}\right) = 3^{N-1} + \text{mult}\left(\mathcal{L}_{N-1}^{(\frac{1}{2}, \frac{1}{2})}, \frac{1}{2}\right) = 3^{N-1} + \frac{3^{N-1} + 3}{2} = \frac{3^N + 3}{2}.$$

(2) The second value in the exceptional set $\frac{3}{4}$ is also in $\sigma(D)$, and satisfies the rest of the conditions in Lemma 3.6-(iii). We also know that $R\left(0, \frac{1}{2}, \frac{3}{4}\right) = 2$. So we get

$$\text{mult}\left(\mathcal{L}_N^{(0, \frac{1}{2})}, \frac{3}{4}\right) = 3^{N-1} \cdot 2 - \frac{3^N + 3}{2} + \text{mult}\left(\mathcal{L}_{N-1}^{(\frac{1}{2}, \frac{1}{2})}, 2\right) = \frac{3^{N-1} - 1}{2}.$$

The next two items deal with the other preimages of $\frac{1}{2}$ and 2 under $R\left(0, \frac{1}{2}, \cdot\right)$.

(3) $\frac{1}{4}$ is the other preimage of $\frac{1}{2}$ under $R\left(\frac{1}{2}, 0, \cdot\right)$, so we use Lemma 3.4 to get

$$\text{mult}\left(\mathcal{L}_N^{(0, \frac{1}{2})}, \frac{1}{4}\right) = \text{mult}\left(\mathcal{L}_{N-1}^{(\frac{1}{2}, \frac{1}{2})}, \frac{1}{2}\right) = \frac{3^{N-1} + 3}{2}.$$

(4) 1 is the other preimage of 2 under $R\left(\frac{1}{2}, 0, \cdot\right)$, so we use Lemma 3.4 to get

$$\text{mult}\left(\mathcal{L}_N^{(\frac{1}{2}, 0)}, 1\right) = \text{mult}\left(\mathcal{L}_{N-1}^{(\frac{1}{2}, \frac{1}{2})}, 2\right) = 1.$$

(5) By the same argument in step (5) of the previous case, all eigenvalues in $\sigma(\mathcal{L}_{N-1}^{(\frac{1}{2}, \frac{1}{2})}) \setminus \{\frac{1}{2}, 2\}$ are in $[\frac{3}{4}, 2]$ and $R\left(0, \frac{1}{2}, \lambda\right) = -4\left(\lambda - \frac{7}{8}\right)^2 + \frac{33}{16}$, so Lemma 3.4 applies and they all have two positive real preimages under $R\left(0, \frac{1}{2}, \cdot\right)$. So in total they contribute to $\sigma(\mathcal{L}_N^{(0, \frac{1}{2})})$

$$\frac{2 \cdot 3^N - 2 \cdot 3^{N-1} - 4}{2}$$

eigenvalues.

The total count of eigenvalues is

$$\frac{3^N + 3}{2} + \frac{3^{N-1} - 1}{2} + \frac{3^{N-1} + 3}{2} + 1 + \frac{2 \cdot 3^N - 2 \cdot 3^{N-1} - 4}{2} = \frac{3^{N+1} + 3}{2} = \dim_N.$$

4.3. Spectrum under non-(half)-integer fluxes. In this subsection we characterize $\sigma(\mathcal{L}_N^\omega)$ in Cases II, III, and IV, thereby proving Theorem 2. Recall from Proposition 4.1 that $\mathbb{R} \ni \lambda \mapsto \Psi(\alpha, \beta, \lambda)$ is \mathbb{C} -valued, so we use Corollary 2.2-(2). In particular the reduced magnetic Laplacian \mathcal{L}_{N-1}^Ω receives a “twist” in the form of a multiplier $e^{2\pi i\theta(\alpha, \beta, \lambda)}$, $\theta(\alpha, \beta, \lambda) = (2\pi)^{-1} \arg \Psi(\alpha, \beta, \lambda)$. The decimation diagram takes the form

$$\mathcal{L}_N^{(\alpha_N, \beta_N)} \xrightarrow{R(\alpha_N, \beta_N, \cdot)} \mathcal{L}_{N-1}^{(\alpha_{N-1}, \beta_{N-1})} \longrightarrow \dots \longrightarrow \mathcal{L}_0^{(\alpha_0, \beta_0)},$$

where for each $n \in \{1, 2, \dots, N\}$, α_{n-1} and β_{n-1} are determined from α_n and β_n via Proposition 2.3. We emphasize again the dependence of the magnetic Laplacians and fluxes on the spectral parameter λ under decimation. That said, to avoid an overcharged notation, we will suppress the flux symbols α_N and β_N in this subsection unless the context requires their presence.

The order of our analysis starts with the case $\Psi(\lambda) \neq 0$, followed by the case $\Psi(\lambda) = 0$.

4.3.1. $\Psi(\lambda) \neq 0$.

Proposition 4.5. *In any of Cases II, III, and IV, suppose $\Psi(\lambda) \neq 0$.*

(G1) *If $\mathcal{D}(\lambda) \neq 0$, then*

$$(4.10) \quad E_\lambda(\mathcal{L}_N^\omega) = \left(\lim_{\mathbb{R} \ni x \rightarrow \lambda} \phi(x) \frac{R(\lambda) - R(x)}{\lambda - x} \right)^{-1} \left(P_\parallel^* - P_\perp^*(D - \lambda)^{-1}C \right) E_{R(\lambda)}(\mathcal{L}_{N-1}^\Omega) \left(P_\parallel - B(D - \lambda)^{-1}P_\perp \right).$$

In particular, $\text{mult}(\mathcal{L}_N^\omega, \lambda) = \text{mult}(\mathcal{L}_{N-1}^\Omega, R(\lambda))$.

(G2) *If $\mathcal{D}(\lambda) = 0$, then λ is a simple zero of \mathcal{D} .*

On the one hand, suppose $\lim_{\mathbb{R} \ni x \rightarrow \lambda} \frac{1}{|\Psi(x)|} \frac{\mathcal{D}(x)(\lambda - x)}{R(\lambda) - R(x)} = 0$. Then

$$\begin{aligned} E_\lambda(\mathcal{L}_N^\omega) &= P_\perp^* E_\lambda(D) P_\perp \\ &+ \left(\lim_{\mathbb{R} \ni x \rightarrow \lambda} \frac{4\mathcal{D}(x)}{(\lambda - x)|\Psi(x)|} \right) P_\perp^* E_\lambda(D) C (\mathcal{L}_{N-1}^\Omega - R(\lambda))^{-1} (I_\parallel - E_{R(\lambda)}(\mathcal{L}_{N-1}^\Omega)) B E_\lambda(D) P_\perp. \end{aligned}$$

In particular, $E_\lambda(\mathcal{L}_N^\omega)(P_\perp^ E_\lambda(D) P_\perp) = E_\lambda(\mathcal{L}_N^\omega)$,*

$$\text{mult}(\mathcal{L}_N^\omega, \lambda) = 3^{N-1} - \dim_{N-1} + \text{mult}(\mathcal{L}_{N-1}^\Omega, R(\lambda)) = -\frac{3^{N-1} + 3}{2} + \text{mult}(\mathcal{L}_{N-1}^\Omega, R(\lambda)),$$

and the corresponding eigenfunction vanishes on V_{N-1} .

On the other hand, suppose $\lim_{\mathbb{R} \ni x \rightarrow \lambda} \frac{1}{|\Psi(x)|} \frac{\mathcal{D}(x)(\lambda - x)}{R(\lambda) - R(x)} \neq 0$. Then

$$(4.11) \quad \begin{aligned} E_\lambda(\mathcal{L}_N^\omega) &= P_\perp^* E_\lambda(D) P_\perp \\ &+ \left(\lim_{\mathbb{R} \ni x \rightarrow \lambda} \frac{4\mathcal{D}(x)}{(\lambda - x)|\Psi(x)|} \right) P_\perp^* E_\lambda(D) C (\mathcal{L}_{N-1}^\Omega - R(\lambda))^{-1} (I_\parallel - E_{R(\lambda)}(\mathcal{L}_{N-1}^\Omega)) B E_\lambda(D) P_\perp \\ &+ \left(P_\parallel^* - P_\perp^*(D - \lambda)^{-1}C \right) \left(\lim_{\mathbb{R} \ni x \rightarrow \lambda} \frac{1}{\phi(x)} \frac{\lambda - x}{R(\lambda) - R(x)} \right) E_{R(\lambda)}(\mathcal{L}_{N-1}^\Omega) \left(P_\parallel - B(D - \lambda)^{-1}P_\perp \right), \end{aligned}$$

and in general

$$\text{mult}(\mathcal{L}_N^\omega, \lambda) = 3^{N-1} - \dim_{N-1} + 2\text{mult}(\mathcal{L}_{N-1}^\Omega, R(\lambda)) = -\frac{3^{N-1} + 3}{2} + 2\text{mult}(\mathcal{L}_{N-1}^\Omega, R(\lambda)).$$

That said, if none of the corresponding eigenfunctions vanishes on V_{N-1} , then the first two terms on the RHS of (4.11) vanish, and $\text{mult}(\mathcal{L}_N^\omega, \lambda) = \text{mult}(\mathcal{L}_{N-1}^\Omega, R(\lambda))$.

Proof. (G1): We are in the setting of Lemma 3.4. The only thing to justify is the existence of the limit on the RHS of (4.10). Indeed, from (2.26) and (2.27) we get

$$\begin{aligned} \phi(x) \frac{R(\lambda) - R(x)}{\lambda - x} &= \frac{|\Psi(x)|}{4\mathcal{D}(x)} \frac{1}{\lambda - x} \left(\frac{A(\lambda) - 64\mathcal{D}(\lambda)(1 - \lambda)}{16|\Psi(\lambda)|} - \frac{A(x) - 64\mathcal{D}(x)(1 - x)}{16|\Psi(x)|} \right) \\ &= \frac{1}{64\mathcal{D}(x)} \frac{1}{\lambda - x} \left(\frac{|\Psi(x)|}{|\Psi(\lambda)|} (A(\lambda) - 64\mathcal{D}(\lambda)(1 - \lambda)) - (A(x) - 64\mathcal{D}(x)(1 - x)) \right) \\ &= \frac{1}{64\mathcal{D}(x)} \left(\frac{F(\lambda) - F(x)}{\lambda - x} + \frac{|\Psi(x)| - |\Psi(\lambda)|}{\lambda - x} \cdot \frac{F(\lambda)}{|\Psi(\lambda)|} \right) \end{aligned}$$

where $F(x) = A(x) - 64\mathcal{D}(x)(1 - x)$, which is analytic. On the other hand, $|\Psi(x)|^2$ is a quadratic polynomial in $x \in \mathbb{R}$. Therefore $|\Psi(x)| = \sqrt{|\Psi(x)|^2}$ is differentiable on \mathbb{R} so long as $\Psi(x) \neq 0$. The claim now follows from the given assumptions.

(G2): By Lemma 4.2, a multiple zero λ of \mathcal{D} occurs only if $\beta = 0$ or $\beta = \frac{1}{2}$, *i.e.*, under Case II. Moreover, by Table 2, λ is also a zero of Ψ . Therefore under the stated conditions λ can only be a simple zero of \mathcal{D} .

Since Ψ is continuous, $\Psi(\lambda) \neq 0$, and $\mathcal{D}(\lambda) = 0$, it follows that $\lim_{\mathbb{R} \ni x \rightarrow \lambda} [\phi(x)]^{-1} = 0$. Thus we are in the setting of either Lemma 3.6-(iii) or Lemma 3.6-(vi), provided that the following two limits exist:

$$(4.12) \quad \lim_{\mathbb{R} \ni x \rightarrow \lambda} \frac{1}{\phi(x)(\lambda - x)} \quad \text{and} \quad \lim_{\mathbb{R} \ni x \rightarrow \lambda} \frac{1}{\phi(x)} \frac{\lambda - x}{R(\lambda) - R(x)}.$$

For the first ratio in (4.12), since λ is a simple zero of \mathcal{D} , and $\Psi(\lambda) \neq 0$,

$$\frac{1}{\phi(x)(\lambda - x)} = \frac{4\mathcal{D}(x)}{|\Psi(x)|(\lambda - x)} = -\frac{4}{|\Psi(x)|} (x - r_1)(x - r_2) \quad \text{for some } r_1, r_2 \neq \lambda.$$

This has a well-defined nonzero limit as $x \rightarrow \lambda$. For the second ratio in (4.12),

$$(4.13) \quad \frac{1}{\phi(x)} \frac{\lambda - x}{R(\lambda) - R(x)} = \frac{4}{|\Psi(x)|} \frac{\mathcal{D}(x)(\lambda - x)}{R(\lambda) - R(x)},$$

the existence of the limit as $x \rightarrow \lambda$ is clear. If this limit is zero (resp. nonzero), Lemma 3.6-(iii) (resp. Lemma 3.6-(vi)) applies. \square

Given our knowledge of the functions \mathcal{D} , Ψ , and A , it would be more satisfying to give concrete criteria for whether the limit of (4.13) is zero. Below is our best attempt using elementary analysis.

By assumption we may write $\mathcal{D}(x) = -(x - \lambda)(x - a)(x - b)$, $a, b \neq \lambda$ being the two other zeros of \mathcal{D} . Also, since $\mathcal{D}(\lambda) = 0$ and $\Psi(\lambda) \neq 0$,

$$\begin{aligned} R(\lambda) - R(x) &= \frac{A(\lambda)}{16|\Psi(\lambda)|} - \frac{A(x) - 64\mathcal{D}(x)(1 - x)}{16|\Psi(x)|} \\ &= \frac{1}{16|\Psi(x)|} (A(\lambda) - A(x) + 64\mathcal{D}(x)(1 - x)) + \frac{A(\lambda)}{16} \left(\frac{1}{|\Psi(\lambda)|} - \frac{1}{|\Psi(x)|} \right). \end{aligned}$$

Therefore (4.13) rewrites as

$$(4.14) \quad 64(x - a)(x - b) \left[\frac{(\lambda - x)^2}{A(\lambda) - A(x) + 64\mathcal{D}(x)(1 - x)} + \frac{|\Psi(\lambda)|}{A(\lambda)} \frac{(\lambda - x)^2}{|\Psi(x)| - |\Psi(\lambda)|} \right].$$

assuming $A(\lambda) \neq 0$. (If $A(\lambda) = 0$, then only the first term inside the square bracket in (4.14) survives.)

Let us note the elementary identity

$$\frac{1}{|\Psi(x)| - |\Psi(\lambda)|} = \frac{|\Psi(x)| + |\Psi(\lambda)|}{|\Psi(x)|^2 - |\Psi(\lambda)|^2}.$$

By Taylor approximation, $|\Psi(\cdot)|^2 - |\Psi(\lambda)|^2$ has a multiple zero at λ if and only if $\frac{d}{dx}|\Psi(x)|^2|_{x=\lambda} = 0$. Therefore the second term in the square bracket in (4.14) converges to 0 as $\mathbb{R} \ni x \rightarrow \lambda$ if and only if $\frac{d}{dx}|\Psi(x)|^2|_{x=\lambda} \neq 0$.

The same reasoning applies to the first term in the square bracket in (4.14). By construction, the polynomial in the denominator must contain at least one factor of $(x - \lambda)$. If it contains multiple factors of $(x - \lambda)$, then the first term converges to a nonzero limit. Luckily we can derive an explicit criterion.

Lemma 4.6. *Assume λ is a zero of $\mathcal{D}(\beta, \cdot)$. Set*

$$\mathcal{H}(\alpha, \beta, x) := A(\alpha, \beta, \lambda) - A(\alpha, \beta, x) + 64\mathcal{D}(\beta, x)(1 - x).$$

Then λ is a multiple zero of $\mathcal{H}(\alpha, \beta, \cdot)$ if and only if

$$(4.15) \quad 8(\lambda - 1) \left(1 - 2 \left(\lambda^2 - 2\lambda(3 - \lambda) + \frac{45}{16} \right) \right) = \cos(2\pi\alpha).$$

Remark. Lemma 4.6 is not vacuous; it is easy to see that (4.15) holds with $\alpha \in \{\frac{1}{4}, \frac{3}{4}\}$, $\beta \in \{\frac{1}{4}, \frac{3}{4}\}$, and $\lambda = 1$. More generally, observe that the LHS of (4.15) depends only on β , whereas the RHS depends only on α . So as long as the LHS has modulus ≤ 1 , there exists α for which (4.15) holds.

Proof of Lemma 4.6. Using (2.17) for $A(\alpha, \beta, \cdot)$, as well as the factorization $\mathcal{D}(\beta, x) = -(x - \lambda)(x - a)(x - b)$, we get

$$\begin{aligned} \mathcal{H}(\alpha, \beta, x) &= 16(\lambda^2 - x^2) - (32 + 4\cos(2\pi\alpha))(\lambda - x) + 64(\lambda - x)(x - a)(x - b)(1 - x) \\ &= 4(\lambda - x) [4(\lambda + x) - 8 - \cos(2\pi\alpha) + 16(x - a)(x - b)(1 - x)]. \end{aligned}$$

Thus λ is a multiple zero of $\mathcal{H}(\alpha, \beta, \cdot)$ if and only if the expression in the square bracket vanishes when $x = \lambda$, *i.e.*,

$$8(\lambda - 1) (1 - 2(\lambda - a)(\lambda - b)) = \cos(2\pi\alpha).$$

We can then replace $a + b$ and ab in terms of λ and coefficients of the cubic polynomial $\mathcal{D}(\beta, \cdot)$ to obtain (4.15). \square

We summarize the above discussions in Table 4.

TABLE 4. Criterion table for Proposition 4.5-(G2)

$\frac{d}{dx} \Psi(x) ^2 _{x=\lambda} = 0$	(4.15) holds	$\lim_{\mathbb{R} \ni x \rightarrow \lambda} \frac{1}{ \Psi(x) } \frac{\mathcal{D}(x)(\lambda - x)}{R(\lambda) - R(x)}$
F	F	0
T	F	nonzero
F	T	nonzero
T	T	0 (if cancellation occurs) or nonzero

4.3.2. $\Psi(\lambda) = 0$. Recall that in Case IV, $\Psi(\lambda) \neq 0$ for any $\lambda \in \mathbb{R}$, so Proposition 4.5 settles the spectral decimation problem in this case. It remains to treat the exceptional values λ in Cases II and III where $\Psi(\lambda) = 0$. These are established in the next two propositions. We begin with the (much) more straightforward case.

Proposition 4.7. *In Case III, if $\lambda = 1 + \frac{1}{2} \cos(2\pi\alpha_N)$, then $\text{mult}(\mathcal{L}_N^\omega, \lambda) = 0$.*

Proof. In this case $\Psi(\lambda) = 0$ and $\mathcal{D}(\lambda) \neq 0$, so $\phi(\lambda) = 0$, $\lim_{\mathbb{R} \ni x \rightarrow \lambda} [R(x)]^{-1} = 0$, and $(\lambda - x)[\phi(x)]^{-1}$ stays bounded as $x \rightarrow \lambda$. Thus we are in the setting of Lemma 3.6-(vii). \square

Now we come to the subtler case. Since $\Psi(x) = (x - \lambda)(x - a)$ for some $a \in \mathbb{C}$, $a \neq \lambda$, it follows that

$$\lim_{x \uparrow \lambda} e^{i(\arg \Psi(x))} = - \lim_{x \downarrow \lambda} e^{i(\arg \Psi(x))},$$

and this implies that the connection $\Omega(x)$ in the reduced Laplacian \mathcal{L}_{N-1}^Ω differs by an overall sign when $x \uparrow \lambda$ compared to when $x \downarrow \lambda$. Precisely we have the identity

$$(4.16) \quad \lim_{x \uparrow \lambda} \operatorname{sgn}(\lambda - x)(\mathcal{L}_{N-1}^\Omega - 1) = \lim_{x \downarrow \lambda} \operatorname{sgn}(\lambda - x)(\mathcal{L}_{N-1}^\Omega - 1).$$

With this in mind we can now state and prove the last remaining case.

Proposition 4.8. *In Case II:*

(II.1) *If either $\alpha_N = 0$, $\beta_N \notin \{0, \frac{1}{2}\}$, and $\lambda = \frac{3}{2}$, or $\alpha_N = \frac{1}{2}$, $\beta_N \notin \{0, \frac{1}{2}\}$, and $\lambda = \frac{1}{2}$, then*

$$E_\lambda(\mathcal{L}_N^\omega) = \left(P_\parallel^* - P_\perp^*(D - \lambda)^{-1}C \right) \left(\lim_{\mathbb{R} \ni x \rightarrow \lambda} \frac{1}{\chi_0(x)} (\mathcal{L}_{N-1}^\Omega - R(x))^{-1} \right) (P_\parallel - B(D - \lambda)^{-1}P_\perp),$$

where $\chi_0(x) = \frac{4(\lambda - x)\mathcal{D}(x)}{|\Psi(x)|}$. In particular, $\operatorname{mult}(\mathcal{L}_N^\omega, \lambda) = \dim_{N-1} = \frac{3^N + 3}{2}$.

(II.2) *If λ is a double zero of \mathcal{D} —that is, either $\beta_N = 0$, $\alpha_N \notin \{0, \frac{1}{2}\}$, and $\lambda = \frac{5}{4}$, or $\beta_N = \frac{1}{2}$, $\alpha_N \notin \{0, \frac{1}{2}\}$, and $\lambda = \frac{3}{4}$ —then the following dichotomy holds.*

On the one hand, if $\alpha_N \in \{\frac{1}{6}, \frac{5}{6}\}$ in the case $\beta_N = 0$ and $\lambda = \frac{5}{4}$, or $\alpha_N \in \{\frac{1}{3}, \frac{2}{3}\}$ in the case $\beta_N = \frac{1}{2}$ and $\lambda = \frac{3}{4}$, then

$$(4.17) \quad \begin{aligned} E_\lambda(\mathcal{L}_N^\omega) &= P_\perp^* E_\lambda(D) P_\perp \\ &+ P_\perp^* E_\lambda(D) C \left(\lim_{\mathbb{R} \ni x \rightarrow \lambda} \frac{1}{\psi_0(x)} (\mathcal{L}_{N-1}^\Omega - R(x))^{-1} \right) (I_\parallel - E_{R(\lambda)}(\mathcal{L}_{N-1}^\Omega)) B E_\lambda(D) P_\perp \\ &+ \left(P_\parallel^* - P_\perp^*(D - \lambda)^{-1}C \right) \left(\lim_{\mathbb{R} \ni x \rightarrow \lambda} \frac{1}{\phi(x)} \frac{\lambda - x}{R(\lambda) - R(x)} E_{R(x)}(\mathcal{L}_{N-1}^\Omega) \right) (P_\parallel - B(D - \lambda)^{-1}P_\perp), \end{aligned}$$

where $\psi_0(x) = \frac{(\lambda - x)|\Psi(x)|}{4\mathcal{D}(x)}$. In general,

$$\operatorname{mult}(\mathcal{L}_N^\omega, \lambda) = 2 \cdot 3^{N-1} - \dim_{N-1} + 2\operatorname{mult}(\mathcal{L}_{N-1}^\Omega, R(\lambda)) = \frac{3^{N-1} - 3}{2} + 2\operatorname{mult}(\mathcal{L}_{N-1}^\Omega, R(\lambda)).$$

That said, if none of the corresponding eigenfunctions vanishes on V_{N-1} , then the first two terms on the RHS of (4.17) vanish, and $\operatorname{mult}(\mathcal{L}_N^\omega, \lambda) = \operatorname{mult}(\mathcal{L}_{N-1}^\Omega, R(\lambda))$.

On the other hand, for all other scenarios

$$\begin{aligned} E_\lambda(\mathcal{L}_N^\omega) &= P_\perp^* E_\lambda(D) P_\perp \\ &+ P_\perp^* E_\lambda(D) C \left(\lim_{\mathbb{R} \ni x \rightarrow \lambda} \frac{1}{\psi_0(x)} (\mathcal{L}_{N-1}^\Omega - R(x))^{-1} \right) (I_\parallel - E_{R(\lambda)}(\mathcal{L}_{N-1}^\Omega)) B E_\lambda(D) P_\perp, \end{aligned}$$

In particular, $E_\lambda(\mathcal{L}_N^\omega)(P_\perp^ E_\lambda(D) P_\perp) = E_\lambda(\mathcal{L}_N^\omega)$,*

$$\operatorname{mult}(\mathcal{L}_N^\omega, \lambda) = 2 \cdot 3^{N-1} - \dim_{N-1} + \operatorname{mult}(\mathcal{L}_{N-1}^\Omega, R(\lambda)) = \frac{3^{N-1} - 3}{2} + \operatorname{mult}(\mathcal{L}_{N-1}^\Omega, R(\lambda)),$$

and the corresponding eigenfunction vanishes on V_{N-1} .

Proof. (II.1): We have $\Psi(\lambda) = 0$, $\mathcal{D}(\lambda) \neq 0$, and thus $\phi(\lambda) = 0$. Nominally this would fall under the scenario of Lemma 3.6-(ii), but we need to address the connection sign change at λ . First we

carry out a tedious but elementary computation to get

$$R(0, \beta, x) = 1 + \frac{x - \frac{3}{2}}{|x - \frac{3}{2}|} \frac{-32x^3 + 80x^2 - 58x + 11 - \cos(2\pi\beta)}{2|4x - 4 - e^{-2\pi i\beta}|}, \text{ if } \alpha = 0, \beta \notin \left\{0, \frac{1}{2}\right\}, \lambda = \frac{3}{2};$$

$$R\left(\frac{1}{2}, \beta, x\right) = 1 + \frac{x - \frac{1}{2}}{|x - \frac{1}{2}|} \frac{-32x^3 + 112x^2 - 122x + 41 - \cos(2\pi\beta)}{2|4x - 4 - e^{-2\pi i\beta}|}, \text{ if } \alpha = \frac{1}{2}, \beta \notin \left\{0, \frac{1}{2}\right\}, \lambda = \frac{1}{2}.$$

In either case we find

$$(4.18) \quad R(x) - 1 = \frac{\lambda - x}{|\lambda - x|} \mathfrak{F}(x)$$

where \mathfrak{F} is bounded in an \mathbb{R} -neighborhood of λ . Consequently,

$$\begin{aligned} \frac{\lambda - x}{\phi(x)} (\mathcal{L}_{N-1}^\Omega - R(x))^{-1} &= 4\mathcal{D}(x) \frac{\lambda - x}{|\Psi(x)|} ((\mathcal{L}_{N-1}^\Omega - 1) - (R(x) - 1))^{-1} \\ &= \frac{4\mathcal{D}(x)}{|x - a|} \frac{\lambda - x}{|\lambda - x|} \left((\mathcal{L}_{N-1}^\Omega - 1) - \frac{\lambda - x}{|\lambda - x|} \mathfrak{F}(x) \right)^{-1} = \frac{4\mathcal{D}(x)}{|x - a|} (\operatorname{sgn}(\lambda - x) (\mathcal{L}_{N-1}^\Omega - 1) - \mathfrak{F}(x))^{-1}, \end{aligned}$$

which has a well-defined nonzero limit as $\mathbb{R} \ni x \rightarrow \lambda$ by (4.16).

(II.2): Since $\Psi(\lambda) = 0$, and λ is a double zero of \mathcal{D} , we have $\lim_{\mathbb{R} \ni x \rightarrow \lambda} [\phi(x)]^{-1} = 0$. This suggests that we are in the setting of either Lemma 3.6-(iii) or Lemma 3.6-(vi), though again we need to account for the connection sign change at λ . A tedious but elementary computation shows that

$$R(\alpha, 0, x) = 1 + \frac{x - \frac{5}{4}}{|x - \frac{5}{4}|} \frac{(4x - 3 - \cos(2\pi\alpha)) + 2(2x - 1)(4x - 5)(1 - x)}{|4x - 3 - e^{-4\pi i\alpha} - 2e^{-2\pi i\alpha}|}, \text{ if } \beta = 0, \alpha \notin \left\{0, \frac{1}{2}\right\}, \lambda = \frac{5}{4};$$

$$R\left(\alpha, \frac{1}{2}, x\right) = 1 + \frac{x - \frac{3}{4}}{|x - \frac{3}{4}|} \frac{(4x - 5 - \cos(2\pi\alpha)) + 2(2x - 3)(4x - 3)(1 - x)}{|4x - 5 + e^{-4\pi i\alpha} - 2e^{-2\pi i\alpha}|}, \text{ if } \beta = \frac{1}{2}, \alpha \notin \left\{0, \frac{1}{2}\right\}, \lambda = \frac{3}{4}.$$

So once again $R(x) - 1$ has the form (4.18). Consequently, the limit as $\mathbb{R} \ni x \rightarrow \lambda$ of

$$\frac{1}{\phi(x)(\lambda - x)} (\mathcal{L}_{N-1}^\Omega - R(x))^{-1} = \frac{4}{|x - a|} \frac{\mathcal{D}(x)}{(\lambda - x)^2} (\operatorname{sgn}(\lambda - x) (\mathcal{L}_{N-1}^\Omega - 1) - \mathfrak{F}(x))^{-1}$$

exists and is nonzero on the image of $I_{\parallel} - E_{R(\lambda)}(\mathcal{L}_{N-1}^\Omega)$. The other quantity to analyze is

$$\begin{aligned} \frac{\lambda - x}{\phi(x)} (\mathcal{L}_{N-1}^\Omega - R(x))^{-1} &= \frac{4\mathcal{D}(x)}{|x - a|} (\operatorname{sgn}(\lambda - x) (\mathcal{L}_{N-1}^\Omega - 1) - \mathfrak{F}(x))^{-1} \\ &= \frac{4(x - r_3)}{|x - a|} \frac{(\lambda - x)^2}{\mathfrak{F}(\lambda) - \mathfrak{F}(x)} (\mathfrak{F}(\lambda) - \mathfrak{F}(x)) (\operatorname{sgn}(\lambda - x) (\mathcal{L}_{N-1}^\Omega - 1) - \mathfrak{F}(x))^{-1}, \end{aligned}$$

where r_3 is the third zero of \mathcal{D} . Since this term acts on the image of $E_{R(\lambda)}(\mathcal{L}_{N-1}^\Omega)$, it remains to determine whether

$$(4.19) \quad \lim_{\mathbb{R} \ni x \rightarrow \lambda} \frac{(\lambda - x)^2}{\mathfrak{F}(\lambda) - \mathfrak{F}(x)}$$

is nonzero, *i.e.*, whether $\mathfrak{F}(\lambda) - \mathfrak{F}(\cdot)$ has a multiple zero at λ . After a computation aided by Mathematica, we verify that the limit (4.19) is nonzero iff: $\alpha \in \left\{\frac{1}{6}, \frac{5}{6}\right\}$ in the case $\beta = 0$ and $\lambda = \frac{5}{4}$; or $\alpha \in \left\{\frac{1}{3}, \frac{2}{3}\right\}$ in the case $\beta = \frac{1}{2}$ and $\lambda = \frac{3}{4}$. In these scenarios we are in the setting of Lemma 3.6-(vi), and otherwise, Lemma 3.6-(iii). \square

Proof of Theorem 2. Combine Propositions 4.5, 4.7, and 4.8 to obtain (1.5). \square

Proof of Proposition 1.3. Proposition 4.5-(G2) and Proposition 4.8-(II.2) implies Item (1) and Item (2), respectively. \square

Proof of Corollary 1.4. By assumption there is no λ which is a double zero of $\mathcal{D}(\beta_N, \cdot)$. Incorporating Proposition 1.3 into Theorem 2 yields (1.7). Now recall from Proposition 4.3 that if $\alpha_N, \beta_N \notin \{0, \frac{1}{2}\}$, then $\Psi(\alpha_N, \beta_N, \cdot)$ has a \mathbb{R} -valued zero iff $3\alpha_N + \beta_N = \frac{1}{2} \pmod{1}$. By Proposition 4.7 this zero is not in the spectrum. This allows us to deduce (1.8) from (1.5) and (1.7). \square

5. MAGNETIC LAPLACIAN DETERMINANTS AND CRSF ASYMPTOTIC COMPLEXITY

In this section we prove Theorem 3 and Corollary 1.7.

First let us recall some simple identities. Let $P(x) = a_d x^d + a_{d-1} x^{d-1} + \dots + a_0$ be a polynomial of degree d . Then

$$\begin{aligned} \{z : z \in P^{-1}(\alpha)\} &= \left\{ z : \alpha = a_d z^d + a_{d-1} z^{d-1} + \dots + a_0 \right\} \\ &= \left\{ z : a_d z^d + a_{d-1} z^{d-1} + \dots + (a_0 - \alpha) = 0 \right\}. \end{aligned}$$

It follows that

$$(5.1) \quad \sum_{z \in P^{-1}(\alpha)} z = -\frac{a_{d-1}}{a_d} \quad \text{and} \quad \prod_{z \in P^{-1}(\alpha)} z = (-1)^d \frac{a_0 - \alpha}{a_d}.$$

Assume $R(x) = b_2 x^2 + b_1 x$ is a quadratic polynomial function with the property that $R(0) = 0$. It can be shown using (5.1) and induction on n that

$$(5.2) \quad \prod_{z \in R^{-n}(\alpha)} z = -\alpha \frac{b_2}{(b_2)^{2^n}}.$$

See [2, Lemma 3.3] for a more general version where R is a rational function satisfying $R(0) = 0$.

For our purposes, we need to involve two additional quadratic polynomials P and Q , without the requirement that $P(0) = 0$ or $Q(0) = 0$.

Lemma 5.1. *Let $P(x) = a_2 x^2 + a_1 x + a_0$ and $R(x) = b_2 x^2 + b_1 x$. Then*

$$F(n, \alpha) := \prod_{z \in P^{-1}(R^{-n}(\alpha))} z = c_{n,1} \alpha + c_{n,0},$$

where $c_{n,1} = -\frac{b_2}{(a_2 b_2)^{2^n}}$, $c_{n,0} = \frac{1}{(a_2 b_2)^{2^n}} \left(H(n) - \frac{b_1}{2} \right)$, and $G(n)$ satisfies the recurrence relation

$$(5.3) \quad H(0) = a_0 b_2 + \frac{b_1}{2}, \quad \text{and for } n \geq 1, \quad H(n) = [H(n-1)]^2 + \frac{b_1(2-b_1)}{4}.$$

Proof. We prove this by induction on n . When $n = 0$, we have by (5.1) that $F(0, \alpha) = \frac{a_0 - \alpha}{a_2}$. Now suppose $F(n, \alpha) = c_{n,1} \alpha + c_{n,0}$ holds. Then denoting the two preimages of R by $R_{(1)}^{-1}$ and $R_{(2)}^{-1}$, we have

$$\begin{aligned} F(n+1, \alpha) &= \prod \left\{ P^{-1}(R^{-(n+1)}(w)) : w = \alpha \right\} = \prod \left\{ P^{-1}(R^{-n}(w)) : w \in R^{-1}(\alpha) \right\} \\ &= F(n, R_{(1)}^{-1}(\alpha)) F(n, R_{(2)}^{-1}(\alpha)) \\ &= c_{n,1}^2 \left(R_{(1)}^{-1}(\alpha) R_{(2)}^{-1}(\alpha) \right) + c_{n,0} c_{n,1} \left(R_{(1)}^{-1}(\alpha) + R_{(2)}^{-1}(\alpha) \right) + c_{n,0}^2 \quad (\text{induction hypothesis}) \\ &= c_{n,1}^2 \left(\frac{-\alpha}{b_2} \right) + c_{n,0} c_{n,1} \left(-\frac{b_1}{b_2} \right) + c_{n,0}^2 \quad (\text{by (5.1)}) \\ &= \left(-\frac{c_{n,1}^2}{b_2} \right) \alpha + \left[c_{n,0}^2 - \frac{b_1}{b_2} c_{n,0} c_{n,1} \right]. \end{aligned}$$

We have thus obtained a system of quadratic recurrence relations

$$c_{n+1,1} = -\frac{1}{b_2}c_{n,1}^2, \quad c_{n+1,0} = c_{n,0}^2 - \frac{b_1}{b_2}c_{n,0}c_{n,1}$$

with initial condition $c_{0,1} = -\frac{1}{a_2}$ and $c_{0,0} = \frac{a_0}{a_2}$. It readily follows that $c_{n,1} = -b_2/(a_2b_2)^{2^n}$ and

$$c_{n+1,0} = c_{n,0}^2 + \frac{b_1}{(a_2b_2)^{2^n}}c_{n,0}.$$

To better see the latter relation, we perform a change of variables $g(n) = c_{n,0} + \frac{1}{2} \frac{b_1}{(a_2b_2)^{2^n}}$ to obtain

$$g(n+1) = [g(n)]^2 + \frac{1}{4} \frac{b_1(2-b_1)}{(a_2b_2)^{2^{n+1}}}.$$

Making another change of variables to $H(n) = g(n)(a_2b_2)^{2^n}$, we deduce (5.3). \square

In general the quadratic recurrence (5.3) cannot be solved in closed form, unless the constant term on the RHS is either 0 or -2 [45], or under specific initial conditions. For instance of the latter, if we assume $a_0 = 0$, then $G(n) = \frac{b_1}{2}$ —and hence $c_{n,0} = 0$ —for all n .

Lemma 5.2. *Let P and R be as in Lemma 5.1, and $Q(x) = q_2x^2 + q_1x + q_0$. Then*

$$\tilde{F}(n, \alpha) := \prod_{z \in Q^{-1} \circ P^{-1}(R^{-n}(\alpha))} z = \tilde{c}_{n,1}\alpha + \tilde{c}_{n,0},$$

where $\tilde{c}_{n,1} = -\frac{b_2}{(q_2^2 a_2 b_2)^{2^n}}$, $\tilde{c}_{n,0} = \frac{1}{(q_2^2 a_2 b_2)^{2^n}} \left(\tilde{H}(n) - \frac{b_1}{2} \right)$, and $\tilde{H}(n)$ satisfies the recurrence relation

$$(5.4) \quad \tilde{H}(0) = a_2 b_2 \left(q_0^2 + q_0 \frac{a_1}{a_2} + \frac{a_0}{a_2} \right) + \frac{b_1}{2}, \quad \text{and for } n \geq 1, \quad \tilde{H}(n) = [\tilde{H}(n-1)]^2 + \frac{b_1(2-b_1)}{4}.$$

Proof. We focus on the initial step $n = 0$:

$$\begin{aligned} \tilde{F}(0, \alpha) &= \left(Q_{(1)}^{-1}(P_{(1)}^{-1}(\alpha)) Q_{(2)}^{-1}(P_{(1)}^{-1}(\alpha)) \right) \left(Q_{(1)}^{-1}(P_{(2)}^{-1}(\alpha)) Q_{(2)}^{-1}(P_{(2)}^{-1}(\alpha)) \right) \\ &= \left(\frac{q_0 - P_{(1)}^{-1}(\alpha)}{q_2} \right) \left(\frac{q_0 - P_{(2)}^{-1}(\alpha)}{q_2} \right) \quad (\text{by (5.1)}) \\ &= \frac{1}{q_2^2} \left(q_0^2 - q_0(P_{(1)}^{-1}(\alpha) + P_{(2)}^{-1}(\alpha)) + P_{(1)}^{-1}(\alpha)P_{(2)}^{-1}(\alpha) \right) \\ &= \left(-\frac{1}{q_2^2 a_2} \right) \alpha + \frac{1}{q_2^2} \left(q_0^2 + q_0 \frac{a_1}{a_2} + \frac{a_0}{a_2} \right) \quad (\text{by (5.1)}). \end{aligned}$$

The induction step is the same as in the proof of Lemma 5.1, except for the changes triggered by the initial conditions. The details are therefore omitted. \square

Proof of Theorem 3. Recall Theorem 1. The computation of $\det'(\mathcal{L}_N^{(0,0)})$ uses (5.2) to treat the preimages $R(0, 0, \cdot)^{-k}(\alpha)$, $\alpha \in \{\frac{3}{4}, \frac{5}{4}\}$. For details we refer the reader to e.g. [2, Theorem 5.1].

Thus we concentrate on the new results. For $\det(\mathcal{L}_N^{(\frac{1}{2}, \frac{1}{2})})$, we use Lemma 5.1 to treat the preimages $R(\frac{1}{2}, \frac{1}{2}, \dots)^{-1} \circ R(0, 0, \cdot)^{-k}(\alpha)$, $\alpha \in \{\frac{3}{4}, \frac{5}{4}\}$. Taking into account multiplicities we obtain

$$\begin{aligned} \det(\mathcal{L}_N^{(\frac{1}{2}, \frac{1}{2})}) &= \left(\frac{1}{2}\right)^{\frac{3^N+3}{2}} \left(\frac{3}{4}\right)^{\frac{3^{N-1}-1}{2}} \left(\frac{5}{4}\right)^{\frac{3^{N-1}+3}{2}} \cdot 2 \\ &\quad \times \left[\prod_{k=0}^{N-2} \left(\left(4 \cdot \frac{3}{4} + H(k) - \frac{5}{2}\right) \frac{1}{16^{2^k}} \right)^{\frac{3^{N-k-2}+3}{2}} \right] \left[\prod_{k=0}^{N-3} \left(\left(4 \cdot \frac{5}{4} + H(k) - \frac{5}{2}\right) \frac{1}{16^{2^k}} \right)^{\frac{3^{N-k-2}-1}{2}} \right], \end{aligned}$$

where $H(0) = 26.5$, and for $k \geq 1$, $H(k) = [H(k-1)]^2 - \frac{15}{4}$.

For the other two determinants, we apply Lemma 5.2 to treat the preimages and obtain

$$\begin{aligned} \det(\mathcal{L}_N^{(0, \frac{1}{2})}) &= \left(\frac{1}{2}\right)^{\frac{3^N+3}{2}} \left(\frac{5}{4}\right)^{\frac{3^{N-1}-1}{2}} \left(\frac{7}{4}\right)^{\frac{3^{N-1}+3}{2}} \cdot \left(\frac{3+\frac{3}{4}}{4}\right)^{\frac{3^{N-2}-1}{2}} \left(\frac{3+\frac{5}{4}}{4}\right)^{\frac{3^{N-2}+3}{2}} \\ &\quad \times \left[\prod_{k=0}^{N-3} \left(\left(4 \cdot \frac{3}{4} + \tilde{H}(k) - \frac{5}{2}\right) \frac{1}{64^{2^k}} \right)^{\frac{3^{N-k-3}+3}{2}} \right] \left[\prod_{k=0}^{N-4} \left(\left(4 \cdot \frac{5}{4} + \tilde{H}(k) - \frac{5}{2}\right) \frac{1}{64^{2^k}} \right)^{\frac{3^{N-k-3}-1}{2}} \right], \end{aligned}$$

where $\tilde{H}(0) = 302.5$, and for $k \geq 1$, $\tilde{H}(k) = [\tilde{H}(k-1)]^2 - \frac{15}{4}$.

$$\begin{aligned} \det(\mathcal{L}_N^{(\frac{1}{2}, 0)}) &= \left(\frac{1}{4}\right)^{\frac{3^{N-1}+3}{2}} \left(\frac{3}{4}\right)^{\frac{3^{N-1}-1}{2}} \left(\frac{3}{2}\right)^{\frac{3^N+3}{2}} \cdot \left(\frac{1+\frac{3}{4}}{4}\right)^{\frac{3^{N-2}-1}{2}} \left(\frac{1+\frac{5}{4}}{4}\right)^{\frac{3^{N-2}+3}{2}} \\ &\quad \times \left[\prod_{k=0}^{N-3} \left(\left(4 \cdot \frac{3}{4} + \hat{H}(k) - \frac{5}{2}\right) \frac{1}{64^{2^k}} \right)^{\frac{3^{N-k-3}+3}{2}} \right] \left[\prod_{k=0}^{N-4} \left(\left(4 \cdot \frac{5}{4} + \hat{H}(k) - \frac{5}{2}\right) \frac{1}{64^{2^k}} \right)^{\frac{3^{N-k-3}-1}{2}} \right], \end{aligned}$$

where $\hat{H}(0) = 86.5$, and for $k \geq 1$, $\hat{H}(k) = [\hat{H}(k-1)]^2 - \frac{15}{4}$. \square

Proof of Corollary 1.7. We present the proof of $\mathfrak{h}(SG, \mathcal{L}_\infty^{(\frac{1}{2}, \frac{1}{2})})$ only, the other two being similar. In particular, we only demonstrate the contribution to the forest entropy from one of the inhomogeneous products, say,

$$\begin{aligned} (5.5) \quad \frac{1}{|V_N|} \log \left[\prod_{k=0}^{N-2} \left(4 \cdot \frac{3}{4} + H(k) - \frac{5}{2} \right)^{\frac{3^{N-k-2}+3}{2}} \right] &= \frac{2}{3^{N+1}+3} \sum_{k=0}^{N-2} \frac{3^{N-k-2}+3}{2} \log \left(H(k) + \frac{1}{2} \right) \\ &= \frac{2}{9} \cdot \frac{1}{3} \sum_{k=0}^{N-2} \left(\frac{3^{-k}}{2} + O(3^{-N}) \right) \log \left(H(k) + \frac{1}{2} \right). \end{aligned}$$

Let us observe that if there exists a fixed constant C such that $H(k) = [H(k-1)]^2 + C$ for all $k \geq 1$, then

$$\log H(k) = 2 \log H(k-1) + \log \left(1 + \frac{C}{[H(k-1)]^2} \right),$$

or

$$\frac{\log H(k)}{2^k} - \frac{\log H(k-1)}{2^{k-1}} = \frac{1}{2^k} \log \left(1 + \frac{C}{[H(k-1)]^2} \right) \leq \frac{1}{2^k} \frac{C}{[H(k-1)]^2}.$$

where we used the inequality $1+x \leq e^x$. Since $\sum_k \frac{1}{2^k [H(k-1)]^2}$ is summable, it follows that $\lim_{k \rightarrow \infty} 2^{-k} \log H(k)$ exists. By the same rationale, $\xi_k := 2^{-k} \log(H(k) + \frac{1}{2})$ converges as $k \rightarrow \infty$.

Thus we can rewrite the RHS of (5.5) as

$$\frac{2}{9} \cdot \frac{1}{3} \sum_{k=0}^{N-2} \left(\frac{3^{-k} 2^k}{2} + O(3^{-N}) 2^k \right) \xi_k = \frac{2}{9} \cdot \frac{1}{3} \sum_{k=0}^{N-2} \left(\frac{2}{3} \right)^k \frac{\xi_k}{2} + O \left(\left(\frac{2}{3} \right)^N \right),$$

with the intention of collecting terms of order unity. (Recall the identity $\frac{1}{3} \sum_{k=0}^{\infty} \left(\frac{2}{3} \right)^k = 1$. Also, roughly speaking, the reason for the factor 2 in $\xi_k/2$ is to account for the double preimages under $R(\frac{1}{2}, \frac{1}{2}, \cdot)$.) \square

Acknowledgements. We thank Alexander Teplyaev and Richard Kenyon for useful conversations during the initial stage of this work, and Quan Vu for his numerical contributions to cycle-rooted spanning forests on the Sierpinski gasket.

APPENDIX A. NUMERICAL APPROXIMATION OF THE FILLED JULIA SET IN FIGURE 3

To numerically approximate the filled Julia set associated with the evolution map \mathcal{U} , we initialize with a uniform sample of points $w = (\alpha, \lambda)$ in the rectangle $[0, 1] \times [0, 2]$. We then discard points w for which $|\mathcal{U}^k(w)|$ exceeds a threshold (10) after $k(=20)$ iterations, and keep those points which remain bounded within. Below is a working MATLAB code written by the second-named author.

```

1 clear;clc
2
3 dpts=1001;
4 lb=0;
5 ub=2;
6 th=10;
7 num_iter=20;
8
9 x=@(a,b,l) cos(2*pi*a);
10 xs=@(a,b,l) sin(2*pi*a);
11 y=@(a,b,l) cos(2*pi*b);
12 ys=@(a,b,l) sin(2*pi*b);
13 cosapplusb=@(a,b,l) x(a,b,l)*y(a,b,l)-xs(a,b,l)*ys(a,b,l);
14 cosa2plusb=@(a,b,l) (x(a,b,l)^2-xs(a,b,l)^2)*y(a,b,l)-2*xs(a,b,l)*x(a,b,l)
    *ys(a,b,l);
15 sinapplusb=@(a,b,l) xs(a,b,l)*y(a,b,l)+x(a,b,l)*ys(a,b,l);
16 sina2plusb=@(a,b,l) 2*xs(a,b,l)*x(a,b,l)*y(a,b,l)+ys(a,b,l)*(x(a,b,l)^2-xs
    (a,b,l)^2);
17 A=@(a,b,l) -64*l^4+256*l^3-356*l^2+(200-4*x(a,b,l)-2*y(a,b,l))*l+4*x(a,b,l)
    )...
18 +2*y(a,b,l)+cosapplusb(a,b,l)-37;
19 re_psi=@(a,b,l) 8*l^2-(2*cosa2plusb(a,b,l)+4*x(a,b,l)+16)*l+2*cosa2plusb(a
    ,b,l)...
20 +0.5*(x(a,b,l)^2-xs(a,b,l)^2)+4*x(a,b,l)+cosapplusb(a,b,l)+15/2;
21 im_psi=@(a,b,l) (-2*sina2plusb(a,b,l)-4*xs(a,b,l))*l+2*sina2plusb(a,b,l)+
    xs(a,b,l)*x(a,b,l)...
22 +4*xs(a,b,l)+sinapplusb(a,b,l);
23 R=@(a,b,l) 1+A(a,b,l)/2/sqrt(re_psi(a,b,l)^2+im_psi(a,b,l)^2);
24
25 aset=linspace(0,1,dpts);
26 lset=linspace(lb,ub,dpts);
27 figure

```

```

28 hold on
29
30 for i=1:dpts
31     for j=1:dpts
32         al=aset(i);
33         be=aset(i);
34         lmd=lset(j);
35         count=0;
36         while abs(lmd)<th
37             count=count+1;
38             psi=re_psi(al,be,lmd)+1i*im_psi(al,be,lmd);
39             theta=angle(psi);
40             if count==num_iter
41                 plot(aset(i),lset(j),'.','color','k')
42                 break
43             end
44             lmd=R(al,be,lmd);
45             al_dummy=al;
46             be_dummy=be;
47             al=mod(3*al_dummy+be_dummy+3*theta/2/pi,1);
48             be=mod(3*be_dummy+al_dummy-3*theta/2/pi,1);
49         end
50     end
51 end
52 xlabel('\alpha')
53 ylabel('\lambda')
54 title('Filled Julia set of U')

```

REFERENCES

- [1] Shlomo Alexander, *Some properties of the spectrum of the Sierpiński gasket in a magnetic field*, Phys. Rev. B (3) **29** (1984), no. 10, 5504–5508. MR743875 ↑2, 3, 22
- [2] Jason A. Anema and Konstantinos Tsoungkas, *Counting spanning trees on fractal graphs and their asymptotic complexity*, J. Phys. A **49** (2016), no. 35, 355101, 21. MR3537208 ↑3, 11, 13, 41, 42
- [3] N. Bajorin, T. Chen, A. Dagan, C. Emmons, M. Hussein, M. Khalil, P. Mody, B. Steinhurst, and A. Teplyaev, *Vibration modes of 3n-gaskets and other fractals*, J. Phys. A **41** (2008), no. 1, 015101, 21. MR2450694 ↑2, 3, 10, 23, 24, 26, 32
- [4] Jean Bellissard, *Renormalization group analysis and quasicrystals*, Ideas and methods in quantum and statistical physics (Oslo, 1988) (1992), 118–148. MR1190523 ↑2, 3, 10, 22
- [5] Antoni Brzoska, Aubrey Coffey, Madeline Hansalik, Stephen Loew, and Luke G. Rogers, *Spectra of magnetic operators on the diamond lattice fractal*, arXiv preprint (2017). available at <https://arxiv.org/abs/1704.01609>. ↑2, 10
- [6] Robert Burton and Robin Pemantle, *Local characteristics, entropy and limit theorems for spanning trees and domino tilings via transfer-impedances*, Ann. Probab. **21** (1993), no. 3, 1329–1371. MR1235419 ↑11
- [7] Shu-Chiuan Chang, Lung-Chi Chen, and Wei-Shih Yang, *Spanning trees on the Sierpinski gasket*, J. Stat. Phys. **126** (2007), no. 3, 649–667. MR2294471 ↑11
- [8] Joe P. Chen and Jonah Kudler-Flam, *Laplacian growth & sandpiles on the Sierpinski gasket: limit shape universality and exact solutions*, Ann. Inst. Henri Poincaré D (2019+), to appear, with preprint available at <https://arxiv.org/abs/1807.08748>. ↑16
- [9] Joe P. Chen and Alexander Teplyaev, *Singularly continuous spectrum of a self-similar Laplacian on the half-line*, J. Math. Phys. **57** (2016), no. 5, 052104, 10. MR3505182 ↑7, 10
- [10] Joe P. Chen, Alexander Teplyaev, and Konstantinos Tsoungkas, *Regularized Laplacian determinants of self-similar fractals*, Lett. Math. Phys. **108** (2018), no. 6, 1563–1579. MR3797758 ↑13, 15

- [11] Frank Daerden, Vyacheslav B. Priezzhev, and Carlo Vanderzande, *Waves in the sandpile model on fractal lattices*, Phys. A **292** (2001), no. 1-4, 43–54. MR1822430 ↑16
- [12] Frank Daerden and Carlo Vanderzande, *Sandpiles on a Sierpinski gasket*, Physica A: Statistical Mechanics and its Applications **256** (1998), no. 3, 533–546. ↑16
- [13] Eytan Domany, Shlomo Alexander, David Bensimon, and Leo P. Kadanoff, *Solutions to the Schrödinger equation on some fractal lattices*, Phys. Rev. B (3) **28** (1983), no. 6, 3110–3123. MR717348 ↑2, 3
- [14] Robin Forman, *Determinants of Laplacians on graphs*, Topology **32** (1993), no. 1, 35–46. MR1204404 ↑12
- [15] Fabien Friedli, *The bundle Laplacian on discrete tori*, Ann. Inst. Henri Poincaré D **6** (2019), no. 1, 97–121. MR3911691 ↑15
- [16] Bent Fuglede and Richard V. Kadison, *Determinant theory in finite factors*, Ann. of Math. (2) **55** (1952), 520–530. MR52696 ↑13
- [17] Masatoshi Fukushima and Tadashi Shima, *On a spectral analysis for the Sierpiński gasket*, Potential Anal. **1** (1992), no. 1, 1–35. MR1245223 ↑2, 3, 5, 10
- [18] J. M. Ghez, Yin Yu Wang, Rammal Rammal, B. Pannetier, and Jean Bellissard, *Band spectrum for an electron on a Sierpinski gasket in a magnetic field*, Solid State Communications **64** (1987dec), no. 10, 1291–1294. ↑2, 3, 10, 11, 22
- [19] Michael Hinz, *Magnetic energies and Feynman-Kac-Itô formulas for symmetric Markov processes*, Stoch. Anal. Appl. **33** (2015), no. 6, 1020–1049. MR3415232 ↑3
- [20] Michael Hinz and Luke Rogers, *Magnetic fields on resistance spaces*, J. Fractal Geom. **3** (2016), no. 1, 75–93. MR3502019 ↑3
- [21] Michael Hinz and Alexander Teplyaev, *Dirac and magnetic Schrödinger operators on fractals*, J. Funct. Anal. **265** (2013), no. 11, 2830–2854. MR3096991 ↑3
- [22] Douglas R. Hofstadter, *Energy levels and wave functions of Bloch electrons in rational and irrational magnetic fields*, Phys. Rev. B **14** (1976), no. 6, 2239. ↑2, 10
- [23] Jessica Hyde, Daniel Kelleher, Jesse Moeller, Luke Rogers, and Luis Seda, *Magnetic Laplacians of locally exact forms on the Sierpinski gasket*, Commun. Pure Appl. Anal. **16** (2017), no. 6, 2299–2319. MR3693883 ↑2
- [24] Adrien Kassel and Richard Kenyon, *Random curves on surfaces induced from the Laplacian determinant*, Ann. Probab. **45** (2017), no. 2, 932–964. MR3630290 ↑12, 13, 15, 16
- [25] Adrien Kassel and David B. Wilson, *The looping rate and sandpile density of planar graphs*, Amer. Math. Monthly **123** (2016), no. 1, 19–39. MR3453533 ↑16
- [26] Sander N. Kempkes, Marlou R. Slot, Saoirse E. Freeney, Stephan J. M. Zevenhuizen, Daniël Vanmaekelbergh, Ingmar Swart, and Cristiane Morais Smith, *Design and characterization of electrons in a fractal geometry*, Nature Physics **15** (2019), no. 2, 127. ↑16
- [27] Richard Kenyon, *Spanning forests and the vector bundle Laplacian*, Ann. Probab. **39** (2011), no. 5, 1983–2017. MR2884879 ↑12, 13
- [28] Brigita Kutnjak-Urbanc, Stefano Zapperi, Sava Milošević, and H. Eugene Stanley, *Sandpile model on the Sierpinski gasket fractal*, Phys. Rev. E **54** (1996Jul), 272–277. ↑16
- [29] Gregory F. Lawler and José A. Trujillo Ferreras, *Random walk loop soup*, Trans. Amer. Math. Soc. **359** (2007), no. 2, 767–787. MR2255196 ↑13
- [30] Russell Lyons, *Asymptotic enumeration of spanning trees*, Combin. Probab. Comput. **14** (2005), no. 4, 491–522. MR2160416 ↑13
- [31] ———, *Identities and inequalities for tree entropy*, Combin. Probab. Comput. **19** (2010), no. 2, 303–313. MR2593624 ↑13, 15
- [32] Satya N. Majumdar and Deepak Dhar, *Equivalence between the Abelian sandpile model and the $q \rightarrow 0$ limit of the Potts model*, Physica A: Statistical Mechanics and its Applications **185** (1992), no. 1-4, 129–145. ↑16
- [33] Leonid Malozemov and Alexander Teplyaev, *Self-similarity, operators and dynamics*, Math. Phys. Anal. Geom. **6** (2003), no. 3, 201–218. MR1997913 ↑2, 7, 10
- [34] Michel Matter, *Abelian Sandpile Model on randomly rooted graphs*, Ph.D. Thesis, 2012. Université Genève, available at <https://archive-ouverte.unige.ch/unige:21849>. ↑16
- [35] John Milnor, *Dynamics in one complex variable*, 3rd ed., Annals of Mathematics Studies, vol. 160, Princeton University Press, Princeton, NJ, 2006. MR2193309 ↑6
- [36] Robin Pemantle, *Choosing a spanning tree for the integer lattice uniformly*, Ann. Probab. **19** (1991), no. 4, 1559–1574. MR1127715 ↑13
- [37] Jean-François Quint, *Harmonic analysis on the Pascal graph*, J. Funct. Anal. **256** (2009), no. 10, 3409–3460. MR2504530 ↑15
- [38] Rammal Rammal and Gérard Toulouse, *Spectrum of the Schrödinger equation on a self-similar structure*, Phys. Rev. Lett. **49** (1982), no. 16, 1194–1197. MR675246 ↑2, 3
- [39] Rammal Rammal and Gérard Toulouse, *Random walks on fractal structures and percolation clusters*, Journal de Physique Lettres **44** (1983), no. 1, 13–22. ↑3, 10

- [40] Tadashi Shima, *On eigenvalue problems for Laplacians on p.c.f. self-similar sets*, Japan J. Indust. Appl. Math. **13** (1996), no. 1, 1–23. MR1377456 ↑2, 10
- [41] Masato Shinoda, Elmar Teufl, and Stephan Wagner, *Uniform spanning trees on Sierpiński graphs*, ALEA Lat. Am. J. Probab. Math. Stat. **11** (2014), no. 1, 737–780. MR3331590 ↑11
- [42] Alexander Teplyaev, *Spectral analysis on infinite Sierpiński gaskets*, J. Funct. Anal. **159** (1998), no. 2, 537–567. MR1658094 ↑2, 3, 7, 10, 15, 32
- [43] Elmar Teufl and Stephan Wagner, *The number of spanning trees in self-similar graphs*, Ann. Comb. **15** (2011), no. 2, 355–380. MR2813521 ↑11
- [44] UConn Math REU program, *Magnetic spectrum on the Sierpinski gasket*. <https://mathreu.uconn.edu/wp-content/uploads/sites/1724/2016/05/sierpinski-gasket.png> (accessed: 2019-09-05). ↑10
- [45] Frpzzd (<https://math.stackexchange.com/users/438055/frpzzd>), *Closed form solution for quadratic recurrence relations*. <https://math.stackexchange.com/q/2578046> (version: 2017-12-23). ↑42
- [46] David Bruce Wilson, *Generating random spanning trees more quickly than the cover time*, Proceedings of the Twenty-eighth Annual ACM Symposium on the Theory of Computing (Philadelphia, PA, 1996), 1996, pp. 296–303. MR1427525 ↑13

(Joe P. Chen) DEPARTMENT OF MATHEMATICS, COLGATE UNIVERSITY, HAMILTON, NY 13346, USA.

E-mail address: jpchen@colgate.edu

URL: <http://math.colgate.edu/~jpchen>

(Ruoyu Guo) DEPARTMENT OF MATHEMATICS, COLGATE UNIVERSITY, HAMILTON, NY 13346, USA.

E-mail address: rguo@colgate.edu